UNIVERSITY OF BIRMINGHAM

Four Essays on Modelling Asset Returns in the Chinese Financial Market

by

Shixuan Wang

A thesis submitted to the University of Birmingham for the degree of DOCTOR OF PHILOSOPHY

Department of Economics
Birmingham Business School
College of Social Science
University of Birmingham

March 2017

ABSTRACT

Firstly, we employ a three-state hidden semi-Markov model (HSMM) to explain the time-varying distribution of the Chinese stock market returns. Our results indicate that the time-varying distribution depends on the hidden states, represented by three market conditions, namely the bear, sidewalk, and bull markets.

Secondly, we further employ the three-state HSMM to the daily returns of the Chinese stock market and seven developed markets. Through the comparison, three unique characteristics of the Chinese stock market are found, namely "Crazy Bull", "Frequent and Quick Bear", and "No Buffer Zone".

Thirdly, we propose a new diffusion process referred to as the "camel process" to model the cumulative return of a financial asset. Its steady state probability density function could be unimodal or bimodal, depending on the sign of the market condition parameter. The price reversal is realised through the non-linear drift term.

Lastly, we take the tools in functional data analysis to understand the term structure of Chinese commodity futures and forecast their log returns at both short and long horizons. The FANOVA has been applied to examine the calendar effect of the term structure. An h-step functional autoregressive model is employed to forecast the log return of the term structure.

Acknowledgements

First and foremost, I sincerely appreciate my supervisors, Prof Zhenya Liu and Prof David Dickinson, for their academic guidance and incredible support during my PhD study. Prof Liu taught me how to think independently and critically. Prof Dickinson supported me without any reserve for all my academic activities. This thesis could not be completed without their continuously generous help.

My deep gratitude goes to Prof Lajos Horváth and Dr William Pouliot. I learnt the way of thinking in statistics from Prof Horváth. Dr Pouliot taught me how to perform Monte Carlo simulation. The statistical knowledge I learnt from them greatly contributes to this thesis.

My great appreciation goes to my parents who always supported and encouraged me in every possible way for my life and studies. It is their unconditional love makes me move forward. Additionally, my heartfelt thanks go to my girlfriend, Wan Li, who gave up a comfortable life in China and chose to stay with me in the UK for a tough life. Her countless praise on my research provides me energy to carry on in my dark time.

Last, but not least, I am grateful for the financial support from the Economic and Social Research Council, UK, grant ES/J50001X/1 and a Royal Economic Society Junior Fellowship.

Contents

List of Figures

List of Tables

Introduction

In the introduction, we provide the background information about the Chinese stock market, review the relevant finance theories, and present the research questions, motivations, and contributions.

In this collection of four loosely related essays, several advanced quantitative methods, namely hidden semi-Markov model, diffusion process, and functional data analysis, have been applied to understand and model the asset returns in the Chinese financial market.

Before the discussion on the technical detail of the statistical methods used in each chapter, it is useful to provide general information about Chinese stock market. We present basic statistics of the Chinese stock market, such as market capitalization, trading value, and number of listed companies, along with the discussion of main stock market indices in China. Compared with developed markets, the Chinese stock market has a number of unique features, such as limited openness, heavy regulation, and individual investors dominating structure. Those unique features are closely related to the quantitative results from the statistical methods.

Additionally, it is worthwhile to review the relevant finance theories, including the efficient market hypothesis (EMH), technical analysis, and behavioural finance. Although this thesis does not focus on testing EMH, but the results from the statistical methods can provide some evidence of inefficiency in the Chinese financial market. In Chapter 1, we model the CSI 300 returns by a three-state HSMM and design a simple trading strategy to exploit the arbitrage opportunity in the inefficient market. Our findings contribute to the literature of technical analysis that are on the disapproval side of the EMH. Behavioural finance provides us a solid foundation to explain some results in Chapter 1 and Chapter 2. For example, the disposition effect is the reason of our finding "bull mixed with bear" during 2007. With the consideration of the price reversal and the market conditions, Chapter 3 propose a new diffusion process referred to as the "camel process" in order to model the cumulative return of a financial asset. In Chapter 4, we show the predicability of functional autoregressive models on the term structure of commodity futures in China, which provide the evidence of inefficiency in the Chinese commodity futures market as well.

The Institutional Background

Overview on the Chinese Stock Market

In mainland China, there are two main stock exchanges, namely the Shanghai Stock Exchange (SSE) and the Shenzhen Stock Exchange (SZSE). Table 1 lists the largest ten stock exchanges in the world, ranked by market capitalization in April 2017. SSE and SZSE are ranked at the 4^{th} place and the 8^{th} place, respectively. Although SSE is larger than SZSE in terms of market capitalization, SZSE has more trading value and more number of listed companies.

TABLE 1: Statistics of Stock Exchanges (April 2017)

	Market Cap. (USD millions)	Trading Value (USD millions)	NO. of Listed Companies		
			Total	Domestic	Foreign
1. NYSE	20,134,573.8	1,174,981.3	2,294	1,806	488
2. Nasdaq - US	8,626,325.5	838,643.7	2,895	2,511	384
3. Japan Exchange Group Inc.	5,263,274.0	437,602.4	3,562	3,556	6
4. Shanghai Stock Exchange	4,354,737.9	617,076.6	1,264	1,264	0
5. LSE Group	3,926,537.1	167,447.9	2,492	2,046	446
6. Euronext	3,902,057.1	148,905.5	1,279	1,106	173
7. Hong Kong Exchanges and Clearing	3,557,033.5	114,339.9	2,020	1,915	105
8. Shenzhen Stock Exchange	3,294,346.1	716,443.3	1,959	1,959	0
9. TMX Group	2,056,681.6	96,303.0	3,426	3,378	48
10. BSE India Limited	1,946,001.7	11,411.5	5,823	5,822	1

Source: World Federation of Exchanges members, affiliates, correspondents and non-members.

In the two exchanges, the common shares are classified as A-shares and B-shares. A-shares are denominated by local currency RMB and traded in RMB only by domestic institutional and individual investors. B-shares is also denominated by RMB but traded in foreign currencies (USD in SSE and Hong Kong dollar in SZSE) by licensed foreign and domestic investors. It should be highlighted that A-shares take up the majority (nearly 96%) of the whole market.

During the last two decade, China has developed multi-tier stock market, consisting of main board, SME board, and ChiNext board. The main board in SSE and SZSE lists companies with large capital size and stable profit. Established in May 2004, SME board is primarily targeted to list small and medium size companies with stable revenue. The main sector of companies listed in SME board is the manufacturing, accounting for 75% of the SME board. Launched in October 2009, ChiNext is positioned to serve

innovative and fast-growing enterprises, especially high-tech firms. ChiNext aims to encourage innovation and creativity. The financial requirements of listing in ChiNext are less stringent than those of the main and SME boards. SZSE asserts that ChiNext is not a "mini-board" and it is open to all enterprises size as long as they meet the listing criteria.

There are several major Chinese stock market indices often used by academic research. The SSE Composite Index is a capitalization-weighted index, which represents the overall market movement of all A-shares and B-shares companies listed on SSE. The SZSE Component Index is a capitalization-weighted index, consisting of the 500 top companies listed in SZSE A-shares. The CSI 300 (a.k.a SHZE 300) index is a free-float capitalization-weighted index based on 300 A-shares stocks listed on both SSE and SZSE. There are several SSE size indices, SSE 50, SSE 180, and SSE 380, respectively representing the top 50, 180, 380 companies listed on SSE A-shares by free-float capitalization weight.

Among those market indices, the CSI 300 index is widely accepted as an overall representation for the general movements of the China A-share markets (Yang et al., 2012; Hou & Li, 2014). The index was jointly launched by the SSE and SZSE on April 8^{th} 2005. The index is complied and published by the China Securities Index Company Ltd. It is comprised of 300 large-capitalization and actively traded stocks, which covers roughly 70% of total market capitalization of the two stock markets (Yang et al., 2012). More importantly, the first Chinese stock market index futures contract is based on the CSI 300 index, launched on April 16^{th} 2010. Hence, we will use the CSI 300 index for the overall perfomrance representation of the Chinese stock market throughout this thesis.

Features of the Chinese Stock Market

Compared with developed markets, there are several unique features of the Chinese stock market. Firstly, the Chinese stock market is relatively isolated from the international financial markets because of very limited openness to the international investors. There are no foreign companies listed on SSE and SZSE (see Table1). The only channel for

foreign investors is the qualified foreign institutional investors (QFII). However, the application for the QFII license is strictly examined by the the China Securities Regulatory Commission (CSRC). For the foreign investors with the QFII license, there are still a number of restrictions on their investment behaviour in the Chinese stock market.

Secondly, the Chinese stock market is heavily regulated and intervened by the government. For the purpose of stabilising market, SSE and SZSE apply the rule of price limits that the daily change of individual stock price cannot go beyond more than 10%. In addition to the price limits, CSRC imposed the "Circuit Breaker" [1] on January 1st 2016. In China, the "Circuit Breaker" is based on the abnormal movement of the CSI 300 index. Specifically, the trading of stocks and relevant derivatives will be suspended for 15 minutes if the market index rises/drops 5%, and the trading will be stopped for the rest of day if the market index rises/drops 7%. After the launch of the "Circuit Breaker", it was activated twice in the first week. Nevertheless, the Chinese government decided to stop the "Circuit Breaker" on January 8th 2016, because of the complaint from the investors.

Thirdly, there is a lack of risk management tools in the Chinese stock market. As a matter of fact, short-selling stocks in China is still limited and investors can only buy stocks. Index futures were supposed to be a suitable tool to hedge downside risk. However, the Chinese regulator imposed various restrictions on trading index futures. In August 2015, more restrictions were imposed because the CSRC suspected that some investors participated in "malicious" short-selling index futures. Many private funds and security firms were under investigation for betting on a market drop. The trading volume of index futures shrank more than 90%, from roughly 3 million to 50 thousand per day. At the moment, utilizing index futures to manage risk is still subject to a number of restrictions (e.g. no more than 10 contracts are allowed to open). Due to those restrictions on domestic index future markets, investors are not able to freely trade index futures. Many investors choose to trade Chinese index future products in foreign

[1] Note that "Circuit Breaker" is different from trading halt which occurs when a stock exchange stops trading on a specific stock for a certain time period. When "Circuit Breaker" is activated, the trading of all stocks on the exchange will be affected.

markets, like the FTSE China A50 index futures on the Singapore Exchange and E-mini FTSE China 50 index futures on the Chicago Mercantile Exchange.

Fourthly, the majority of investors are individual investors without professional investment knowledge, who are focusing on short-term speculation rather than long-term investment. In China, individual investors account for 82.24% of total trading volume in 2013 (Han & Li, 2017), whereas institutional investors dominate in developed markets. As indicated by Table 2, there are in total 49 million individual investors in China, while the number of institutional investors is only 71 thousand. Another distinctive feature suggested by Table 2 is that the majority of individual investors has small amount of market value. Specifically, 93.61% individual investors hold less than 0.5 million market value A-shares stocks. The market value of A-shares stocks held by institutional investors is more diversified, with 32.66% larger than 10 million. According to the 2015 annual report of China Securities Depository and Clearing Corporation, 48 % investors are less than 40 years old (see Table 3), and less than 20 % of the individual investors have undergraduate degree or above.

TABLE 2: Market Value Distribution of A-Shares Investors (December 2016)

Market Value (10000 RMB)	**Individuals**		**Institutions**		**Total**	
	No. of Investors	**Ratio**	**No. of Investors**	**Ratio**	**No. of Investors**	**Ratio**
< 1	12,017,997	24.37%	4,536	6.30%	12,022,533	24.35%
1-10	23,627,616	47.92%	8,288	11.51%	23,635,904	47.87%
10-50	10,513,794	21.32%	10,978	15.25%	10,524,772	21.31%
50-100	1,791,721	3.63%	6,055	8.41%	1,797,776	3.64%
100-500	1,195,312	2.42%	13,360	18.56%	1,208,672	2.45%
500-1000	97,822	0.20%	5,257	7.30%	103,079	0.21%
1000 +	63,640	0.13%	23,508	32.66%	87,148	0.18%
Total	49,307,902	100.00%	71,982	100.00%	49,379,884	100.00%

Source: Wind.

Lastly, the Chinese stock market is very liquid with high turnover velocity. The turnover velocity in the Chinese stock market is much higher than the turnover velocity in developed markets. In April 2017, the turnover velocity of SZSE and SSE are 260.97% and 170.04%, ranked in the 2nd and 4th places among all stock exchanges in the world [2]. The possible reason of high turnover velocity is that a large proportion of trading activities

[2]Data source: World Federation of Exchanges members, affiliates, correspondents and non-members.

TABLE 3: Investors Age Distribution

Age	**No. of Investors**	**Ratio**
<20	479,900	0.49%
20 - 30	19,751,000	19.99%
30 - 40	27,334,100	27.66%
40 - 50	24,701,700	25.00%
50 - 60	15,345,500	15.53%
60 +	11,209,400	11.34%
Total	98,821,600	100.00%

Source: 2015 annual report of China Securities Depository and Clearing Corporation.

are speculative rather considered as investments. Many individual investors are heavily influenced by market rumours. Individual investors like to follow the news and purchase stocks in a herding manner (Tan et al., 2008).

Two Notable Historical Events

Split-Share Structure Reform

Before the reform, one of distinct feature in the Chinese stock market was the existence of the non-tradable shares, which were mainly held by the government and its affiliates. The percentage of non-tradable shares in the total shareholdings was approximately two-thirds. At that time, the investors with tradable shares had very limited power in the company governance. The split-share structure induced a number of problems, such as inefficient corporate governance, agency problem, suppression of free trading (Yeh et al., 2009).

On April 29th 2005, the Chinese government imposed a split-share structure reform, which aimed to convert all non-tradable shares to tradable shares. The implementation of the reform took about roughly two years. Initially, the China Securities Regulatory Commission (CSRC) conducted a pilot program on the conversion of four companies in April 2005, followed by another 42 companies in June 2005. In August 2005, the reform was opened to all listed companies. By the end of 2017, more than 97% of listed companies in China has implemented the reform (Nartea et al., 2013). Liao et al. (2014) point out that the reform was a milestone event of China's financial liberalization,

which significantly reduced agency problems and improved the corporate governance of the listed companies. Due to the conversion from non-tradable shares to tradable shares, the reform had provided substantial liquidity to the market.

Other Source Financing

It has been observed that other source financing activities are very active during 2015. Other source financing refers to borrow funds from trust companies, fund-matching companies, etc. Unlike margin loan and margin financing, the regulation on other source financing is much less strict, which would be essential cause for the high leverage. For example, umbrella trusts are not required to register with the China Securities Depository and Clearing Corporation. Umbrella trusts contain two sorts of tranches. Banks purchase the senior tranches, which guarantee fixed returns. Subordinate tranches are sold to private clients, like wealthy individuals, private companies, and fund-matching companies, and provide uncertain returns depending on the performance of the wealth management product. In other words, subordinate tranches would get the rest of investment profits. Jiang (2014) claimed that the Minsheng Bank, China Everbright Bank, and China Merchants Bank were heavily involved in the business of umbrella trusts. There is no accurate data about the size of umbrella trusts but some estimations indicate that they accounted for roughly 200 billion RMB by the end of 2014 (Hsu, 2015). In favour of high interest rates, fund-matching companies lend funds to investors by providing margin loans without sufficient consideration of risk. Yap (2015) pointed out that fund-matching companies channelled 500 billion RMB (June 30, 2015) from opening multiple and subdivided securities accounts with brokerages. These fund-matching companies were subject to a lack of regulation until CSRC imposed restrictions on them in July 2015.

Theoretical Background

The Efficient Market Hypothesis and Anomalies

One of most relevant finance theory is the efficient market hypothesis (EMH). The widely accepted definition of the EMH is proposed by Fama (1970). He defines the EMH as that "A market in which prices always 'fully reflect' available information is called 'efficient' ". He further distinguishes three different forms of the EMH, namely weak form, semi-strong form, and strong form, depending on the information set of historical prices only, public available information, any relevant information, respectively.

In the 1970s, the EMH was generally accepted by the academic researches in financial economics (Shiller, 2003). One straightforward implication of the EMH is that the future stock price is unpredictable. Fama (1965) concludes that the stock price follows a random walk with empirical evidence from the thirty stocks of the Dow-Jones Industrial Average. He verifies the random walk model by separately testing two sub-hypotheses that the successive price changes are independent and the price changes follow some probability distribution. Samuelson (1965) uses a concept of the martingale to prove that anticipated prices fluctuate randomly. The random walk model and the martingale hypothesis severely challenge the proponents of the technical analysis, which will be discussed in depth later.

After the prevalence of the EMH, many researchers in finance and statistics, however, started to doubt the EMH and believe that the stock prices are at least partially predicable (Malkiel, 2003). From the time-series perspective, Campbell et al. (1997) and Lo & MacKinlay (2002) find the short-term momentum that the stocks with short-term (i.e. daily, weakly, and monthly) above-average returns tend to have a high probability of further above-average returns in the subsequent period, which is the evidence rejecting the EMH in the sense that the stock price is not purely random walk. But only 12 percent of the variation in the daily stock market index can be predicted by using the information of the past daily returns (Beechey et al., 2000). At longer horizons (three to fives years), many studies have shown evidence of mean reversion in stock returns (e.g. Fama & French, 1988; Poterba & Summers, 1988). Fama & French (1988) claim that

20 to 40 percent of the variation in the long horizon returns can be predicted by using the information of the past returns.

There are some other anomalies from the cross-sectional perspective, such as the size effect, the value effect, etc. Fama & French (1993) identify that the small-capitalization company stocks tend to have larger returns than those of large-capitalization company stocks and that stocks of companies with high book-to-market ratio (i.e. high value) tend to have larger returns than ones with low book-to-market ratio. They further conclude that the size and the value together can provide explanatory power for stock returns.

A number of researches have found the calender effects of stock returns, such as month-of-the-year and day-of-the-week effects, which uncover the empirical evidence that the average stock returns in a certain calender month or weekday appear to be significantly different from the other months or weekdays. For example, Haugen & Lakonishok (1988) find the relatively higher returns in January (the January effect), and French (1980) documents the significantly higher returns on Monday (the weekend effect). However, Malkiel (2003) claims that these calender effects are comparatively small to the transactions costs when someone actually exploit them in practice.

Due to the joint hypothesis problem indicated by Campbell et al. (1997), the market efficiency is empirically rejected could be because the market is truly inefficient or because the wrong market equilibrium is assumed. In this sense, the EMH is not testable. Throughout this thesis, we focus on the statistical methods in terms of measuring efficiency rather than testing the EMH.

Technical Analysis

Technical analysis, also known as "charting", is to predict the future price movement by identifying the presence of geometric shapes in historical price charts, sometimes also with information of volume and open interest. Under the EMH, the current price has already reflected all past available information, which naturally has the implication

that technical analysis should provide no useful information for forecasting future price movement (Fama, 1965).

Nevertheless, technical analysis has been widely used by traders in practice. For example, more than 90 percent of foreign exchange traders in the London market performed one to four weeks ahead forecasting by technical analysis in 1990s (Allen & Taylor, 1990). It has been a long-standing debate on the usefulness of technical analysis in academia. One difficulty of technical analysis is that the geometric shapes are sometimes difficult to be mathematically define.

The empirical studies show the mixed results whether technical analysis can generate excess returns. On the approval side, a number of studies have found the evidence of excess returns generated by technical analysis (e.g. Pruitt & White, 1988; Brock et al., 1992; Neely et al., 1997; Coutts & Cheung, 2000; Leigh et al., 2002; Okunev & White, 2003). In particular, Lo et al. (2000) employ kernel smoothing technique to automatically recognise ten sophisticated technical charts, such as Head-and-Shoulders, Broadening, and Triangle, and further find several technical indicators do have predictive power. However, some studies suspected the validity of technical analysis because of the data mining problem (e.g. Brock et al., 1992).

On the disapproval side, many researchers show that technical analysis does not outperform simple buy-and-hold strategy (e.g. Curcio et al., 1997; Hamm & Wade Brorsen, 2000; Lucke, 2003). Other studies find that the profits from the technical analysis declines over time (e.g. Guillaume, 2012). In particular, Coutts (2010) re-examines the trading rules in Coutts & Cheung (2000) with a more updated sample period and concludes that those trading rules become defunct.

Behavioural Finance

In the 1990s, the theories of behavioural finance were developed to explain why and how financial markets might be inefficient. Shiller (2003) defines behavioural finance as "finance from a broader social science perspective including psychology and sociology". The key assumption in behavioural finance is that not all investors are rational,

and those irrational investors (often known as noise traders) make the asset prices deviate from their fundamental values. The irrational behaviour comes from a number of human psychological activities, including overconfidence, myopic loss aversion, representativeness, conservatism, belief perseverance, anchoring, and availability biases. Those psychological activities impede investors to form the correct expectation on the asset prices and to further conduct irrational investment decisions.

Two phenomena often discussed by behavioural finance are overreaction and underreaction, which refer to that the investors react disproportionately to new information. DeBondt & Thaler (1985) find that most investors usually overreact to unexpected and dramatic news, suggesting the weak from market inefficiencies. De Bondt & Thaler (1987) further find additional evidence to support the overreaction hypothesis, which contradicts two alternative hypotheses based on the size of company and risk difference. It is not always overreaction, but sometimes be slow or underreaction. Hong & Stein (1999) construct a model with two groups of boundedly rational agents "newwatchers" and "momentum traders" and show the underreaction at short horizons and overreaction at long horizons. Fama (1998) claims that overreaction to information is as frequent as underreaction. Veronesi (1999) uses a dynamic, rational expectations equilibrium model of asset prices to demonstrate that stock prices underreact to good news in bad times and overreact to bad news in good times. Farag (2014) use the system GMM to find strong evidence of price reversal after the overreaction in the Egyptian stock market.

The disposition effect is the phenomena that investors tend to sell assets that have gained profit ("winners") and hold assets that have lost value ("losers"). Weber & Camerer (1998) conduct experiments and find that the experimental subjects did tend to sell winners and keep losers, which can be explained by the multiple reference points affecting framing and guide choices. Barber & Odean (1999) study the disposition effect and concludes that overconfidence is the possible reason. Barberis & Xiong (2009) investigate the driving reason for the disposition effect and conclude that the model with preferences defined over annual gains and losses fails to predict the disposition effect but the model with preferences defined over realized gains and losses predicts the disposition effect more reliably.

Behavioural finance is applied to explain the excess returns of some trading strategies. Lakonishok et al. (1994) investigate the reason for the higher returns of the value strategies and find that these strategies exploit the suboptimal behaviour of the typical investor. Chan et al. (1996) explain the profitability of the momentum strategies as that the market responds gradually to new information, i.e. there is underreaction. Lee & Swaminathan (2000) discover an important link between momentum and value strategies is the past trading volume, and their findings helps to intermediate-horizon underreaction and long-horizon overreaction effects. Apart from explanation using behavioural finance, Frazzini (2006) designs a even-driven trading strategy based on the disposition effect and this trading strategy generates monthly alphas of over 200 basis points.

Research Questions, Motivations, and Contributions

In this collection of four loosely related essays, namely several quantitative methods, hidden semi-Markov model, diffusion process, and functional data analysis, have been applied to understand and model the asset returns in the Chinese financial market.

HSMM is a generalisation of the HMM by explicitly specifying the sojourn time distribution (Yu, 2010). Bulla & Bulla (2006) examine the reproduction of the stylized facts of the asset returns by the US industry stock indices and show that HSMM is superior to HMM because the stylized facts of the daily returns were entirely reproduced. Due to the merits of HSMM in the literature, we employ a three-state HSMM to decode the Chinese stock market returns in Chapter 1. Firstly, it is appropriate to employ a three-state HSMM to explain the time-varying distribution of Chinese stock market returns. Secondly, the hidden states in the HSMM correspond to the market conditions, namely the bear, sidewalk, and bull market. Unlike the definition of market conditions in the literature (Fabozzi & Francis, 1977; Chauvet & Potter, 2000; Edwards & Caglayan, 2001; Lunde & Timmermann, 2004; Gonzalez et al., 2006; Cheng et al., 2013), we provide a systematic way to find the timing of three-category classification, namely the bull, sidewalk, and bear market, for the daily data. Thirdly, we show the

inefficiency of the market by design a trading strategy based on the expanding window decoding. The trading strategy generates risk-adjusted return with a Sharpe ratio of 1.14 in the testing sample.

The by-product of Chapter 1 is our statistical definition of market conditions, i.e. bear, sidewalk, and bull markets, which correspond to the three states in the HSMM. As discussed above, the regulation and the investor structure of the Chinese stock market are different from the developed markets. It is natural to question the difference in terms of market conditions between the Chinese stock market and developed market. In Chapter 2, we employ the three-state HSMM to the daily returns of the Chinese stock market and the other seven developed markets. Using the Viterbi algorithm to globally decode the most likely sequence of the market conditions, we systematically find the precise timing of bear, sidewalk, and bull markets for all eight markets. Through the comparison of the estimation and decoding results, many unique characteristics of the market conditions in China are found, such as "Crazy Bull", "Frequent and Quick Bear", and "No Buffer Zone". In China, the bull market is more volatile than in developed markets, the bear market occurs more frequently than in developed markets, and the sidewalk market has not functioned as a buffer zone since 2005. Lastly, possible causes of the unique characteristics are discussed and implications for policy-making are suggested.

As indicated in the first two chapters, the asset returns behaves differently in different market conditions. Additionally, the overreaction has been widely studied in behavioural finance. To the best of our knowledge, there is no diffusion process considering both market condition and overreaction. In Chapter 3, we propose a new diffusion process referred to as the "camel process" in order to model the cumulative return of a financial asset. The process considers the market condition and the price reversal. This new process includes three parameters, the market condition parameter α, the overreaction correction parameter β, and the volatility parameter γ. Its steady state probability density function could be unimodal or bimodal, depending on the sign of the market condition parameter. The price reversal is realised through the non-linear drift term which incorporates the cube term of the instantaneous cumulative return. The time-dependent solution of its Fokker-Planck equation cannot be obtained analytically, but

can be numerically solved using the finite difference method. The properties of the camel process are confirmed by our empirical estimation results of ten market indexes in two different periods. The nature of the research in Chapter 3 is more theoretical rather than empirical.

In the last chapter, we shift from the stock market to the commodity futures market because the stringent constraints on short selling stocks make it very difficult to manage the downside risk and investing in commodity futures is an effect way to diversify against falling stock prices (Edwards & Caglayan, 2001; Jensen et al., 2002; Wang & Yu, 2004; Erb & Harvey, 2006). We should not restrict ourselves only in the stock market, and it is worthwhile and meaningful to investigate the commodity futures market in China. Chapter 4 takes the tools in functional data analysis to understand the term structure of Chinese commodity futures and forecast their log returns at both short and long horizons. A functional ANOVA (FANOVA) has been applied in order to examine the calendar effect of the term structure. We use an h-step Functional Autoregressive model to forecast the log return of the term structure. Compared with the naive predictor, the in-sample and out-of-sample forecasting performance indicates that additional forecasting power is gained by using the functional autoregressive structure. Although the log return at short horizons is not predictable, the forecasts appear to be more accurate at long horizons due to the stronger temporal dependence. The predictive factor method has a better in-sample fitting, but it cannot outperform the estimated kernel method for out-of-sample testing, except in the case of 1-quarter-ahead forecasting.

Chapter 1

Decoding Chinese Stock Market Returns: Three-State Hidden Semi-Markov Model, Market Conditions, and Market Inefficiency

In this chapter, we employ a three-state hidden semi-Markov model (HSMM) to explain the time-varying distribution of the Chinese stock market returns since 2005. Our results indicate that the time-varying distribution depends on the hidden states, which are represented by three market conditions, namely the bear, sidewalk, and bull markets. In order to show the inefficiency of the market, we design a simple trading strategy based on expanding window decoding that generates risk-adjusted return with a Sharpe ratio of 1.14.

1.1 Introduction

The term "decoding", originally from the field of speech recognition, is the procedure of deciphering observations into the underlying pattern that drives the mechanism. In this chapter, we aim to decode the Chinese stock market returns through a new developed statistical model, namely hidden semi-Markov Model (HSMM). More specifically, we are going to answer three questions: 1) can we use the HSMM to explain the time-varying distribution of the Chinese stock market returns? 2) what is the economic interpretation of the hidden states in the HSMM? 3) can we design a profitable trading strategy based on the HSMM to show the inefficiency of the market?

The motivation for the first question is based on our observation of the market index. The literature on the Chinese stock market focuses on financial integration, speculative trading, government interventions, information asymmetry, and the relation with bank credit (e.g. Girardin & Liu, 2007; Mei et al., 2009; Los & Yu, 2008; Chan et al., 2008; Girardin & Liu, 2005). Less attention has been paid to the time-varying features of the Chinese stock market after 2005. We have observed that the Chinese stock market behaves quite differently across different periods since 2005. Between 2005 and 2009, the Chinese stock market index (CSI 300) increased approximately six times from 1003 (April 8^{th} 2006) to 5877 (October 16^{th} 2007), and then dropped to 1627.759 (April 11^{th} 2008). Between 2010 and 2014, the CSI 300 had much less volatility and fluctuated between 2000 and 3500. From 2015 onwards, the market became highly volatile again (see Figure 1.1). In this chapter, we will show that a three-state HSMM can be employed to explain the time-varying distribution of the Chinese stock market returns.

The motivation for the second question is followed the answer of the first question. It is naturally to raise the question about the economic interpretation of the hidden states of the HSMM. Based on the estimation results by the expectation-maximization (EM) algorithm, the hidden states behind the return data can interpreted as the three market conditions, namely the bear, sidewalk, and bull markets. The underlying sequence of hidden states is globally decoded by the Viterbi algorithm. The evolution of the market conditions of the Chinese stock market over the last decade is then reviewed.

FIGURE 1.1: CSI 300 and its Returns

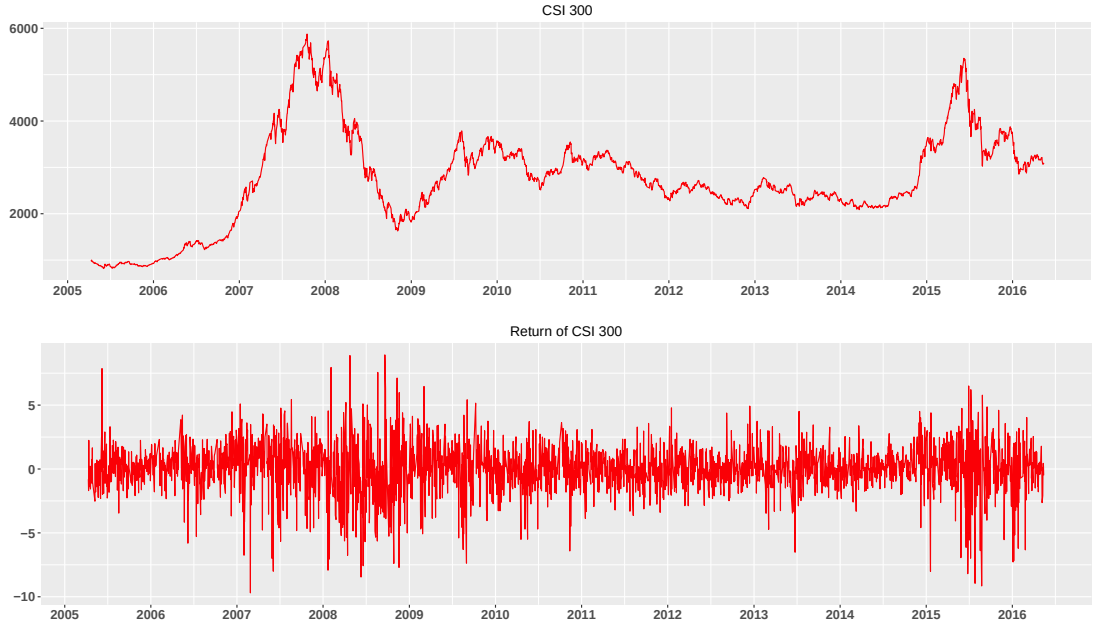

The motivation for the third question is arisen from the efficient market hypothesis (EMH). Under the EMH, the prices always 'fully reflect' available information and follow a random walk. Our three-state HSMM shows some merits of fitting the empirical data in terms of the stylized facts of asset returns, which are not considered by the random walk. Although testing the EMH is not the focus of this chapter, it is worthwhile to use our three-state HSMM to provide some evidence for the inefficiency of the Chinese stock market. Following the literature of technical analysis, we design a simple trading strategy based on expanding window decoding, which generates risk-adjusted return with a Sharpe ratio of 1.14. With the profitable trading strategy, we broaden the readership of this research to both academic researchers and practitioners.

We contribute to the literature along three main dimensions. Firstly, we make use of a new statistical model, HSMM, to explain the time-varying distribution of the Chinese stock market returns. To the best of our knowledge, this model has never been used in any emerging market. Secondly, we provide the economic interpretation of the hidden states. To the best of our knowledge, this is the first research to associate market conditions to the hidden states in the HSMM. The by-product is that we provide a new systematic way to find the timing of different market conditions, which will be

used in Chapter 2. Thirdly, we contribute to the literature of technical trading rules by proposing a new profitable trading strategy based on our model.

The remainder of the chapter is structured as follows. Section 1.2 reviews the literature of relevant studies. Section 1.3 describes our data and its descriptive statistics. Section 1.6 briefly introduces the HSMM, estimation method, decoding techniques and our model set-up. In Section 1.7, the estimation results and the decoding results are presented and their economic meanings are discussed, followed by the model evaluation and comparison in Section 1.8. Section 1.9 presents a simple trading strategy with a Sharpe ratio of 1.14. Section 1.10 summarises the chapter.

1.2 Literature Review

Stylized Facts of Asset Returns

The stylized facts of asset returns in the developed markets are well documented in the literature (Granger & Ding, 1995; Pagan, 1996; Cont, 2001). They can be classified into two categories, namely distributional properties and temporal properties. Distributional properties relate to the non-Gaussianity of the distribution of asset returns, whilst temporal properties refer to the time dependence of asset returns and of the squared/absolute asset returns.

In the early studies exploring distributional properties, normal distributions with stationary parameters were often selected in order to model daily asset returns. However, Mandelbrot (1997) doubted the Gaussian hypothesis of asset returns and stated that stable Paretian distributions with characteristic exponents of less than 2 are better suited to fit the empirical distribution of assets (Mandelbrots hypothesis). Fama (1965) undertook extensive testing on empirical data and found that extreme tail values are more frequent than the Gaussian hypothesis (a.k.a. leptokurtosis), which supports the Mandelbrots hypothesis. In order to explain the notion of leptokurtosis, Fama tried two modified versions of the Gaussian model: a Gaussian mixture model and a non-stationary Gaussian model. However, his empirical evidence supports neither of them. Praetz (1972) and

Blattberg & Gonedes (1974) employed t-distributions with small degrees of freedom in order to capture the fat-tail of the empirical distribution of asset returns. Granger & Ding (1995) suggested that the appropriate distribution is the double exponential distribution with zero mean and unit variance. Mittnik & Rachev (1993) inspected various stable distributions for asset returns and found that the Weibull distribution gave the best fit for the S&P 500 daily returns between 1982 and 1986.

In terms of temporal properties, the ARCH-family models are often used for volatility clustering. The original ARCH model was introduced by Engle (1982) in order to model non-constant variances. Bollerslev (1986) generalised the ARCH model by allowing past conditional variances to affect current conditional variances. Afterwards, variants of the GARCH were developed, including EGARCH, GJR, GARCH-M, and so forth. Bollerslev et al. (1992) comprehensively reviewed many types of GARCH models. As for the continuous-time set-up, stochastic volatility models were introduced by Taylor (1986) in an attempt to overcome the main drawback of the Black-Scholes model characterised by a constant volatility. Stochastic volatility models facilitate analysis of a variety of option pricing problems. A review of the stochastic volatility models was conducted by Jäckel (2004).

Hidden (Semi-)Markov Models

The HMM is suitable to capture both distributional and temporal properties of the stylized facts of asset returns. The state process of the model evolves as a Markov chain, providing the channel of time dependency. Its distribution is a mixture of several distributions, enabling it to explain the fat tails. Rydén et al. (1998) adopted an HMM with component distributions as normal distributions (zero mean but different variance) in order to reproduce most of the stylized facts of the daily returns. However, the HMM fails to reproduce the slow decay in the autocorrelation function (ACF) of the squared returns. For the Chinese stock market, Girardin & Liu (2003) use a switch-in-the-mean-and-variance model (MSMH(3)-AR(5)) in order to examine the market conditions on the Shanghai A-share market from 1994 to 2002. They found three regimes: a speculative market, a bull market and a bear market.

There are two ways to improve the HMM. The first way is to change the component distribution into other types of distribution. Rogers & Zhang (2011) proposed a two-state HMM with non-Gaussian component distributions. They examined various component distributions. By using the Kolmogorov-Smirnov test, the symmetric hyperbolic distribution is found to be the most appropriate component distribution. With the inclusion of a regularisation term, they can reproduce the slow decay of the ACF in the absolute returns. Their model setting mainly focused on statistical properties and lacked meaning for the field of economics. The second way is to generalise the sojourn time distribution of the HMM. Bulla & Bulla (2006) modelled daily returns of US industry stock indices with the HSMM, which is a generalisation of the HMM by explicitly specifying the sojourn time distribution. They utilised both normal distributions and Student's t-distributions as the component distributions. The stylized facts of the daily returns were entirely reproduced by the HSMM. Their research focused on analysing the variances but ignored the means of the component distributions. We believe that the means of the component distributions are also worth investigating because they lead to different market conditions.

Definition of Market Conditions

In practice, investors tend to determine market conditions arbitrarily and different conclusions might be drawn for the same market in the same period. In the existing academic literature, the definition of market conditions varies considerably. In one of the early study, Fabozzi & Francis (1977) propose three ways to define market conditions. In the first classification of Bull and Bear Markets, the rule places most months when the market rises in the bull market (BB), but months when the market rose near the bearish months were treated as part of the bear market. In the second classification of Up and Down Markets (UD), months in which return was non-negative are defined as Up months and months in which return was negative are defined as Down months. In the third classification of Substantial Up and Down Months (SUD), there are three categories: months when the market moved Up-substantially, months when the market

moved Down-substantially, and months when the market moved neither Up-substantially nor Down-substantially. The threshold of substantial move was arbitrarily defined.

In the modern study, a loose definition by Chauvet & Potter (2000) proposed that market prices generally increase (decrease) in a bull (bear) market. Edwards & Caglayan (2001) use a simple classification that bull market months are defined as those in which the S&P index rises by 1% or more and bear market months are defined as those in which the S&P index falls by 1% or more. Lunde & Timmermann (2004) claim that a bull (bear) market starts when the market price increases (decreases) a certain percentage, say 20%, from the previous local bottom (peak). Gonzalez et al. (2006) utilized two formal turning point methods to detect the timing of bull and bear markets. Cheng et al. (2013) define bull (bear) markets as the periods with at least three consecutive months of positive (negative) returns.

Market Efficiency and Technical Trading Rules

Under the EMH, the current price has already reflected all past available information, which naturally has the implication that technical trading rules cannot generate excess returns than a buy-and-hold trading strategy Fama (1965).

The empirical studies show the mixed results. Park & Irwin (2007) have conducted a survey about the profits of technical analysis. In general, technical trading rules are profitable for the stock market indices in emerging markets even after transaction costs(Ratner & Leal, 1999; Ito, 1999; Coutts & Cheung, 2000; Gunasekarage & Power, 2001). However, the profits of technical trading rules are negligible after transaction costs or have declined as time goes by (Hudson et al., 1996; Mills et al., 1997; Ito, 1999; Day & Wang, 2002).

1.3 Data

1.3.1 Data Information

The raw data is the closing price of the CSI 300, which is a free-floating weighted stock market index of 300 A-share stocks listed on both the Shanghai Stock Exchange and the Shenzhen Stock Exchange. The sample period is from April 8^{th} 2005 (the launch date of the CSI 300) to May 13^{th} 2016. The number of observations accounts for 2697 in total. Our data was downloaded from Wind. The daily return is defined as 100 times the first-order difference of the natural logarithm of the price series.

$$r_t = 100 \times (log(P_t) - log(P_{t-1})) \tag{1.1}$$

where P_t is the closing price of the CSI 300.

1.3.2 Rationale for the CSI 300

There are several major Chinese stock market indices often used by academic research. The SSE Composite Index is a capitalization-weighted index, which represents the overall market movement of all A-shares and B-shares listed on SSE. The SZSE Component Index is a capitalization-weighted index, consisting of the 500 top companies listed in SZSE A-shares. The CSI 300 (a.k.a SHZE 300) index is a free-float capitalization-weighted index based on 300 A-shares stocks listed on both SSE and SZSE. There are several SSE size indices, SSE 50, SSE 180, and SSE 380, representing the top 50, 180, 380 companies listed on SSE A-shares by free-float capitalization weight.

Among those market indices, the CSI 300 index is widely accepted as an overall representation for the general movements of the China A-share markets (Yang et al., 2012; Hou & Li, 2014). The index is jointly launched by the SSE and SZSE on April 8^{th} 2005, and complied and published by the China Securities Index Company Ltd. It is comprised of 300 large-capitalization and actively traded in both SSE and SZSE, which covers roughly 70% of total market capitalization of the two stock markets (Yang et al., 2012). More importantly, the first Chinese stock market index futures contract is based on the CSI

TABLE 1.1: Descriptive Statistics

	CSI 300	SSE Composite	SZSE Component	SSE 50	SSE 180	SSE 380
Mean	0.042	0.030	0.039	0.034	0.039	0.067
Std. Err.	1.898	1.785	2.014	1.908	1.900	2.110
Skewness	-0.516	-0.561	-0.488	-0.317	-0.487	-0.799
Kurtosis	6.089	6.655	5.490	6.291	6.216	5.903
Correlation Matrix						
CSI 300	1.000	0.980	0.959	0.962	0.995	0.905
SSE Composite	0.980	1.000	0.931	0.950	0.980	0.897
SZSE Component	0.959	0.931	1.000	0.877	0.932	0.912
SSE 50	0.962	0.950	0.877	1.000	0.982	0.775
SSE 180	0.995	0.980	0.932	0.982	1.000	0.873
SSE 380	0.905	0.897	0.912	0.775	0.873	1.000

300 index, launched on April 16th 2010. Table 1.1 presents the first four moments of the daily returns of the six major stock market indices in China. As can be observed, the moments of all six major market indices are similar and they are highly correlated. All market indices lead to similar results. Hence, we will only use the CSI 300 index for the overall perfomrance representation of the Chinese stock market throughout this thesis.

1.4 Descriptive Statistics

As for the CSI 300, the mean is roughly 0.042 and the standard deviation is 1.898. The third moment, skewness, shows that the daily return is negatively skewed. The fourth moment, kurtosis, is larger than the double of the normality benchmark. This implies that the daily returns of the CSI 300 have the leptokurtosis and the fat tails. The third and fourth moments indicate that the distribution of the daily returns deviates from the normal distribution. The non-Gaussianity can be confirmed by the Kolmogorov-Smirnov test with statistics of 0.953 and a P-value of approximately zero.

In order to inspect non-Gaussianity, we fit a normal distribution to the empirical distribution and compare it to the empirical kernel density in Figure 1.2(a). As it may be observed, the empirical kernel density has the leptokurtosis in the middle and the fat tails at the two sides. The empirical density is highly inconsistent with the fitted normal density. For the purpose of visualising the magnitude of the fat tails, Figure 1.2(b) shows

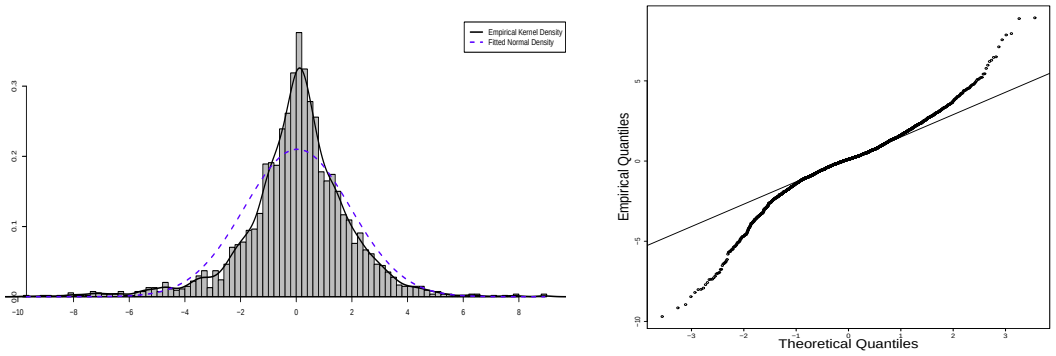

(a) Empirical Kernel Density vs. Fitted Normal Density

(b) QQ Plot

the QQ plot of the empirical distribution to a theoretical normal distribution. While the empirical quantiles fit the normal quantiles in the middle part, they diverge at the two tails. The QQ plot confirms the heavy tail of the daily returns of the CSI 300.

1.5 Distributional and Temporal Properties

1.5.1 Distributional Properties

In order to study the distributional properties, we fit various parametric distributions to our empirical data, the daily returns of the CSI 300. Most parametric distributional types studied in the literature are considered here. Four evaluation tools (log likelihood, AIC, BIC, and the Kolmogorov-Smirnov test) are reported in Table 1.2 for all the fitted parametric distributions.

The normal distribution has the lowest log likelihood, and the highest AIC and BIC, which confirmed the non-Gaussianity shown in Section 1.4. A Student's t-distribution with a degree of freedom 2.145 gives a better fitting than a normal distribution as it can capture the fat-tail to some extent. However, the t-distribution is also rejected by the Kolmogorov-Smirnov Test. The double Weibull, which gave a good fit for S&P 500 (Mittnik & Rachev, 1993), is inferior to the t-distribution for the Chinese stock index returns. A double exponential distribution seems to be the best fitted distribution within the non-mixture distribution category. The Kolmogorov-Smirnov test cannot reject a

double exponential distribution with a P-value of 79.83%. A symmetric hyperbolic distribution is rejected by the Kolmogorov-Smirnov test at the 5% significance level.

If mixture distributions are considered, the Gaussian mixture distribution with two components (Gaussian mixture (2)) is better than the double exponential distribution with a higher log likelihood, lower AIC and BIC, and a Kolmogorov-Smirnov test P-value of 86.20%. With an additional component, a Gaussian mixture distribution with three components (Gaussian mixture (3)) produces a higher log likelihood. It may be argued that the increase in likelihood comes from over-fitting by introducing more parameters. However, the AIC and BIC of Gaussian mixture (3) are lower than those of Gaussian mixture (2). Since the AIC and BIC penalise the additional number of parameters, this suggests that Gaussian mixture (3) is superior to Gaussian mixture (2) for Chinese stock index returns. Furthermore, a Kolmogorov-Smirnov test cannot reject Gaussian mixture (3) at the 5% level.

The study of the fitting of various parametric distributions suggests that Gaussian mixture (3) is a good candidate to capture the distributional properties of Chinese stock index returns, which provides an intuitive foundation for using the three-state HSMM in this paper.

1.5.2 Temporal Properties

"Long-memory"

As can be seen in Figure 1.4(a), the autocorrelation functions are insignificant [1] for most lags with a small number of exceptions. Thus, daily returns are uncorrelated. Figure 1.4(b) and Figure 1.4(c) show that the autocorrelation functions of both squared returns and absolute returns are significant for all lags and decay slowly. This slowly decaying autocorrelation is referred to as the "long-memory" in the literature. Both squared returns and absolute returns are two types of volatility measure. The reason behind the "long-memory" could be volatility clustering, which results from the fact that the

[1] The 95% confidence band for the autocorrelation function is calculated by $\pm 1.96/\sqrt{N}$, where N is the sample size.

TABLE 1.2: Various Parametric Distribution Fittings

Type of Distribution	Fitted Parameters	Log Likelihood	AIC	BIC	Kolmogorov-Smirnov Test (P-value)
Normal	mean sd 0.042 1.897	-5554.054	11112.110	11123.910	0.00%
Student's t	df 2.145	-5396.709	10795.420	10801.320	0.00%
Double Weibull	alpha -0.911	-5446.249	10894.500	10900.400	0.00%
Double Exponential	location scale 0.111 1.332	-5339.219	10682.440	10694.240	79.83%
Symmetric Hyperbolic	location scale 0.101 1.802	-5366.661	10737.320	10749.120	4.70%
Gaussian Mixture (2)	Component 1 mean sd weight -0.232 2.861 33.86% Component 2 mean sd weight 0.182 1.093 66.14%	-5350.699	10713.400	10748.800	86.20%
Gaussian Mixture (3)	Component 1 mean sd weight -0.704 3.194 20.01% Component 2 mean sd weight 0.029 0.610 23.90% Component 3 mean sd weight 0.313 1.532 56.08%	-5328.992	10675.980	10729.080	12.20%

Note: *We use a one-parameter double Weibull distribution* $F(x) = exp(-(-x)^{-\alpha})\mathbf{1}_{x\leqslant 0} + \mathbf{1}_{x>0}$ *the same as Cont (2001).*

volatility of the past returns will affect the volatility of future returns for a considerably long period of time.

The temporal property of "long-memory" implies that there is some time dependence for the squared/absolute returns. This time dependence is very persistent for the volatility of returns. The GARCH-family models and the stochastic volatility models are usually used to capture volatility clustering. A Markov chain or semi-Markov chain is also capable of modelling volatility clustering in a discrete way. The advantage of a Markov chain or semi-Markov chain is that they can be associated with various distributions. Hence, the study of temporal properties gives us another incentive to use our three-state HSMM.

Taylor Effect

Taylor (1986) found that the autocorrelations of the power of absolute returns are the highest when the power coefficient is one. In a mathematical definition, this is represented as:

$$corr\left(|r_t|, |r_{t+k}|\right) > corr\left(|r_t|^{\theta}, |r_{t+k}|^{\theta}\right) \qquad for \quad any \quad \theta \neq 1 \tag{1.2}$$

Figure 1.2 illustrates the Taylor effect for the daily returns of the CSI 300. One horizontal dimension is the lag number and the other is the power coefficient θ. The vertical dimension is the autocorrelation function values. The surface has the highest value in the middle where $\theta = 1$ for all lags. The surface is declining when θ deviates from 1 and reaches its lowest values at the sides of the space. $|r_t|^{\theta}$ is a volatility measure with different scales. The Taylor effect implies that the volatility measured by $|r_t|$ has the strongest time dependence.

FIGURE 1.3: ACF of Original Returns, Squared Returns, and Absolute Returns

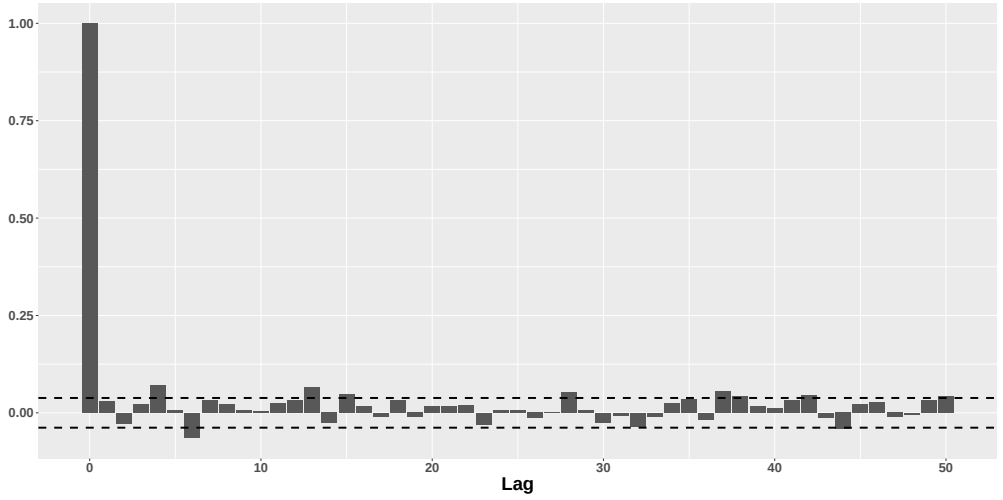

(a) ACF of Original Returns

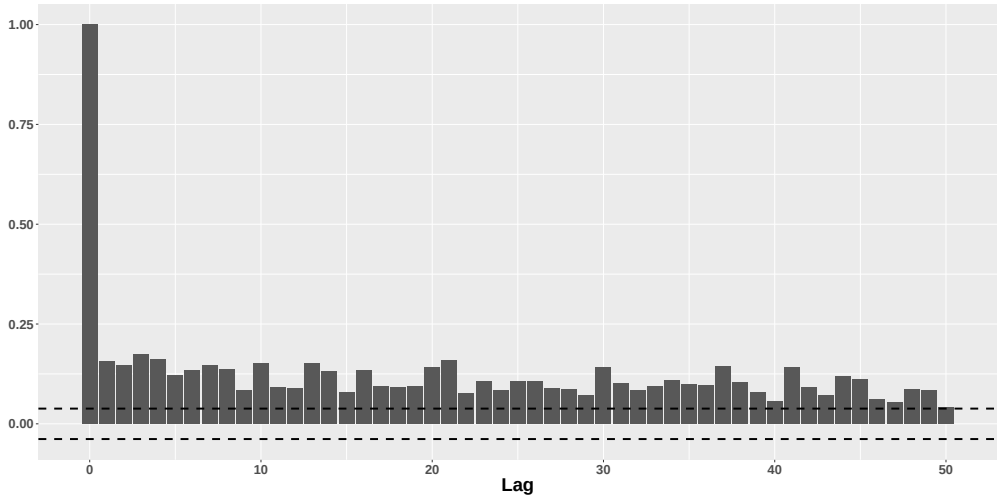

(b) ACF of Squared Returns

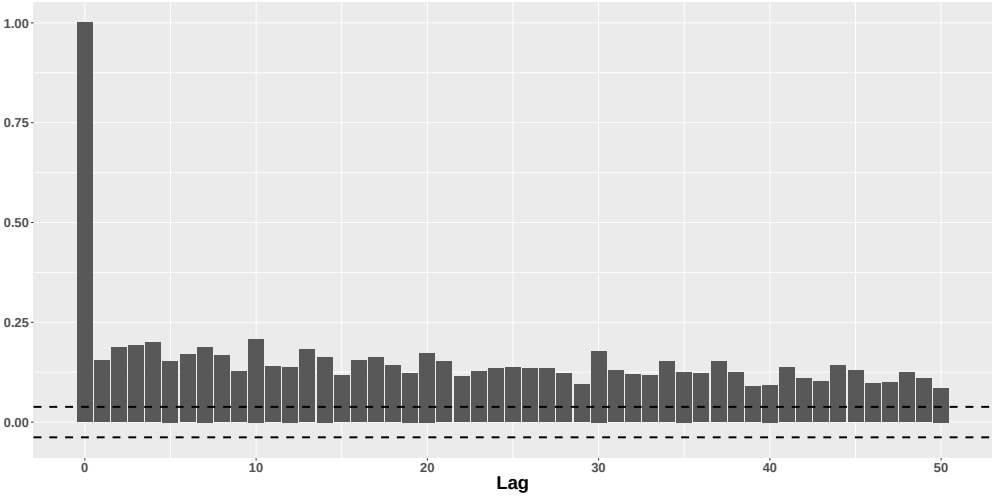

(c) ACF of Absolute Returns

FIGURE 1.2: Taylor Effect

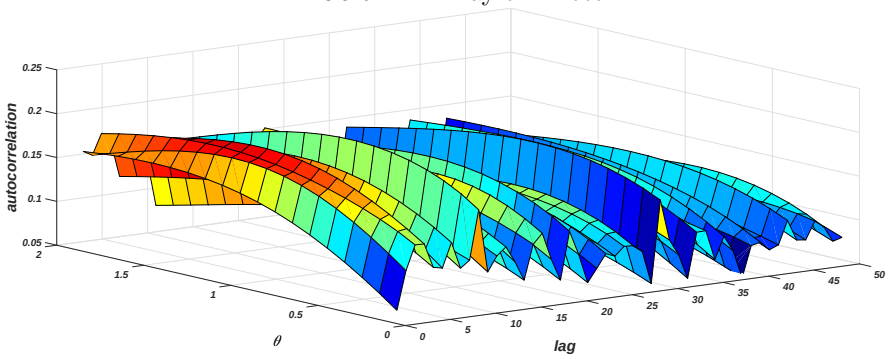

In summary, the combination of a Gaussian mixture model and the "long-memory" time dependence can correspond to HMM/HSMM where the distributional dimension is a Gaussian mixture distribution and the time dependence is captured by a hidden Markov chain/hidden semi-Markov chain. The distributional properties and the temporal properties of our empirical data provide the intuitive support to adopt the HMM/HSMM for Chinese stock index returns. The HSMM is finally chosen because it is a generalisation of the HMM and Rydén et al. (1998) found that the HMM could not reproduce the stylized fact of the "long-memory".

1.6 Methodology

1.6.1 Hidden Semi-Markov Model

One limitation of the HMM is that its sojourn time [2] has to follow a geometric distribution (Yu, 2010; Bulla & Bulla, 2006). The HSMM generalises the HSMM by allowing the sojourn time distribution to follow other distributions. In other words, the sojourn time d of a given state is explicitly specified for the HSMM. Similarly to the HMM, the HSMM also entails two processes, an unobservable state process $\boldsymbol{S}_1^T = \boldsymbol{s}_1^T$ and an observation process $\boldsymbol{X}_1^T = \boldsymbol{x}_1^T$, where $\boldsymbol{s}_1^T$ is the notation for the realised states $s_1, s_2, ..., s_T$ and $\boldsymbol{x}_1^T$ is the notation for observations $x_1, x_2, ..., x_T$. The hidden state process $\boldsymbol{S}_1^T$ is

[2]The sojourn time is also known as the dwell time, occupancy time, or duration time.

an unobservable semi-Markov chain with m states. The observation process $\boldsymbol{X}_1^T$ is associated with the hidden state process through component distributions [3]. Equation 1.3 shows the component distribution for state i at time t.

$$\mathbb{P}_i(x_t) = \mathbb{P}(x_t|s_t = i) \quad \text{where} \quad i \in \{1, 2, ..., m\} \tag{1.3}$$

Equation 1.4 defines the state transition probability from state i to state j.

$$\gamma_{ij} = \mathbb{P}(s_{t+1} = j|s_t = i) \quad \text{where} \quad i \neq j, \quad i, j \in \{1, 2, ..., m\} \tag{1.4}$$

Unlike the HMM, the transition probability from one state to the same state in the HSMM is zero, i.e. $\gamma_{ij} = 0$. The sojourn time in the HSMM is controlled by the sojourn time distribution defined in Equation 1.5.

$$d_i(u) = \mathbb{P}(s_{t+u+1} \neq i, \boldsymbol{s}_{t+1}^{t+u} = i|s_{t+1} = i, s_t \neq i) \tag{1.5}$$

where the variable u is the length of the sojourn time which can follow nonparametric or parametric distributions. The sojourn time distribution for each state i can follow different types of distribution or the same type of distribution but with different values of the parameters.

The transition probability matrix (TPM) has entries for the transition probabilities γ_{ij} at row i and column j. The diagonal elements in the TPM of the HSMM are zeros.

$$\boldsymbol{\Gamma} = \begin{pmatrix} 0 & \gamma_{12} & \cdots & \gamma_{1m} \\ \gamma_{21} & 0 & \cdots & \gamma_{2m} \\ \vdots & \vdots & \ddots & \vdots \\ \gamma_{m1} & \gamma_{m2} & \cdots & 0 \end{pmatrix} \tag{1.6}$$

We estimate the model using the EM algorithm (see 1.A). The most likely sequence of the states is globally decoded by the Viterbi algorithm (see 1.B.1). Additionally, we use local decoding to compute the conditional probabilities for each state at time t given the

[3] The component distribution is also known as emission distribution, conditional distribution, or marginal distribution.

observation (see 1.B.2). Our implementation is based on the R package 'hsmm' (Bulla & Bulla, 2013).

The number of states in our HSMM is set to three. The Gaussian mixture (3) gives a better fit than Gaussian mixture (2) based on the likelihood and the information criteria. The normal distribution is chosen to be the component distribution for our HSMM. Other distributions could be considered, but the empirical results of the Chinese stock index returns show that the HSMM with normal components is sufficient to explain our data. Moreover, it is convenient to conduct various tests on a normal distribution, like the z-test in order to examine the significance of the mean. Additionally, the normal component distribution enables us to give a straightforward interpretation for the HSMM.

As for the sojourn time distribution, the logarithmic distribution is selected because it can produce stable estimation results while the EM algorithm may not converge under many other sojourn time distributions. The logarithmic distribution has only one parameter and can avoid overfitting by introducing more parameters. The negative Binomial distribution used by Bulla & Bulla (2006) is also a suitable candidate but it produces similar results as the logarithmic distribution. Other sojourn time distributions could be used, but the logarithmic distribution is sufficient for our data.

1.6.2 Definition of Market Conditions

It is inevitable to propose our own definition of market conditions for three reasons. Firstly, there is no generally accepted definition of the market conditions. Secondly, most definitions of the market conditions are based on the monthly data. Lastly and mostly importantly, the current definition are mainly for two-category classification, i.e. the bull or bear market (or up or down market). The only three-category classification is the SUD in Fabozzi & Francis (1977), but their threshold of substantial move was arbitrarily defined. We define the bear, sidewalk, and bull market conditions from the perspective of the distributional features.

Definition 1.1. A Bear Market

- The mean of the distribution of the daily returns conditional on a bear market is significantly less than 0.
- The frequency of the positive returns is expected to be larger than that of the negative returns.
- Because of the above statistical properties, the price in a bear market is generally decreasing.

Definition 1.2. A Sidewalk Market

- The mean of the distribution of the daily returns conditional on a sidewalk market should be insignificantly different from 0.
- It is expected to observe a roughly equal number of positive and negative returns.
- Because of the above statistical properties, the price in a sidewalk market stays in a band and shows a mean-reversion pattern.

Definition 1.3. A Bull Market

- The mean of the distribution of the daily returns conditional on a bull market should be significantly larger than 0.
- The frequency of the positive returns is expected to be larger than that of the negative returns.
- Because of the above statistical properties, the price in a bull market is generally increasing.

In straight-forward notation, the mean in each market is as follows:

$$\mu(S_t) = \mu_1 < 0, \text{ if } S_t = 1 \text{ (bear market)}$$

$$\mu(S_t) = \mu_2 \approx 0, \text{ if } S_t = 2 \text{ (sidewalk market)}$$

$$\mu(S_t) = \mu_3 < 0, \text{ if } S_t = 3 \text{ (bull market)}$$

The variance of each market can be denoted as

$$\sigma^2(S_t) = \sigma_1^2, \text{ if } S_t = 1 \text{ (bear market)}$$
$$\sigma^2(S_t) = \sigma_2^2, \text{ if } S_t = 2 \text{ (sidewalk market)}$$
$$\sigma^2(S_t) = \sigma_3^2, \text{ if } S_t = 3 \text{ (bull market)}$$

where we expect that the bear market should have highest variance (i.e. $\sigma_1^2 > \sigma_2^2$, and $\sigma_1^2 > \sigma_3^2$) because it is normally the most volatile market.

1.7 Empirical Results

1.7.1 Estimation Results

Through the EM algorithm, the parameters of the HSMM are estimated, including the parameters of the component distributions, transition probability matrix, and sojourn time distribution. Table 1.3 presents the estimated parameters of the component distributions. Based on the estimated mean and standard deviation, it is able to compute one-sample z-statistics in order to test the significance of the mean. The formula to compute the z-statistics is as follows.

$$z_i = \frac{\bar{x}_i}{\sigma_i/\sqrt{n_i}} \quad for \quad i \in \{1, 2, 3\} \tag{1.7}$$

where $\bar{x}_i$ is the mean of state i, σ_i is the standard deviation of state i, and n_i is the sample size of state i. The one-sample z-test suggests that the mean of state 1 is significantly below 0 at the 1% significance level; the mean of state 3 is significantly above 0 at the 1% significance level; whilst the mean of state 2 is insignificant from 0.

The results indicate that the time-varying distribution of the returns depends on the hidden states, which can be interpreted as the market conditions. Specifically, state 1 corresponds to the bear market, state 2 corresponds to the sidewalk market, and state 3 corresponds to the bull market.

TABLE 1.3: Component Distribution Parameters

	State 1	**State 2**	**State 3**
Mean	-0.510	-0.020	0.622
Std. Dev.	3.113	1.156	1.440
Sample Size	572	1430	695
z-statistics	3.918***	-0.654	11.387***

Note: *p<0.1; **p<0.05; ***p<0.01

Table 1.4 presents the empirical frequency of the positive and negative returns for the fitted component distributions and confirms our interpretation of the three underlying states of the HSMM. As can be seen, the frequency of the positive return of state 3 is 67.19%, while the frequency of the negative return is 32.81%. There are negative returns in the bull market as well, but positive returns are more frequent. This statistical evidence empowers the price in the bull market to increase. Hence, state 3 can be regarded as a bull market according to its statistical features. Using the same logic, state 1 has a significant negative mean and corresponds to the bear market where the price shows a downward trend because the negative returns (52.97%) occur more often than the positive returns (47.03%). As for state 2, the frequency of the positive and negative returns is nearly the same at around 50%. State 2 corresponds to the sidewalk market where the price displays a mean-reversion pattern.

TABLE 1.4: Frequency of Positive and Negative Returns

	State 1	**State 2**	**State 3**
Positive Return Freq.	47.03%	50.49%	67.19%
Negative Return Freq.	52.97%	49.51%	32.81%

Based on the estimated parameters in the component distribution, Figure 1.4 displays the histogram of the daily returns of the CSI 300, the empirical density, and three fitted component distribution densities. By separating the empirical distribution into three component distributions, the HSMM is able to explain the leptokurtosis and fat tail effects. The over-peak in the middle part of the empirical distribution mainly results from the sidewalk market, whereas the bear market plays a vital role in the fat tails. The standard deviation of the bear market is 3.113, which is much higher than for the

other two markets. Hence, the bear market is the most volatile market, followed by the bull market. Conversely, the sidewalk market is the most stable market.

FIGURE 1.4: Empirical and Component Density

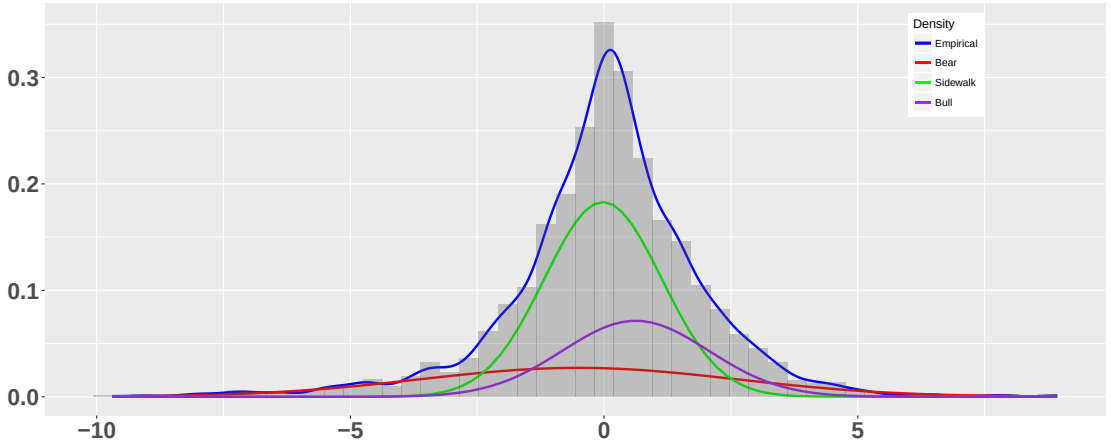

The existing literature often ignores the analysis of the mean of component distribution. However, the component mean is important for price behaviour. Although the mean of state 3 (0.622) is very small, it is still significantly larger than zero. This small but significant positive mean ensures that positive returns occur more frequently than the negative returns, which is the key feature of the bull market. The same logic can be applied to state 1. The insignificant mean of state 2 ensures that its distribution is almost symmetrical around 0 and the frequency of positive returns and negative returns is nearly the same.

Table 1.5 presents the number of days, the number of times, and average sojourn time for different market conditions. Our results show that the bull market has a slightly longer sojourn time than the bear market. Additionally, the average sojourn time for the sidewalk market is the longest with 204.29 days, which is much longer than in the case the other two types of markets.

TABLE 1.5: Sojourn Information

	State 1 (Bear)	**State 2 (Sidewalk)**	**State 3 (Bull)**
Number of Days	572	1430	695
Number of Times	22	7	25
Average Sojourn	26.00	204.29	27.80

Table 1.6 gives the estimated transition probability matrix (TPM) of the HSMM for the CSI 300 returns. The sojourn time of the HSMM is controlled by the sojourn time distribution rather than by the diagonal entries in the TPM. Hence, the diagonal entries are all zeros for the HSMM. There are a few interesting economic implications that can be drawn from the TPM.

TABLE 1.6: Transition Probability Matrix

From\ To	**State 1 (Bear)**	**State 2 (Sidewalk)**	**State 3 (Bull)**
State 1 (Bear)	0	0.02%	99.98%
State 2 (Sidewalk)	49.56%	0	50.44%
State 3 (Bull)	74.08%	25.92%	0

- After a bear market, it is highly likely (99.98%) that a bull market will follow. This situation often occurs at the end of a crisis when the market starts to recover.
- A bear market and a bull market have equal possibility (around 50%) to occur after a sidewalk market. In other words, it is unclear whether a bull or bear market will follow after the price fluctuates within a certain range for a long period.
- At the end of a bull market, the market has a high probability (74.08%) to be bear and a low probability (25.92%) to be sidewalk. These circumstances usually ensue after a bubble burst, such as the financial crisis in 2008.

1.7.2 Decoding Results

The global decoding is conducted by the Viterbi algorithm. Figure 1.5 shows the global decoding states with reference to the CSI 300 original series, while Figure 1.6 is correlated with the daily returns of the CSI 300. The purple background represents the bull market, the red background denotes the bear market, and the green background stands for the sidewalk market. We review the evolution of the transition between the different market conditions for the Chinese stock market in our sample period.

- At the beginning of our sample period (April 8^{th} 2005), the Chinese stock market was in a sidewalk market and lasted for about one year until April 27^{th} 2006.

After a short period of bull (April 28th 2006 to July 14th 2006), the market became sidewalk again and lasted for approximately 4 months (July 17th 2006 to November 13th 2006).

- At the end of 2006, the CSI 300 started to climb and reached its historically high peak at 5877.20 on October 10th 2007. One possible reason of the boom in 2007 is the split-share structure reform, which aimed to convert all non-tradable shares to tradable shares. The implementation of the reform took about roughly two years from 2005 to 2007. Due to the conversion from non-tradable shares to tradable shares, the reform had provided substantial liquidity to the market, and it is highly likely to be one of reason for the very promising market during that period.

- Interestingly, it is common to believe that the year 2007 is a "pure" bull market, but our decoding results show that this period was not purely bull, but was in fact mixed with some periods of the bear market. The mixture of the bull and bear market can be explained by the disposition effect in the behavioural finance, which is the phenomena that investors tend to sell assets that have gained profit and hold assets that have lost value. In other words, investors used to cash in to achieve capital gain following increase in stock prices and this will lead to price reversals.

- After the financial crisis (March 12th 2007), the market went into a "pure" bear market and the CSI 300 dropped from its peak to the bottom of 1627.76 on November 4th 2008, which is the largest drop in the history of the Chinese stock market. After the market collapsed, it started to be bull and recover.

- Afterwards, the Chinese stock market experienced some periods of bear, sidewalk, and bull alternatively. It went into a remarkably long period of sidewalk from November 19th 2011 to November 20th 2014. During that period, the CSI 300 stayed in the range of 2000 to 3500 and displayed a mean-reversion pattern.

- From December 11th 2014, the Chinese stock market became bull and rocketed from 3183.01 to 5335.12 on June 12th 2015, which represented an astonishing increase of 67.61%. From the technical analysis perspective, there was a breakout

through the resistance line at the end of 2014, after several years of sidewalk market. From the fundamental analysis perspective, one of the reason for this boom was the substantial liquidity provided from the other source financing. After this bull market, the Chinese stock market abruptly transited into a bear market. The CSI 300 shrank to 3025.70 on August 26^{th} 2015, which was a dramatic 43.29% decrease. The reason of this dramatical drop in the market was highly likely to be related to the regulations and restrictions on other source financing imposed by CRSC in July 2015. The detail of the other source financing will be discussed in Chapter 2.

- From September 18^{th} 2015 to December 25^{th} 2015, the Chinese stock market was a bull market over the course of three months. Afterwards, a short bear market and a short bull market occurred, followed by a sidewalk market.

The local decoding (Figure 1.7) offers a more detailed probability of each state along with time in the sample period. The local decoding results confirm our understanding on the transition of the market conditions of the Chinese stock market. Before 2007, state 2 remained at a high level of probability. During 2007 and 2008, state 1 and state 3 alternatively reached high probabilities. After the financial crisis, state 1 remained at a high probability for about one year, while the other two remained low. From 2011 to 2014, the probability of state 2 was almost 100% with a few exceptions. After 2015, the probability of state 3 reached a relatively high level again and was followed by a comparatively high level of state 1. State 2 has had the highest probability recently. The local decoding results are consistent with the global decoding results.

FIGURE 1.5: CSI 300 and Market Conditions (Global Decoding)

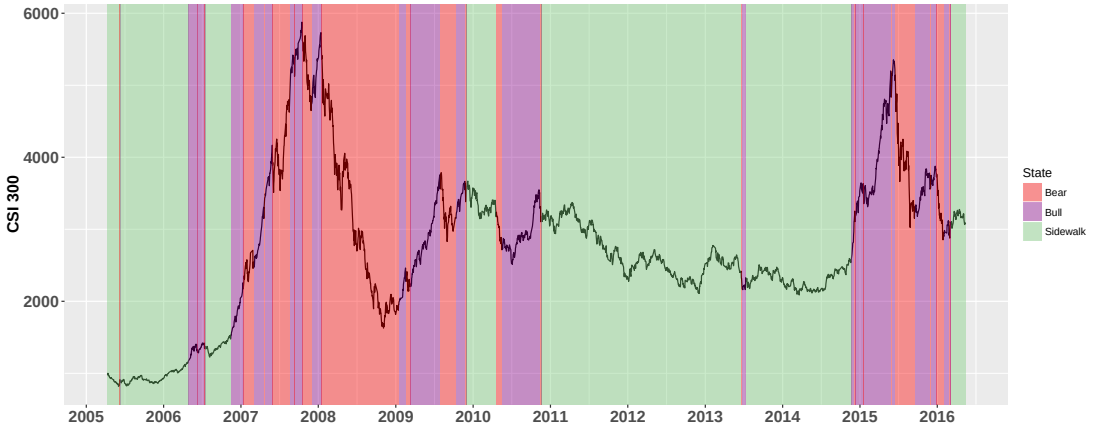

FIGURE 1.6: Daily Returns of CSI300 and Market Conditions (Global Decoding)

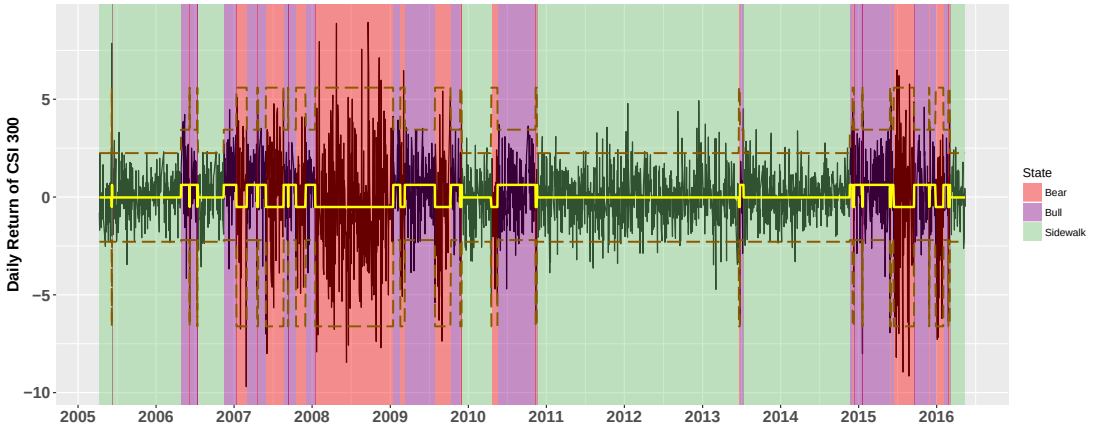

FIGURE 1.7: Local Decoding

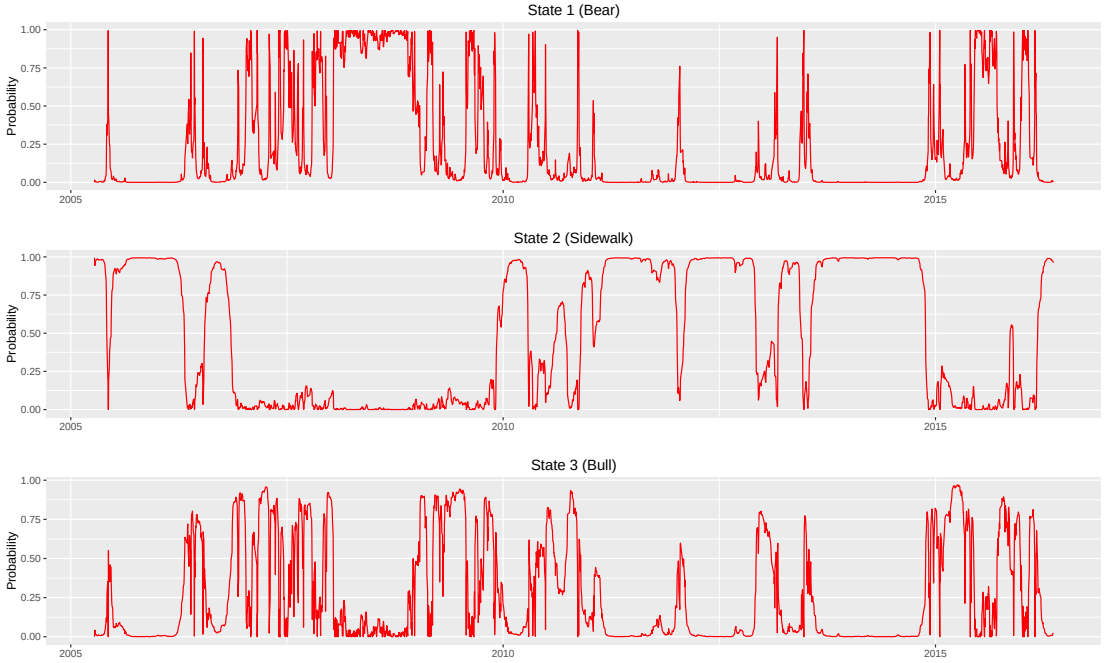

1.8 Model Evaluation and Comparison

In this section, we compare the empirical performance of our three-state HSMM with a stochastic volatility (SV) model and a tGARCH(1,1) model in terms of three stylized facts, namely the fat tails, the "long-memory", and the Taylor effect.

It is worthwhile to mention the advantages and disadvantages of the HSMM and the other alternative models. Although GARCH models are now widely used and simple to estimate, there are three main disadvantages of these models pointed out by Nelson (1991). Firstly, GARCH models rule out the possible situation of the negative correlation between current returns and future returns volatility. Secondly, The parameter restrictions of GARCH models can often be violated by empirical data. Thirdly, it is difficult in GARCH models to interpret whether the shocks to conditional variance is persist or not. As for our choice of the specific GARCH model, Hansen & Lunde (2005) find no evidence that the GARCH(1,1) is inferior to other sophisticated ARCH-family models by using DM-$exchange rate and daily IBM returns data. Additionally, the only complication of tGARCH(1,1) from GARCH(1,1) is that the conditional distribution is set to be the Student's t-distribution in order to capture the fat-tail.

Allowing the volatility to be an unobserved continuous-time random process, SV models overcome the disadvantages of GARCH models and fit more naturally to the modern finance theories (Platanioti et al., 2005). Taylor (1994) show that SV models have simple continuous-time analogues for option pricing. Yu (2002) show that the SV model is superior to the GARCH models according to three different asymmetric loss functions and Root Mean Square Error for the forecasting of the volatility of the New Zealand market index. Although the evidence of superiority of SV models over GARCH models, their empirical application has been limited because it is difficult to estimate the parameters for SV model because the likelihood functions is hard to evaluate (Broto & Ruiz, 2004).

The most prominent advantage of the HSMM is that we can systemically find the hidden states and infer the most likely sequence of the the hidden states. The main limitation of the HSMM is that the empirical results can be largely changed by the model setting, such as the number of states, the component distribution, and the sojourn time

distribution. Finding the appropriate model settings can involve many times of trial and error. Additionally, using the Viterbi algorithm to conduct the global decoding is a computational expensive procedure. To the best of our knowledge, there is no study on the empirical performance comparison between SV models and HSMM.

Our comparison focuses on the aspects of reproducing stylized facts of asset returns. The economic significance of the three stylized facts is as follows. Fat tails are related to the Value-at-Risk, which plays a vital important role in financial risk management. If the model cannot capture the correct left tail risk, the Value-at-Risk could be underestimated. In this circumstance, the investors may encounter an extra loss they do not expect. It is found that the return itself is not autocorrelated but that the squared return and the absolute return are autocorrelated and their ACF are slowly decaying. Note that the squared return and the absolute return are both volatility measures. Hence, the stylized fact of the "long-memory" is associated with volatility clustering, i.e. a large volatility tends to be followed by a large volatility and a small volatility tends to be followed by a small volatility. A good model should capture the persistence of the volatility in asset returns. The Taylor effect is a famous statistical observation. Taylor (1986) has initially found that the absolute return with power one has the highest autocorrelation. The following literatures treat the reproduction of the Taylor effect as an important benchmark (e.g. Rydén et al., 1998; Bulla & Bulla, 2006; Rogers & Zhang, 2011). If the model fails to reproduce the Taylor effect, then the data generation process in the model could not fully represent the empirical asset return.

Additionally, we also compare our model with a two-state HSMM, a three-state HMM, and a two-state HMM with respect to log likelihood, AIC, and BIC. This is for the model selection purpose and confirms our choice of a three-state HSMM.

1.8.1 Comparison with Other Volatility Models

Following Jacquier et al. (1994) and Kim et al. (1998), the stochastic volatility model is specified as

$$y_t = e^{h_t/2}\varepsilon_t \tag{1.8}$$

$$h_t = \mu + \phi(h_{t-1} - \mu) + \sigma\eta_t \tag{1.9}$$

where y_t is the demeaned log return, h_t is the latent time-varying log volatility process, μ is the mean level of the log volatility, ϕ is the persistence coefficient for the volatility process, σ is the volatility of the log volatility, and ε_t and η_t are uncorrelated standard normal white noise shocks.

We use the MCMC method developed by Kastner & Frühwirth-Schnatter (2014) to estimate the stochastic volatility model. As for the mean level $\mu \in \mathbb{R}$, we choose the usual normal prior $\mu \sim \mathcal{N}(\log(var(y_t)), 1)$. The persistence parameter $\phi \in (-1, 1)$ is equipped with the Beta prior $(\phi + 1)/2 \sim \mathcal{B}(20, 1)$. In terms of the volatility of the log volatility $\sigma \in \mathbb{R}^+$, we choose $\sigma^2 \in 0.1 \times \chi_1^2$. For the MCMC setting, the thinning parameter is set to be 10, the burn-in parameter is 5000, and the number of draw is 55000. Table 1.7 presents the posterior draws of the parameters. The posterior mean is employed for the point estimation of the parameters.

The second benchmark model we consider is the tGARCH(1,1), which has the form

$$r_t = \mu + \sigma_t\varepsilon_t, \qquad \varepsilon_t \sim t(\nu) \tag{1.10}$$

$$\sigma_t^2 = \omega + \alpha_1 y_{t-1}^2 + \beta_1\sigma_{t-1}^2 \tag{1.11}$$

where $\omega > 0$, $\alpha_1 > 0$, $\beta_1 > 0$, and $\alpha_1 + \beta_1 < 1$. r_t is the log return calculated in Equation 2.1. The conditional distribution is set to be the Student's t-distribution with the degree of freedom ν. We use the quasi-maximum likelihood method (Bollerslev & Wooldridge, 1992) to estimate the tGARCH(1,1) model, and the estimation results are reported in Table 1.8.

TABLE 1.7: Estimation for the SV Model

	Mean	**Std. Error**	**5%**	**50%**	**95%**
μ	0.933	0.198	0.622	0.932	1.255
ϕ	0.985	0.005	0.976	0.985	0.992
σ	0.141	0.017	0.115	0.140	0.171
$e^{\mu/2}$	1.602	0.160	1.365	1.594	1.873
σ^2	0.020	0.005	0.013	0.019	0.029

TABLE 1.8: Estimation for the tGARCH(1,1)

	Estimate	**Std. Error**	**t-stat**	**P-value**
μ	0.083	0.027	3.043	0.002
ω	0.026	0.010	2.719	0.007
α_1	0.056	0.009	6.368	0.000
β_1	0.939	0.009	102.187	0.000
ν	5.280	0.567	9.318	0.000

Fat Tail Reduction

Figure 1.8 shows the QQ plots of the log returns in the overall sample and three market conditions with respect to the theoretical normal distribution. The overall sample has tremendously fat tails since the QQ line deviates heavily from the diagonal line. After the separation of the whole sample into 3 states by our HSMM, the bear market and the bull market have close to normal distributions with slight tails, while the sidewalk market has modest tails. The QQ plots suggest that the distributions of the three market conditions are close to normal distributions. The reduction of fat tails can be confirmed by the kurtosis. The kurtosis of log returns is 6.089 in the overall sample, 3.002 in State 1 (Bear), 3.865 in State 2 (Sidewalk), and 3.283 in State 3 (Bull). The kurtosis of the three market conditions is close to 3. Hence, the assumption of the normal component distribution is suitable for our data. This confirms that the distributional property of the Chinese stock market returns could be a mixture of Gaussian distributions.

Figure 1.9 depicts the standardized residuals from three models and their QQ plot with respect to the theoretical normal distribution. The standardized residual of HSMM is defined as $(r_t - \bar{x}_i)/\sigma_i, i = 1, 2, 3$, the standardized residual of the SV model is ε_t in Equation 1.8, and the standardized residual of tGARCH is ε_t in Equation 1.10. Both the HSMM and the SV model can significantly reduce the fat tail, while the

FIGURE 1.8: QQ Plots of the Log Returns

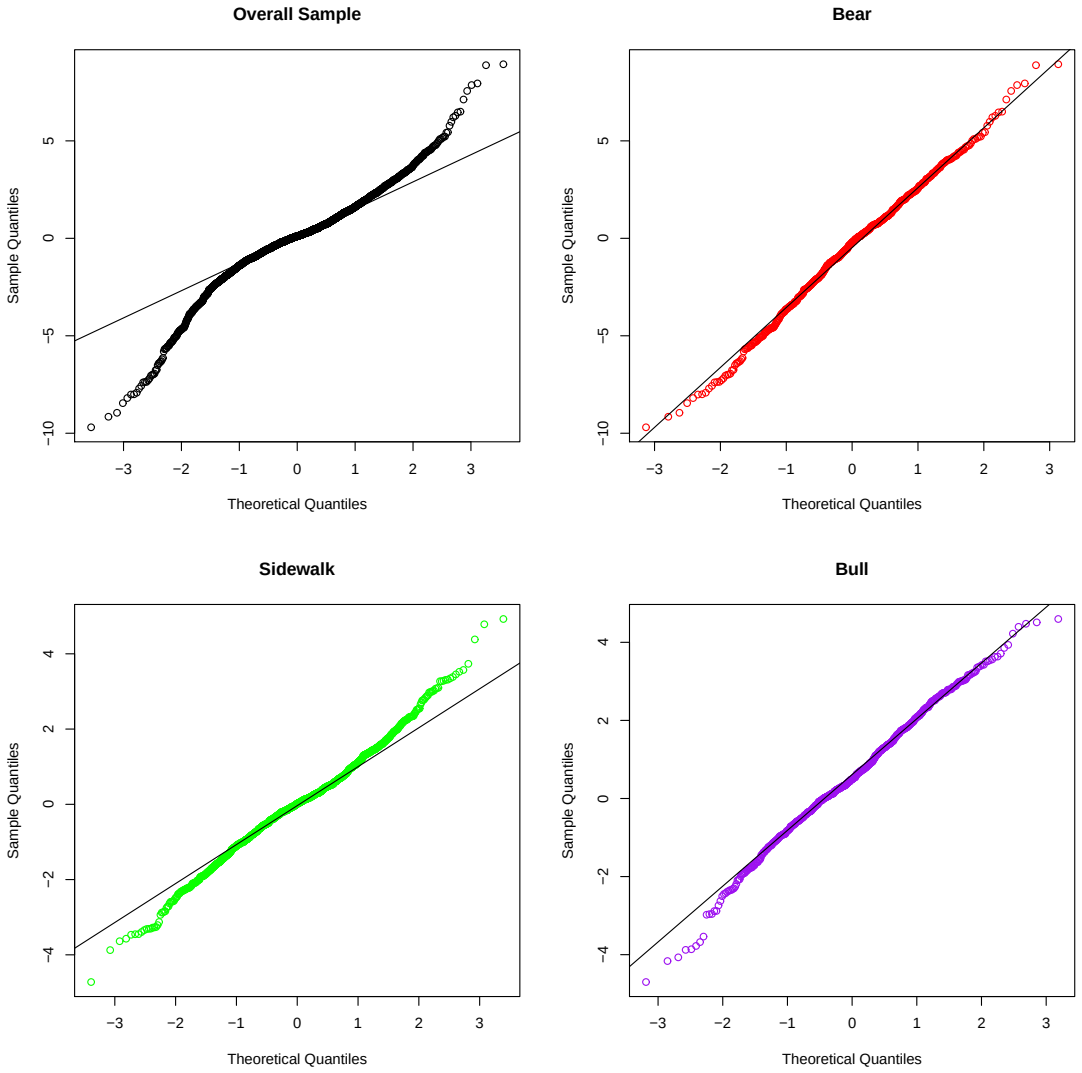

GARCH(1,1) still presents fat tails in its standardized residuals. The right tail of the standardized residuals in the SV model is slightly smaller than that in the HSMM. We further compare the kurtosis of the standardized residuals in the three models. The kurtosis of the standardized residuals is 3.560 in the HSMM, 3.285 in the SV model, and 4.678 in the tGARCH. In terms of fat tail reduction, the HSMM slightly underperforms the SV model, but they both outperform the tGARCH.

FIGURE 1.9: Standardized Residuals and their QQ Plots

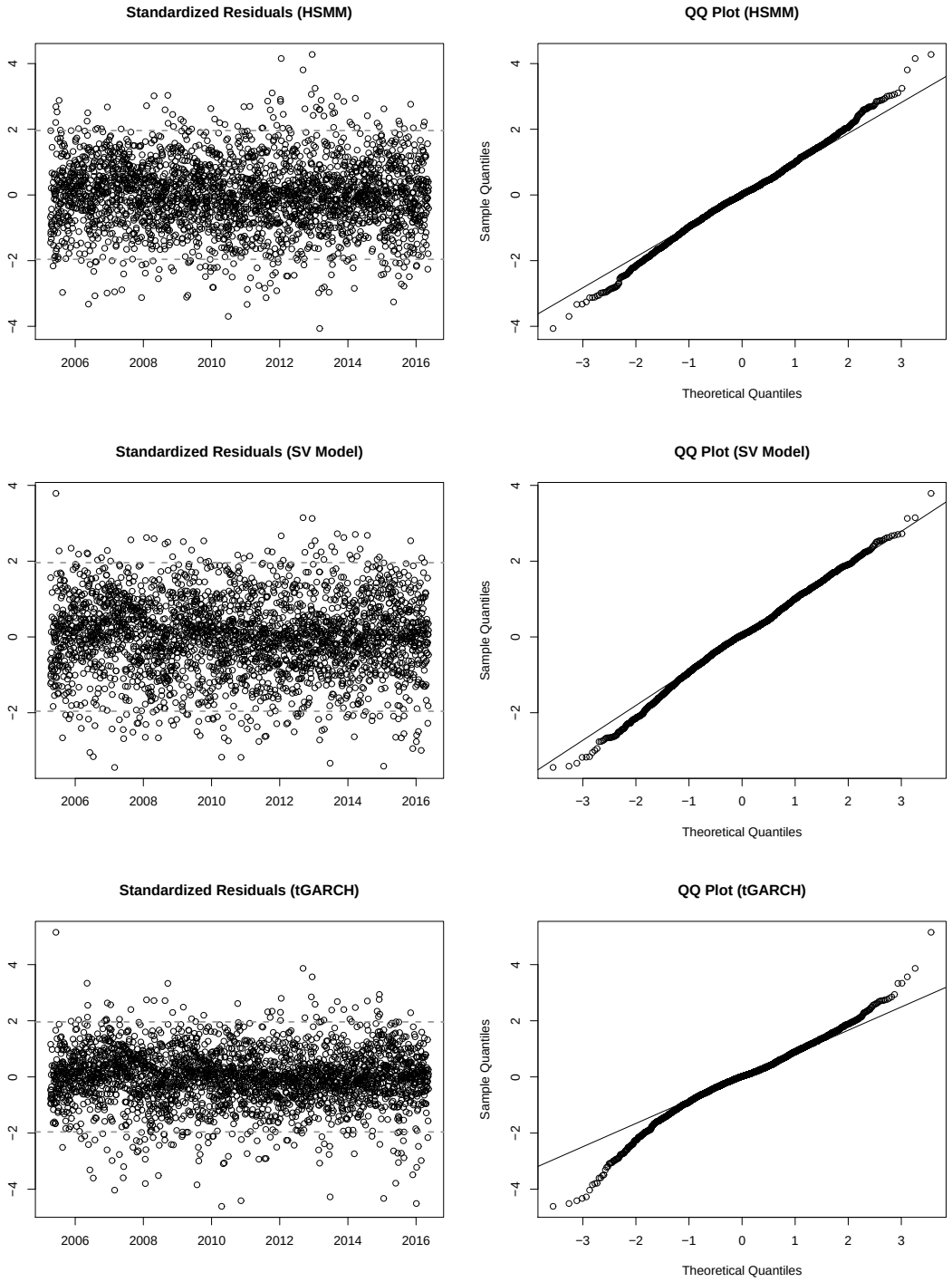

"Long-memory"

Rydén et al. (1998) could not reproduce the slow decay of the ACF of the squared or absolute returns by the HMM. It is interesting to examine the "long-memory" property of our model and two benchmark models. We simulate data from those three models based on the estimated parameters from our empirical CSI 300 log return data. The number of the Monte Carlo simulation accounts for 5000 repetitions. Figure 1.10 shows the empirical ACF and the model ACF for squared and absolute returns. The grey bars represent the empirical ACF while the red line is the model ACF.

Generally, all three models can reproduce the "long-memory" property because they all have slow decaying ACF. There are some differences between the ACF of the three models. Firstly, the model ACF of the HSMM is close to the empirical ACF before Lag 10, but it is slightly underestimated for large lags. Secondly, tGARCH has best fitting for the empirical ACF of the squared return, while the model ACF of the HSMM is underestimated and that of the SV model is overestimated. Thirdly, the SV model gives the best fitting for the empirical ACF of the absolute return, while the model ACF of the HSMM is still underestimated and that of the tGARCH is overestimated.

Our simulation results of the tGARCH are consistent with Ding et al. (1993). Their Monte Carlo simulation study also shows that ARCH type models can facilitate the "long-memory" property for both squared returns and absolute returns. Ding & Granger (1996) also derived the theoretical ACF for various GARCH(1,1) models and found them to be exponential decreasing.

Taylor Effect

The autocorrelation functions of different power values θ (i.e. $corr\left(|r_t|^{\theta}, |r_{t-k}|^{\theta}\right)$) for the three models are also simulated by the same Monte Carlo procedure with 5000 repetitions. Figure 1.11 displays the Taylor effect of all three models. The surface of the simulated Taylor effect is much smoother than that of the empirical Taylor effect in Figure 1.2.

FIGURE 1.10: Empirical ACF and Model ACF

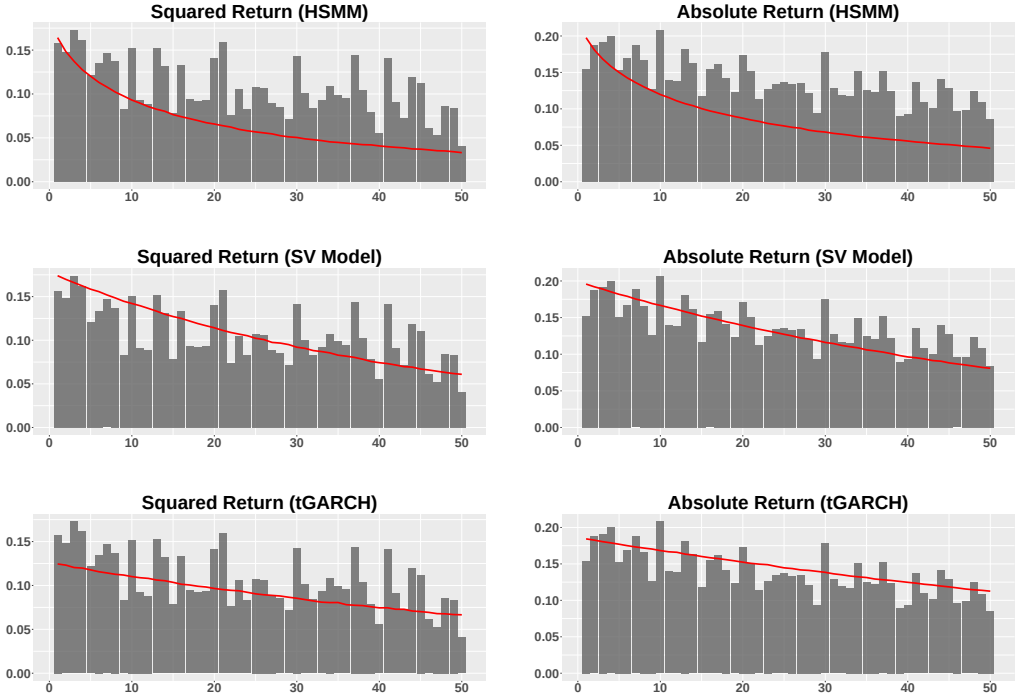

Generally, all three models can reproduce the stylized fact of the Taylor effect, i.e. the autocorrelation function with power value $\theta = 1$ is the highest among the other power values. As can be seen in the 3-D plot, the surface decreases slowly when θ deviates from 1 and reaches the lowest values at two sides. Nevertheless, the shape of autocorrelation functions surface is different for the three models. The surface of the HSMM has a more evident curvature before Lag 10 and becomes much flatter with larger lags. The surface of the SV model and the tGARCH has a consistent curvature in terms of the lag numbers. The tGARCH has a more blended surface than the SV model.

1.8.2 Comparison with the Hidden Markov Models

Our three-state HSMM is compared with the two-state HSMM used by Bulla & Bulla (2006), the three-state HMM adopted by Rydén et al. (1998), and the two-state HMM employed by Rydén et al. (1998) in terms of log likelihood, AIC, and BIC. Table 1.9 summarises the performance of all of the models for the return data of the CSI 300. Our three-state HSMM has the highest log likelihood among the other models. This indicates that our model fits the empirical return of the CSI 300 better than the other

FIGURE 1.11: Taylor Effect from Simulation

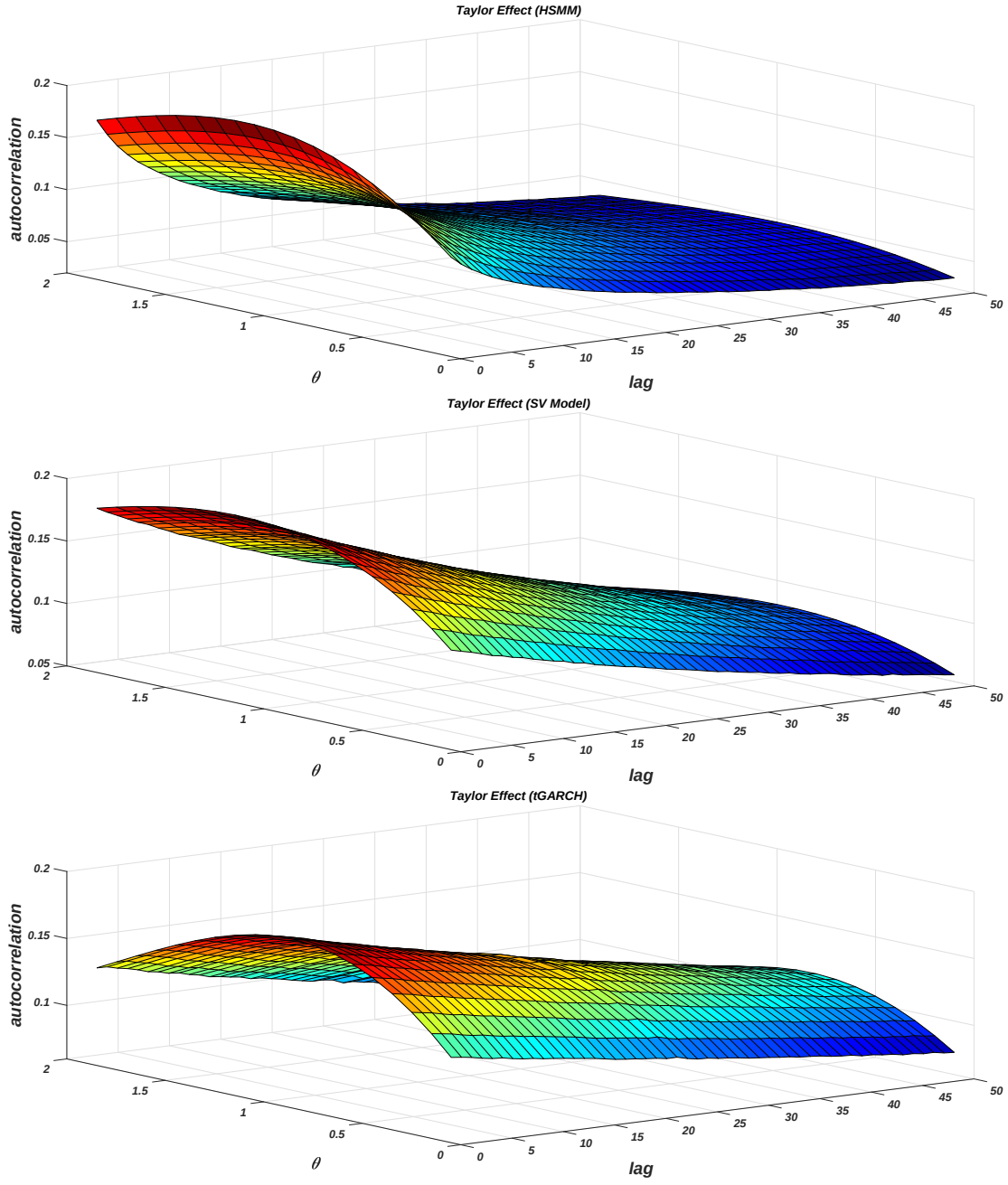

models. However, it is not fair to evaluate model performance purely on the log likelihood because different models may have different numbers of parameters. Introducing more parameters usually increases the log likelihood but may result in overfitting.

The Akaike information criterion (AIC) and the Bayesian information criterion (BIC) are fair model comparison tools. The AIC penalises the number of parameters and the BIC takes into consideration both the number of parameters as well as the sample

size. A better model has a smaller AIC/BIC. The three-state HSMM has the smallest AIC and BIC. This implies that the HSMM does not over-fit the data and additional parameters are sensibly introduced to model the data.

TABLE 1.9: Model Comparison with Hidden Markov Models

	3-State HSMM	**2-State HSMM**	**3-State HMM**	**2-State HMM**
Iteration No.	130	18	234	45
Log Likelihood	-5178.911	-5213.159	-5186.953	-5229.820
AIC	10385.820	10440.320	10401.910	10473.640
BIC	10468.420	10481.620	10484.500	10514.940

1.9 Trading Strategy

Under the EMH, the current prices always 'fully reflect' available information and follow a random walk., which naturally has the implication that technical trading rules cannot generate excess returns than a buy-and-hold trading strategy Fama (1965). Our three-state HSMM shows some merits of fitting the empirical data in terms of the stylized facts of asset returns, which are not considered by the random walk. Although testing the EMH is not the focus of this chapter, it is worthwhile to use our three-state HSMM to provide some evidence of the inefficiency of the Chinese financial market.

We design a simple trading strategy [4] based on our three-state HSMM. In order to test the profit of the trading strategy, we split the data into two parts, a training sample (April 8$^{\text{th}}$ 2005 to December 31$^{\text{st}}$ 2013) and a testing sample (January 1$^{\text{st}}$ 2014 to May 13$^{\text{th}}$ 2016). The three-state HSMM is estimated by the data in the training sample.

In order not to use future information, we use the expanding window to recursively decode the most likely sequence of states. Specifically, we fix the start date of the window to April 8$^{\text{th}}$ 2005 and move the end date of the window to each date in the testing sample. The performance of the trading strategy is only evaluated for the testing sample.

For each expanding window, we conduct global decoding for the data and take the last decoded state in the window. The trading rule is as follows:

[4] This is only a numerical demonstration of the trading strategy. Investors cannot directly trade the CSI 300 in China, but the index ETF can be its proxy.

- If the last decoded state is the bear market $\longrightarrow$ Short and hold in the next trading day
- If the last decoded state is the sidewalk market $\longrightarrow$ No position in the next trading day
- If the last decoded state is the bull market $\longrightarrow$ Long and hold in the next trading day

Figure 1.12 shows the cumulative return of the trading strategy in the upper panel, drawdown in the middle panel and trading signal in the lower panel. This trading strategy is profitable with an annualised return of 37.59% and a Sharpe ratio of 1.14 [5]. The maximum drawdown occurred at -21.34% in January 2015. There are three remarkable periods. The trading strategy does not have any position (trading signal: 0) before December 2014; it takes a long position (trading signal: 1) in April 2014; and it takes a short position (trading signal: -1) from June 2015 to October 2015 and from January 2016 to March 2016. The majority of the profit in the trading strategy comes from the short position. During the same trading period, the buy-and-hold trading strategy has an annual return of 13.36% and a Sharpe ratio of 0.28. Nevertheless, it should be highlighted that the maximum drawdown of the buy-and-hold trading strategy is -62.92%. Our simple trading strategy is superior to the buy-and-hold strategy in terms of higher risk-adjusted return.

For the robustness test, we follow Gencay (1998) to examine the trading performance in different out-of-sample periods. We conduct three other data split schemes and this trading strategy still shows high profit. The robustness test results are shown in 1.C. The robust performance of our simple trading strategy is consistent with the previous studies shown that technical trading strategies are profitable for the stock market indices in emerging markets (Ratner & Leal, 1999; Ito, 1999; Coutts & Cheung, 2000; Gunasekarage & Power, 2001).

1.10 Conclusion

With the aim to decode the Chinese stock market returns, three research sub-questions have been answered. Firstly, it is appropriate to employ a three-state HSMM to explain

[5]The risk free rate in China is assumed to be a constant of 4.35% according to `http://www.global-rates.com/interest-rates/central-banks/central-bank-china/pbc-interest-rate.aspx`.

FIGURE 1.12: Performance of the Simple Trading Strategy
(Training Sample: Apr.2005 - Dec.2013; Testing Sample: Jan.2014 - May.2016)

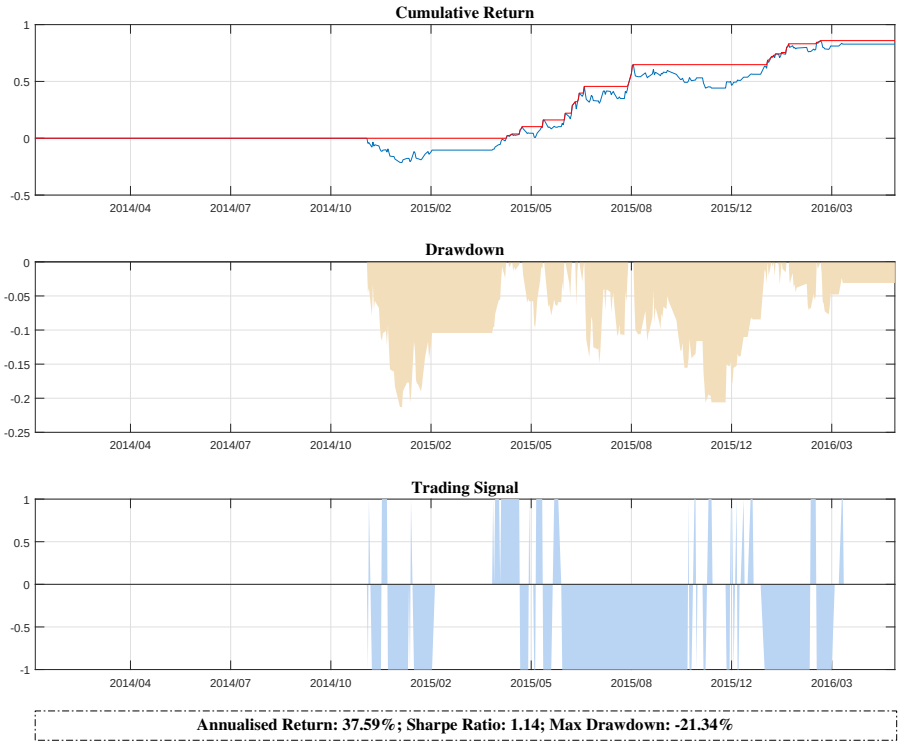

the time-varying distribution of Chinese stock market returns. Secondly, the hidden states in the HSMM correspond to the market conditions, namely the bear, sidewalk, and bull market. Thirdly, we show the inefficiency of the market by design a trading strategy based on the expanding window decoding. The trading strategy generates risk-adjusted return with a Sharpe ratio of 1.14 in the testing sample.

Additionally, we reviewed the evolution of the market conditions in the Chinese stock market over the last decade. The most prominent periods are the bear market (January 16$^{\text{th}}$ 2008 to January 14$^{\text{th}}$ 2009), the long sidewalk market (November 19$^{\text{th}}$ 2011 to November 20$^{\text{th}}$ 2014), and a recent bull market (December 11$^{\text{th}}$ 2014 to May 27$^{\text{th}}$ 2015). In the model evaluation, our three-state HSMM along with a SV model and a tGARCH(1,1) can reproduce the stylized facts of the "long-memory" and the Taylor effect, but tGARCH(1,1) fails to reduce the fat tails.

One limitation of the HSMM is that the empirical results can be largely changed by the model setting. Finding the appropriate model settings can involve many times of trial

and error. Future research may wish to explore the links between market conditions and macroeconomic variables.

Appendix

1.A EM Algorithm

In this appendix, we provide technical details of the EM algorithm for the right-censored HSMM. We adopt the right-censored HSMM because the assumption of the classical HSMM that the last observation always coincides with the exit from a state seems to be unrealistic for financial time series data (Bulla & Bulla, 2006). The right-censored setting releases the assumption that the last observation is always to be the end of a state. In other words, the last visited state will last for some time even after the last observation. There is no immediate jump to other states after the last observation. In the right-censored setting, the sojourn time in the last visited state is modelled by the survivor function, which shown in Equation 1.12.

$$D_i(u) = \sum_{\nu > u} d_i(u) \tag{1.12}$$

Guédon (2003) provided the complete-data likelihood for the right-censored HSMM. The complete-data likelihood function contains the observation $\boldsymbol{X}_1^T$ and the state sequence $\boldsymbol{S}_1^T$, where $u-1$ is the period that the last visited state will continue after the last observation. The last visited state will jump into other states at time $T+u$. The complete-data likelihood for the right-censored HSMM is shown in Equation 1.13.

$$L_c(\boldsymbol{X}_1^T, \boldsymbol{s}_1^{T+u}|\boldsymbol{\theta}) = \mathbb{P}(\boldsymbol{X}_1^T = \boldsymbol{x}_1^T, \boldsymbol{S}_1^T = \boldsymbol{s}_1^T, \boldsymbol{S}_{T+1}^{T+u-1} = s_T, S_{T+u} \neq s_T|\boldsymbol{\theta}) \tag{1.13}$$

The final likelihood function is obtained by summing all possible state sequences and all possible prolongation lengths of the last state, as indicated in Equation 1.14.

$$L(\boldsymbol{\theta}) = \sum_{t=S_1,\ldots,S_T} \sum_{u_{T+}} L_c(\boldsymbol{X}_1^T, \boldsymbol{s}_1^{T+u}|\boldsymbol{\theta}) \tag{1.14}$$

where $\sum_{t=S_1,\ldots,S_T}$ represents the summation of all possible state sequences, and $\sum_{u_{T+}}$ represents the summation over all possible additional sojourn time after time T.

It is difficult to compute the likelihood function in Equation 1.13 because the underlying state sequence is unknown. It needs to consider all possibilities of the state sequence in order to compute the full likelihood, which is not realistic. The expectation-maximization (EM) algorithm provides a suitable procedure to deal with the missing data problem. The EM algorithm (Baum et al., 1970) is an iterative procedure to increase the likelihood until it reaches the convergence criteria. The EM algorithm iteratively conducts the E-step and M-step. Given an initial guess of the parameter vector $\boldsymbol{\theta}$, the E-step firstly computes the Q-function, which is the conditional expectation for the complete-data likelihood.

- **E-step**

$$Q(\boldsymbol{\theta}, \boldsymbol{\theta}^{(t-1)}) = \mathbb{E}\left\{ L_c(\boldsymbol{X}_1^T, \boldsymbol{s}_1^{T+u}|\boldsymbol{\theta}) | \boldsymbol{X}_1^T = \boldsymbol{x}_1^T, \boldsymbol{\theta}^{(t-1)} \right\} \tag{1.15}$$

  Based on the Q-function in Equation (12), the M-step aims to maximise the Q-function with respect to parameter $\boldsymbol{\theta}$.

- **M-step**

$$\boldsymbol{\theta}^{(t)} = \arg\max_{\boldsymbol{\theta}} Q(\boldsymbol{\theta}, \boldsymbol{\theta}^{(t-1)}) \tag{1.16}$$

The parameter vector $\boldsymbol{\theta}$ that maximises the Q-function in the M-step of the previous iteration will be used in the E-step of the next iteration. Along with every iteration, the likelihood is non-decreasing. The algorithm will stop once the convergence criterion is satisfied. Normally, the convergence criterion is the successive change of likelihood is less than a very small number. The EM algorithm is not guaranteed to reach the global maxima and it might be trapped in local maxima. Hence, it is necessary to try different

initial values of parameter vector $\boldsymbol{\theta}$ in order to check that the maximum reached is the global maximum rather than the local maximum.

In this chapter, we focused on the economic interpretation of the HSMM rather than on the mathematical derivation. We direct the reader to the thesis of Bulla (2006) for the mathematical details of the EM algorithm of the HSMM. In his thesis, he decomposes the Q-function of the HSMM into four components, which correspond to the initial probabilities, transition probabilities, sojourn time, and component distributions. The E-step is implemented by the forward-backward algorithm. His decomposition framework facilities the M-step in which the four components can be maximised individually. Bulla shows the close-form solutions for some common distributions for the sojourn time and component distributions, but the numerical solver could be applied if a closed solution does not exist.

Unlike the maximum likelihood method whereby the standard errors can be directly calculated by the Fisher information matrix (FIM), one drawback of the EM algorithm is that the FIM is not a by-product of the algorithm. It is highly unlikely to obtain the FIM by evaluating analytically the second-order derivatives of the marginal log-likelihood of the HSMM. Recent numerical methods are developed to get an approximation of the FIM (see Louis, 1982; Meng & Rubin, 1991; Jamshidian & Jennrich, 2000). However, all these methods have limitations (Meng, 2016). There is no generally accepted method to get diagnosis for the estimation of the HSMM by the EM algorithm. Hence, we do not provide the diagnosis of the estimated parameters in this chapter.

1.B Decoding Technique

It is interesting to decode the most likely states in the Markov chain. There are two decoding techniques for the HSMM, global decoding and local decoding. Global decoding aims to determine the most likely sequence of the states given the observations, while the local decoding computes the conditional probability of each state at times given the observations. Normally, they produce similar but not identical decoding results.

1.B.1 Global Decoding

The purpose of global decoding is to find the most likely sequence of states conditional on the observations. Mathematically speaking, global decoding intends to find a sequence of states with the highest likelihood given the observations, which is shown in Equation 1.17.

$$\hat{\boldsymbol{S}}_1^T = \arg\max_{\boldsymbol{S}_1^T} \mathbb{P}\left(\boldsymbol{S}_1^T | \boldsymbol{X}_1^T\right) \tag{1.17}$$

The exhaustive attack method has the computational complexity level at $\mathcal{O}(m^T)$. This brute force method is not feasible for long sequence data. The Viterbi algorithm (Viterbi, 1967) was developed by utilising the Markov property of the HMM and HSMM. This is an efficient dynamic programming algorithm and its complexity level is $\mathcal{O}(m \times T)$. The Viterbi algorithm works in the following way.

$$\arg\max_{\boldsymbol{S}_1^T} \mathbb{P}\left(\boldsymbol{S}_1^T | \boldsymbol{X}_1^T\right) = \arg\max_{\boldsymbol{S}_1^T} \mathbb{P}\left(\boldsymbol{S}_1^T, \boldsymbol{X}_1^T\right) \tag{1.18}$$

Define

$$\mu_t(S_t) = \max_{\boldsymbol{S}_1^{t-1}} \mathbb{P}(\boldsymbol{S}_1^t, \boldsymbol{X}_1^t) \tag{1.19}$$

The recursion expression for $\max \mathbb{P}(\boldsymbol{S}_1^t, \boldsymbol{X}_1^t)$ can be derived.

$$\begin{aligned}
\max_{\boldsymbol{S}_1^{t-1}} \mathbb{P}(\boldsymbol{S}_1^t, \boldsymbol{X}_1^t) &= \max_{\boldsymbol{S}_1^{t-1}} \mathbb{P}(X_t|S_t)\mathbb{P}(S_t|S_{t-1})\mathbb{P}(\boldsymbol{S}_1^{t-1}, \boldsymbol{X}_1^{t-1}) \\
&= \max_{S_{t-1}} \left\{ \mathbb{P}(X_t|S_t)\mathbb{P}(S_t|S_{t-1}) \max_{\boldsymbol{S}_1^{t-2}} \mathbb{P}(\boldsymbol{S}_1^{t-1}, \boldsymbol{X}_1^{t-1}) \right\} \\
&= \max_{S_{t-1}} \mathbb{P}(X_t|S_t)\mathbb{P}(S_t|S_{t-1})\mu_{t-1}(S_{t-1})
\end{aligned} \tag{1.20}$$

The recursion equation for $\mu_t(S_t)$ is as follows

$$\mu_t(S_t) = \max_{S_{t-1}} \mathbb{P}(X_t|S_t)\mathbb{P}(S_t|S_{t-1})\mu_{t-1}(S_{t-1}) \qquad for \quad t = 2, ..., T \tag{1.21}$$

Equation 1.21 is able to compute the most likely trajectory for each state up to time t. At time T, the state with the highest $\mathbb{P}(\boldsymbol{S}_1^T, \boldsymbol{X}_1^T)$ is picked up and the corresponding trajectory is the solution for the Viterbi algorithm.

1.B.2 Local Decoding

The purpose of local decoding is to compute the conditional probabilities for each state at time t given the observation.

$$\hat{S}_t = \arg\max_{S_t} \mathbb{P}\left(S_t = i | \boldsymbol{X}_1^T = \boldsymbol{x}_1^T\right) \qquad for \quad i = 1, ..., m \tag{1.22}$$

The conditional probability in Equation 1.22 can be decomposed into three terms.

$$\begin{aligned} \mathbb{P}\left(S_t = i | \boldsymbol{X}_1^T = \boldsymbol{x}_1^T\right) = \quad & \mathbb{P}\left(S_{t+1} \neq i, S_t = i | \boldsymbol{X}_1^T = \boldsymbol{x}_1^T\right) \\ & + \mathbb{P}\left(S_{t+1} = i | \boldsymbol{X}_1^T = \boldsymbol{x}_1^T\right) \\ & - \mathbb{P}\left(S_{t+1} = i, S_t \neq i | \boldsymbol{X}_1^T = \boldsymbol{x}_1^T\right) \end{aligned} \tag{1.23}$$

Define $\xi_t(i) = \mathbb{P}(S_t = i | \boldsymbol{X}_1^T = \boldsymbol{x}_1^T)$. It is able to obtain the recursion equation for the conditional probability.

$$\xi_t(i) = \mathbb{P}\left(S_{t+1} \neq i, S_t = i | \boldsymbol{X}_1^T = \boldsymbol{x}_1^T\right) + \xi_{t+1}(i) - \mathbb{P}\left(S_{t+1} = i, S_t \neq i | \boldsymbol{X}_1^T = \boldsymbol{x}_1^T\right) \tag{1.24}$$

With Equation 1.24, $\xi_t(i)$ can be computed based on the $\xi_{t+1}(i)$ and it is able to calculate the conditional probabilities at all time in a backward way (see details in Guédon (2003)).

1.C Robustness Test of the Trading Strategy

We implemented three other data split schemes in order to test the profit of our trading strategy. The first scheme is cutting the sample at the end of 2009 (i.e. trading sample: Apr.2005 - Dec.2009, testing sample: Jan.2010 - May.2016); the second scheme is at the end of 2012 (i.e. trading sample: Apr.2005 - Dec.2012, testing sample: Jan.2013 - May.2016); and the third scheme is at the end of 2014 (i.e. trading sample: Apr.2005 - Dec.2014, testing sample: Jan.2015 - May.2016). For each scheme, the HSMM is estimated by using the training data, and then the trading strategy is tested for the period of the testing sample. The trading strategy still shows high profit for all three

schemes (see Figure 1.C.1 to Figure 1.C.3). The profit of the trading strategy is believed to be robust.

FIGURE 1.C.1: Performance of the Simple Trading Strategy - Period 1

(Training Sample: Apr.2005 - Dec.2009; Testing Sample: Jan.2010 - May.2016)

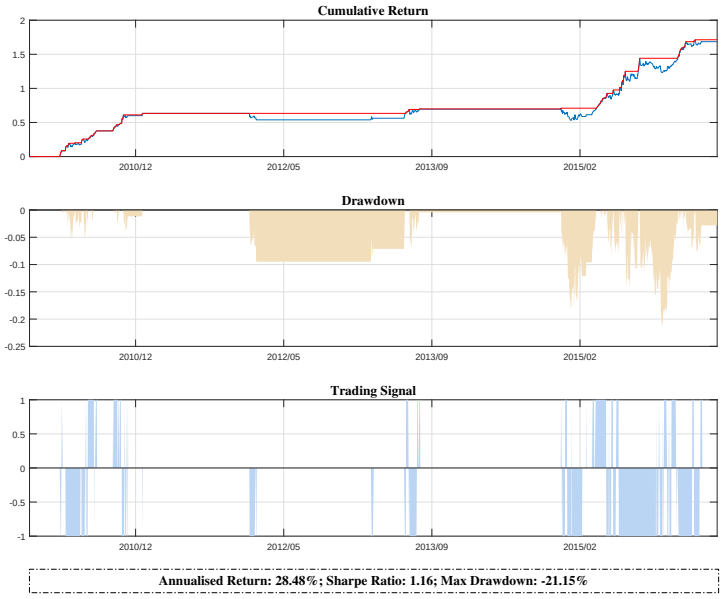

FIGURE 1.C.2: Performance of the Simple Trading Strategy - Period 2

(Training Sample: Apr.2005 - Dec.2012; Testing Sample: Jan.2013 - May.2016)

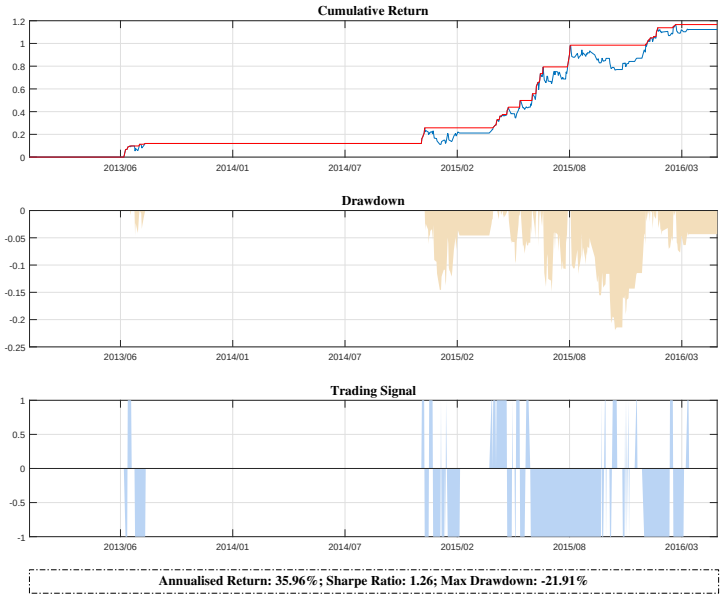

FIGURE 1.C.3: Performance of the Simple Trading Strategy - Period 3

(Training Sample: Apr.2005 - Dec.2014; Testing Sample: Jan.2015 - May.2016)

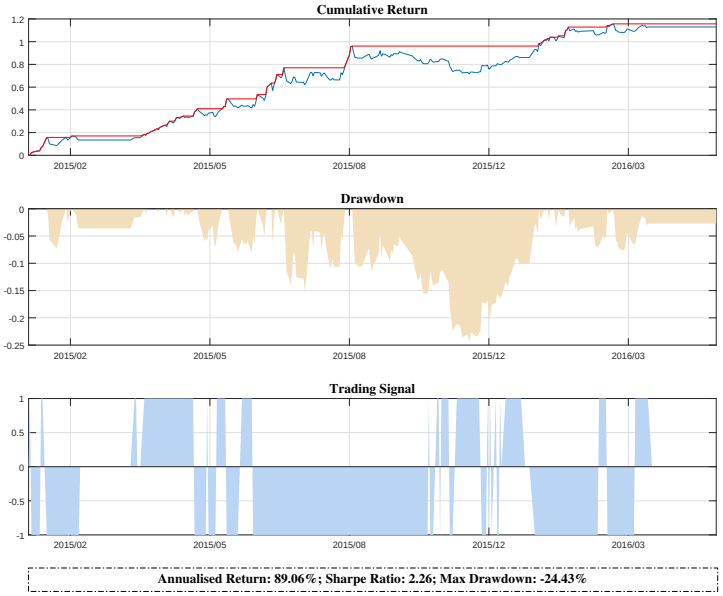

Chapter 2

Understanding the Chinese Stock Market:

International Comparison and Policy Implications

The definition of bear, sidewalk, and bull markets is ambiguous in existing literature. This makes it difficult for practitioners to distinguish between different market conditions. In this chapter, we employ a statistical definition of bear, sidewalk, and bull markets, which correspond to the three states in our hidden semi-Markov model. We employ this analysis to the daily returns of the Chinese stock market and the other seven developed markets investigated. Using the Viterbi algorithm to globally decode the most likely sequence of the market conditions, we systematically find the precise timing of bear, sidewalk, and bull markets for all eight markets. Through the comparison of the estimation and decoding results, many unique characteristics of the Chinese stock market are found, such as "Crazy Bull", "Frequent and Quick Bear", and "No Buffer Zone". In China, the bull market is more volatile than in developed markets, the bear market occurs more frequently than in developed markets, and the sidewalk market has not functioned as a buffer zone since 2005. Lastly, the possible causes of the unique characteristics are discussed and implications for policy-making are suggested.

2.1 Introduction

In the last two decades, China has made significant progress on the development of the stock market. A number of important steps have been carried out, such as the enactment of Qualified Foreign Institutional Investors (QFII) programme in 2002, the split-share structure reform in 2005, and the Qualified Domestic Institutional Investors (QDII) programme in 2006. However, the current rules and structures of the Chinese stock market are still considerably different from those of developed stock markets. Firstly, the Chinese stock market is relatively isolated from the international financial markets because of very limited openness to the international investors. Secondly, the Chinese stock market is heavily regulated and intervened by the government. Thirdly, the Chinese stock market is still under development and lacks financial derivatives to manage risk. Lastly, the majority of investors are individual investors without professional investment knowledge, who are focusing on short-term speculation, rather than long-term investment. Lastly, the Chinese stock market is very liquid with high turnover velocity.

It is natural to raise the question how these different rules and structures reflect on the market behaviour. Many studies have investigated the Chinese stock market. Herding behaviour, overreaction, and speculation in the Chinese stock market are well-documented (Tan et al., 2008; Mei et al., 2009; Ni et al., 2015). However, less attention has been to paid from the perspective of the market condition. To the best of our knowledge, very limited study has identified the difference of the market conditions between the Chinese stock market and developed markets, especially after 2005. In this chapter, we are interested in investigating the unique characteristics of market conditions in China with particular comparison to developed markets. Additionally, we discuss the possible causes of the unique characteristics of market conditions in China and propose several policy suggestions to help the development of the Chinese stock market.

The definition of bear, sidewalk, and bull markets is very vague in the existing literature, making it difficult for practitioners to distinguish between stock markets in different market conditions. We employ a statistical definition of bear, sidewalk, and bull markets, which corresponds to the states in our three-state hidden semi-Markov model (HSMM) in

Chapter 1. We employ this analysis to the daily return of the Chinese stock market and the other seven developed markets analysed. Using the Viterbi algorithm (Viterbi, 1967) to globally decode the most likely sequence of the market conditions, we systematically find the precise timing of bear, sidewalk, and bull markets for all eight markets. Through the comparison of the estimation and decoding results, several unique characteristics of the Chinese stock market are found, such as "Crazy Bull", "Frequent and Quick Bear", and "No Buffer Zone". "Crazy Bull" refers to the observation that the bull market has a considerably high variance. "Frequent and Quick Bear" is the observation that the bear market has short sojourn time and occurs very frequently. "No Buffer Zone" represents the observation that the bull market is typically mixed with the bear market and there is no sidewalk market between them.

Our findings are meaningful for investors and policy makers on two levels. Firstly, at the micro-level, investors have more in-depth understanding of the Chinese stock market, which has several prominent differences from developed markets. In China, the bull market is more volatile, the bear market happens more frequently, and the sidewalk market does not function as a buffer zone. All of these characteristics suggest that investors need to carefully manage the risk of their investment and avoid speculation. Secondly, at the macro-level, it is vital for the government to educate individual investors and develop institutional investors, to provide more accessible risk management tools, and to strengthen regulation on excess leverage from other source financing.

2.2 Literature Review

Many studies have investigated the Chinese stock market. Herding behaviour, overreaction, and speculation in the Chinese stock market are well-documented. Tan et al. (2008) studied heading behaviour in the Chinese stock market, both A-share and B-share. They found that herding happens in both upside and downside market conditions. Particularly, herding behaviour is stronger in upside market conditions in A-share. Investor sentiment and its nonlinear effect on stock returns in China was studied by Ni et al. (2015) through the panel quantile regression model. The nonlinear effect of investor

sentiment turns out to be asymmetric and reversal, which proves the occurrence of overreaction in the Chinese stock market. Additionally, it was observed that Chinese investors are affected by cognitive bias and speculation tendencies.

The market condition has been studied by Markov-switching techniques. Schaller & Norden (1997) considered a two-regime model which allows the mean and/or the variance of returns to vary in different regimes for the US stock market. Nielsen et al. (2001) found that a third regime, the speculative market, exists in some European markets. Girardin & Liu (2003) adopted a switch-in-the-mean plus switch-in-the-variance (MSMH(3)-AR(5)) model for weekly capital gains on the Shanghai A-share market during the period between 1995 and 2002. They also found that there are three market conditions: a speculative market, a bull market and a bear market. They claimed that the bull market is always a buffer zone in the transition between the other two market conditions. It should be noted that the buffer zone defined in the context of Girardin & Liu (2003) is the bull market, while the sidewalk market is regarded as the buffer zone in this chapter.

The hidden Markov model (HMM) and hidden semi-Markov model (HSMM) used in financial studies focus on the reproduction of stylized facts of daily returns. Rydén et al. (1998) firstly adopted a two-state HMM with normal distributions (zero mean but different variance) as the component distribution (a.k.a. marginal distribution) to reproduce most of the stylized facts of daily returns, except for the slow decay in the autocorrelation function of squared returns. Bulla & Bulla (2006) used a two-state HSMM, which is a generalization of HMM, to model daily returns of 18 US sector indexes. The stylized facts of daily returns are reproduced by HSMM, including the long-memory in the autocorrelation function of squared returns. In Chapter 1, we used a three-state HSMM on the daily returns of CSI 300 and showed that the stylized facts of daily return in China also can be reproduced. The empirical results suggest that three-state HSMM is appropriate for the CSI 300, and it is better than two-state HSMM, three-state hidden Markov model, and two-state hidden Markov model model. In this Chapter, we employ the same three-state HSMM as in Chapter 1 to systematically find the precise timing of bear, sidewalk, and bull markets.

This chapter firstly propose the statistical definitions of bear, sidewalk, and bull markets. In the empirical results part, the unique characteristics of the Chinese stock market are identified through the comparison of estimation and decoding results with developed markets. Finally, the possible causes of the unique characteristics are discussed and several policy implications are suggested.

2.3 Definition of Bear, Sidewalk, and Bull

In practice, investors tend to determine market conditions arbitrarily and different conclusions might be drawn for the same market in the same period. In the existing academic literature, the definition of market conditions varies considerably. In one of the early study, Fabozzi & Francis (1977) propose three ways to define market conditions. In the first classification of Bull and Bear Markets, the rule places most months when the market rises in the bull market (BB), but months when the market rose near the bearish months were treated as part of the bear market. In the second classification of Up and Down Markets (UD), months in which return was non-negative are defined as Up months and months in which return was negative are defined as Down months. In the third classification of Substantial Up and Down Months (SUD), there are three categories: months when the market moved Up-substantially, months when the market moved Down-substantially, and months when the market moved neither Up-substantially nor Down-substantially. The threshold of substantial move was arbitrarily defined.

In the modern study, a loose definition by Chauvet & Potter (2000) proposed that market prices generally increase (decrease) in a bull (bear) market. Edwards & Caglayan (2001) use a simple classification that bull market months are defined as those in which the S&P index rises by 1% or more and bear market months are defined as those in which the S&P index falls by 1% or more. Lunde & Timmermann (2004) claim that a bull (bear) market starts when the market price increases (decreases) a certain percentage, say 20%, from the previous local bottom (peak). Gonzalez et al. (2006) utilized two formal turning point methods to detect the timing of bull and bear markets. Cheng

et al. (2013) define bull (bear) markets as the periods with at least three consecutive months of positive (negative) returns.

It is inevitable to propose our own definition of market conditions for three reasons. Firstly, there is no generally accepted definition of the market conditions. Secondly, most definitions of the market conditions are based on the monthly data. Lastly and mostly importantly, the current definition are mainly for two-category classification, i.e. the bull or bear market (or up or down market). The only three-category classification is the SUD in Fabozzi & Francis (1977), but their threshold of substantial move was arbitrarily defined. We define the bear, sidewalk, and bull market conditions from the perspective of the distributional features.

Definition 2.1. A Bear Market

- The mean of the distribution of the daily returns conditional on a bear market is significantly less than 0.
- The frequency of the positive returns is expected to be larger than that of the negative returns.
- Because of the above statistical properties, the price in a bear market is generally decreasing.

Definition 2.2. A Sidewalk Market

- The mean of the distribution of the daily returns conditional on a sidewalk market should be insignificantly different from 0.
- It is expected to observe a roughly equal number of positive and negative returns.
- Because of the above statistical properties, the price in a sidewalk market stays in a band and shows a mean-reversion pattern.

Definition 2.3. A Bull Market

- The mean of the distribution of the daily returns conditional on a bull market should be significantly larger than 0.
- The frequency of the positive returns is expected to be larger than that of the negative returns.
- Because of the above statistical properties, the price in a bull market is generally increasing.

In straight-forward notation, the mean in each market is as follows:

$$\mu(S_t) = \mu_1 < 0, \text{ if } S_t = 1 \text{ (bear market)}$$
$$\mu(S_t) = \mu_2 \approx 0, \text{ if } S_t = 2 \text{ (sidewalk market)}$$
$$\mu(S_t) = \mu_3 < 0, \text{ if } S_t = 3 \text{ (bull market)}$$

The variance of each market can be denoted as

$$\sigma^2(S_t) = \sigma_1^2, \text{ if } S_t = 1 \text{ (bear market)}$$
$$\sigma^2(S_t) = \sigma_2^2, \text{ if } S_t = 2 \text{ (sidewalk market)}$$
$$\sigma^2(S_t) = \sigma_3^2, \text{ if } S_t = 3 \text{ (bull market)}$$

where we expect that the bear market should have highest variance (i.e. $\sigma_1^2 > \sigma_2^2$, and $\sigma_1^2 > \sigma_3^2$) because it is normally the most volatile market.

2.4 Empirical Results

2.4.1 Data Description

We apply the three-state HSMM to analyse the daily returns of stock indexes in eight countries, including the CSI 300 (China), S&P 500 (United States), FTSE 100 (United Kingdom), CAC 40 (France), DAX (Germany), Nikkei 225 (Japan), STI (Singapore), and ASX 200 (Australia). The sample period is from April 8th 2005 to February 26$^{\text{th}}$ 2016 [1], slightly more than a decade. The reason for using this sample period is that the start date is when the CSI 300 was first launched. Additionally, As the split-share structure reform occurred in 2005, the behavior of Chinese stock market has a structural change. Interested readers can refer to Girardin & Liu (2003) the research for the Chinese stock market during 1997 to 2002. There are 2645 observations for each index. The source of our data is Wind.

[1] Note that the sample period is slightly shorter than the sample period used in Chapter 1.

The daily return is defined as 100 times the first-order difference of the natural logarithm of the price series.

$$r_t^i = 100 \times (log(P_t^i) - log(P_{t-1}^i)) \tag{2.1}$$

where P_t^i is the closing price of the market index i at time t.

2.4.2 Component Distribution - Evidence of "Crazy Bull"

It is natural to interpret the three states in our HSMM as bear, sidewalk, and bull according to our definition based on statistical features of return distributions. The estimated parameters of the component distribution in HSMM for all countries are presented in Table 2.1. The means of State 1 in all countries are less than zero and their variances are the highest among the three states. The statistical features of State 1 are consistent with a bear market. It can be observed that the means in State 2 are all close to zero and slightly less to zero. The variance in State 2 is much lower than in State 1. The statistical features of State 2 meet our expectation of a sidewalk market, in which the return distribution should have a mean close to zero, enabling the price in the sidewalk market to fluctuate within a band. State 3 for all countries have positive means with the smallest variance among all of the states, except for the CSI 300. The return distribution with positive mean and small variance allows the price in the bull market to increase steadily, which is an intrinsic feature of a bull market.

The first unique characteristic of the Crazy Bull is the abnormally high variance in the Chinese bull market compared with other countries. The Chinese bull market has a variance of 2.058, almost three times higher than for other countries. Japan has the second most unstable bull market with a variance of 0.693. The bull market in the United States and the United Kingdom are relatively more stable, as indicated by the small variances of 0.244 and 0.297, respectively. It is reasonable to expect that the variance is higher in the bear market for all eight countries since the abrupt price fall during the market crash make the volatility increase. The bear markets in all eight countries show similarly high variances. The bear market in our sample period happened after 2008 triggered by financial crisis. The variance in the Chinese bear market (9.719)

is modest, between the highest variance in Japan (16.169) and the lowest in Australia (6.680). It seems that the volatility of the Chinese bear is normal. There is no significant difference between the sidewalk markets of the eight countries. Interestingly, the means in the sidewalk markets are close to 0 but consistently slightly less than 0. In Table 2.2, one-sample z-statistics show that none of the eight countries has a mean in State 2 which is significantly different from 0.

TABLE 2.1: Component Distribution

	State 1 (Bear)		**State 2 (Sidewalk)**		**State 3 (Bull)**	
	Mean	*Variance*	*Mean*	*Variance*	*Mean*	*Variance*
CSI 300	-0.513	(9.719)	-0.020	(1.343)	0.614	(2.058)
S&P 500	-0.140	(8.726)	-0.042	(1.375)	0.115	(0.244)
FTSE 100	-0.245	(9.346)	-0.018	(1.427)	0.082	(0.297)
CAC 40	-0.330	(11.611)	-0.051	(2.219)	0.123	(0.526)
DAX	-0.316	(10.180)	-0.018	(1.920)	0.187	(0.393)
Nikkei 225	-0.382	(16.169)	-0.056	(2.311)	0.156	(0.693)
STI	-0.084	(8.831)	-0.053	(1.644)	0.061	(0.348)
ASX 200	-0.304	(6.680)	-0.040	(1.449)	0.098	(0.412)

TABLE 2.2: One-Sample z-test

z-statistics of mean in State 2	
CSI 300	-0.653
S&P 500	-1.251
FTSE 100	-0.595
CAC 40	-1.316
DAX	-0.533
Nikkei 225	-1.464
STI	-1.270
ASX 200	-1.185

2.4.3 Sojourn Time - Evidence of "Frequent and Quick Bear"

Based on the global decoding results, Table 2.3 reports the number of days, number of times, and average sojourn for the three market conditions in all eight countries during our sample period. Compared with developed markets, the Chinese stock market shows "Quick Bull", "Frequent and Quick Bear", and "Long Sidewalk".

It should be highlighted that the average sojourn time of the bull market in China (27.72) is the shortest, while for developed markets this is more than 40 trading days. During

our sample period, the Chinese market was in the bull market for 693 trading days, but entered and exited the bull market 25 times. We observe that the United States is also in the bull market a large number of times (27). However, the total number of days the United States is in the bull market (1133) is nearly double that of China, which results in a relatively longer average sojourn in the bull market (41.96).

China, along with the United Kingdom and Japan, are found to have a short average sojourn in the bear market, whilst the other five countries have more than 30 trading days. It should be pointed out that China was in the bear market 22 times, while all of the other countries were around five times in the bear market in our sample period. We can argue that the "Quick Bear" happens in the United Kingdom and Japan but not frequently, while China has a "Frequent and Quick Bear".

The average sojourn of the sidewalk market in China is 230.17, more than twice that of other countries. Additionally, China was only in the sidewalk market six times in the sample period. Every time China entered the sidewalk market, the long-term trend in the stock market cannot be established unless the long sojourn in the sidewalk market has elapsed. The most obvious sidewalk period in China is from 2011 to 2014, where the CSI 300 stayed roughly between 2000 and 3000. During that period, whenever the CSI 300 was near the ceiling or floor, it would eventually return to the band again.

2.4.4 Transition Probability Matrix - Evidence of "No Buffer Zone"

We found a very unique characteristic, "No Buffer Zone", of the Chinese stock market from the estimated transition probability matrix in Table 2.4. The direct transition probability from the bear market to bull market (or the opposite direction) is close to 0% in all developed markets. It is clearly shown that all developed markets always have the sidewalk market as a buffer zone between the bull and bear market. Nevertheless, the transition probability matrix in China is very special with a particularly high transition probability from the bear market to the bull market (nearly 100%) and a relatively high transition probability from the bull market to the bear market (77.05%). The buffer zone effect was not found to exist in China over the sample period. The direct transition between the bull market and the bear market is typical. It was found that the

TABLE 2.3: Days, Times, and Average Sojourn

		State 1 (Bear)	**State 2 (Sidewalk)**	**State 3 (Bull)**
CSI 300	*Number of Days*	570	1381	693
	Number of Times	22	6	25
	Average Sojourn	25.91	230.17	27.72
S&P 500	*Number of Days*	269	1242	1133
	Number of Times	3	30	27
	Average Sojourn	89.67	41.40	41.96
FTSE 100	*Number of Days*	166	1486	992
	Number of Times	7	21	14
	Average Sojourn	23.71	70.76	70.86
CAC 40	*Number of Days*	174	1483	987
	Number of Times	5	18	13
	Average Sojourn	34.80	82.39	75.92
DAX	*Number of Days*	217	1612	815
	Number of Times	3	21	18
	Average Sojourn	72.33	76.76	45.28
Nikkei 225	*Number of Days*	104	1607	933
	Number of Times	5	16	10
	Average Sojourn	20.80	100.44	93.30
STI	*Number of Days*	213	938	1493
	Number of Times	4	16	12
	Average Sojourn	53.25	58.63	124.42
ASX 200	*Number of Days*	188	1251	1205
	Number of Times	4	16	11
	Average Sojourn	47.00	78.19	109.55

bull market and the bear market are mixed together many times in the Chinese stock market. The second difference between the TPM of China and other countries is that in China the transition probability from sidewalk market to the other two markets is roughly 50%, while other developed markets tend to have a much larger probability to be a bull maker after exiting the sidewalk market. The developed market normally has less than 20% probability of exiting the sidewalk market to the bear market. Though this might be due to the short sample period of our data, this is what actually happened in the last decade, including the four stages of the economic and business cycle, namely economic prosperity before 2007, the financial crisis in 2008, financial depression since 2009, and economic rebound after 2010.

TABLE 2.4: Transition Probability Matrix

	From \ To	State 1 (Bear)	State 2 (Sidewalk)	State 3 (Bull)
CSI 300	**State 1 (Bear)**	0.00%	0.04%	99.96%
	State 2 (Sidewalk)	48.45%	0.00%	51.55%
	State 3 (Bull)	77.05%	22.95%	0.00%
S&P 500	**State 1 (Bear)**	0.00%	99.90%	0.10%
	State 2 (Sidewalk)	5.18%	0.00%	94.82%
	State 3 (Bull)	0.00%	100.00%	0.00%
FTSE 100	**State 1 (Bear)**	0.00%	100.00%	0.00%
	State 2 (Sidewalk)	14.61%	0.00%	85.39%
	State 3 (Bull)	0.00%	100.00%	0.00%
CAC 40	**State 1 (Bear)**	0.00%	100.00%	0.00%
	State 2 (Sidewalk)	13.10%	0.00%	86.90%
	State 3 (Bull)	0.00%	100.00%	0.00%
DAX	**State 1 (Bear)**	0.00%	99.93%	0.07%
	State 2 (Sidewalk)	7.81%	0.00%	92.19%
	State 3 (Bull)	0.00%	100.00%	0.00%
Nikkei 225	**State 1 (Bear)**	0.00%	100.00%	0.00%
	State 2 (Sidewalk)	20.33%	0.00%	79.67%
	State 3 (Bull)	0.00%	100.00%	0.00%
STI	**State 1 (Bear)**	0.00%	100.00%	0.00%
	State 2 (Sidewalk)	17.89%	0.00%	82.11%
	State 3 (Bull)	0.00%	100.00%	0.00%
ASX 200	**State 1 (Bear)**	0.00%	100.00%	0.00%
	State 2 (Sidewalk)	16.88%	0.00%	83.12%
	State 3 (Bull)	0.00%	100.00%	0.00%

2.5 Discussion and Policy Implications

By comparing with international markets, we found many unique characteristics of the Chinese stock market. The most prominent three characteristics are "Crazy Bull", "Frequent and Quick Bear", and "No Buffer Zone". All of these characteristics indicate that the Chinese stock market is much more volatile than other developed markets. These three characteristics are of great importance for policy makers. In order to build a more reliable and stable stock market, we would like to discuss the possible causes of the unique characteristics and policy implications from our findings.

2.5.1 "Crazy Bull" - Rational Security Analysis and Adjust Investor Structure

Compared with other developed markets, the Chinese stock market has considerably high variance in the bull market, which could be induced by the herding behaviour of individual investors. Kim & Wei (2002) provide evidence that individual investors are more likely to engage in herding. Kumar & Lee (2006) use more than 1.85 million individual investor transaction at a major US discount brokerage house to show that individual investors buy or sell stocks in concert during 1991-1996. Moreover, they can be easily influenced by news and market sentiment. Barber & Odean (2008) test and confirm that individual investors are net buyers of stocks in the news with public attention.

In order to mitigating the herding behaviour, Lao & Singh (2011) suggest that large financial institutions can bring more rational security analysis to the general public, which can decrease the level of speculative investments activity by the individual investors. Most individual investors have little knowledge of stock markets and focus on speculation of short-term price changes, rather than the fundamental value of listed companies. It is imperative to guide individual investors to focus on the fundamental values of firms and encourage individual investors to make rational investments.

In China, individual investors account for 82.24% of total trading volume in 2013 (Han & Li, 2017), whereas institutional investors dominate in developed markets. Boehmer & Kelley (2009) show that stock with greater institutional ownership are priced more efficiently. The Chinese government needs to adjust investor structure and promote the development of institutional investors, like asset management firms, private funds, and mutual funds. Institutional investors have expert knowledge and skills to manage professional investments that seek long-term returns under the proper risk management.

2.5.2 "Frequent and Quick Bear" - Risk Management Tools

In China, the bear market is quick and occurs more frequently than in developed markets. As a matter of fact, short-selling is limited in the Chinese stock market. Most investors

can only buy stocks in China. Mei et al. (2009) point out that the mispricing can hardly be arbitrage away at both the market level and the individual stock level in a market with the stringent constraints on short selling. It is very difficult to hedge downside risk during the bear market.

Index futures Contracts are appropriate tools to hedge downside risk during a bear market. Lien & Tse (2000) utilize the futures contracts to develop a hedge strategy that minimizes the lower partial moments. Lien & Tse (2002) review the theoretical background and the econometric implementation of various futures hedging. Chen et al. (2003) investigate different theoretical methods to the optimal futures hedge ratios.

Although the China Financial Futures Exchange launched the first index futures contracts, the CSI 300 index futures, on April 16^{th} 2010, the trading of index futures are under strict restrictions. Firstly, there are high barriers for individual investors to participant because of the high deposit requirement and the minimum account size requirement. Secondly, the margin requirements are 15% to 18%, which is much higher than the margin requirement of index futures in developed countries. Thirdly, QFIIs were not eligible to trade the index futures.

In July 2015, more restrictions on index future trading have hampered the development of financial markets. The most strict rule was that the number of opening contracts can not more than 10 per day. This rule made investors to use the index futures to manage risk. In order to develop the Chinese stock market, it is crucial to remove the restrictions on the trading of domestic index future products for investors to hedge the downside risk during the frequent bear market. In this way, the Chinese stock market can stay on the promised path of reform to become more market-oriented rather than policy-oriented.

2.5.3 "No Buffer Zone" - Restriction on Leverage

The most notable characteristic of the Chinese stock market is that the bull market is typically mixed with the bear market and that there is no sidewalk market between them. In developed markets, the sidewalk market always functions as the "buffer zone"

between the bear market and the bull market. The "No Buffer Zone" phenomenon can be explained by the overreaction effect in behavioural finance. DeBondt & Thaler (1985) find that most investors usually overreact to unexpected and dramatic news, suggesting the weak from market inefficiencies. Wang et al. (2004) study the overreaction effect in China during the period between 1994 to 2000 and find that the overreaction effect is most pronounced in A-share market.

More importantly, Hsu (2015) point out that the excess leverage from other source financing exaggerated the effect of the overreaction in China. In 2015, the Chinese stock market encountered a bull market followed by a bear market, which increased volatility to a historically high level. It is highly likely that the abnormally high volatility was caused by excess leverage, specifically through other source financing, like umbrella trusts and fund-matching companies (Hsu, 2015). By margin loan and margin financing, brokerages can increase funding by up to twice the margin (i.e. ratio at 1:2). Through umbrella trusts, one could leverage up to five times the margin (i.e. ratio at 1:5).

The excess leverage of other source financing exaggerates the downside risk of the Chinese stock market, which caused the contagion of the market crisis. It is inevitable that detailed regulation needs to be imposed on umbrella trusts and fund-matching companies (Tian, 2015). There should be strict rules in the banking sector to provide funding for umbrella trusts (Jiang, 2014). Leverage should be capped at a much lower level. The monitoring of fund-matching companies needs to be significantly reinforced. Finally, information on other source financing should be more transparent to the public.

2.6 Conclusion

The definition of bear, sidewalk, and bull markets is ambiguous in existing literature. This makes it difficult for practitioners to distinguish between different market conditions. In this chapter, we employ a statistical definition of bear, sidewalk, and bull markets, which correspond to the three states in our hidden semi-Markov model. Through the comparison with seven developed markets, we found three unique characteristics of

the Chinese stock market, namely "Crazy Bull", "Frequent and Quick Bear", and "No Buffer Zone".

"Crazy Bull" refers to the fact that the variance of the bull market in the Chinese stock market is noticeably higher than for developed markets. "Frequent and Quick Bear" is implied by the fact that the bull market occurs frequently in China and the sojourn time of the Chinese bull market is short. "No Buffer Zone" is the most prominent characteristic. It is observed that the sidewalk in developed markets always functions as a buffer zone between the bear and bull markets, while this case never occurs in China.

The possible causes of those three characteristics were discussed. Based on the discussion, it is very important to adjust the investor structure, to provide risk management tools, and to strengthen supervision on the excess leverage from other source financing.

Chapter 3

Asset Return & Camel Process: Beauty and the Beast

In this chapter, we propose a new diffusion process referred to as the "camel process" in order to model the cumulative return of a financial asset. The process considers the market condition and the price reversal. This new process includes three parameters, the market condition parameter α, the price reversal parameter β, the volatility parameter γ. Its steady state probability density function could be unimodal or bimodal, depending on the sign of the market condition parameter. The price reversal is realised through the non-linear drift term which incorporates the cube term of the instantaneous cumulative return. The time-dependent solution of its Fokker-Planck equation cannot be obtained analytically, but can be numerically solved using the finite difference method. The properties of the camel process are confirmed by our empirical estimation results of ten market indexes in two different periods.

3.1 Introduction

Diffusion processes have been widely used in the asset pricing. One of most popular parametric diffusion process is the geometric Brownian motion in the Black-Scholes model (see Black & Scholes, 1973; Merton, 1973). The geometric Brownian motion has the assumption of independent multiplicative increments, which is often violated by the empirical observation of the asset returns, i.e. stylized facts of asset returns. Many other parametric diffusion processes have been developed to improve the Black-Scholes by explaining the stylized facts (e.g. Mandelbrot, 1997; Jäckel, 2004; Bingham & Kiesel, 2001; Eberlein & Keller, 1995; Merton, 1976). To the best of our knowledge, there is no parametric diffusion process considering the market condition and the price reversal, although they have been widely studied in the literature of technical analysis and behavioural finance. Our new proposed "camel process" contributes to the fill this literature gap.

Financial economists often argue that asset price may behaves differently in different market conditions. Levy (1974) suggest to estimate separate beta coefficients for bull and bear market. Not all study are in favour of different behaviours in different market conditions. Fabozzi & Francis (1977) conclude the coefficients of the sing-index market model are not significantly different in three types of market condition definition, Bull and Bear, Up and Down, Substantial Up and Down. However, Kim & Zumwalt (1979) extend the design of Fabozzi & Francis (1977) and show the evidence that more stock exhibited significantly difference between Up-market and Dow-market betas. Chen (1982) uses the time-varying beta approach to avoid the multicollinearity problem in Kim & Zumwalt (1979) and re-examine the difference in Up-market and Dow-market betas. The results obtained from time-varying beta approach is consistent with Kim & Zumwalt (1979) and support that betas tend to be different in Up-market and Down-market. Using three-state hidden semi-Markov Model, Chapter 1 has shown that asset returns follow different distributions in different market conditions. To the best of our knowledge again, there is no diffusion process in the finance study considering the market condition.

Additionally, the violation of EMH can often be explained by behavioural finance. One of the important explanation is the overreaction hypothesis [1] that investors tend to overreact to new information, such as positive and negative shocks. The overreaction can be observed at the individual stock level (Keynes, 1964; Williams, 1938; Arrow, 1982) as well as the market level (DeBondt & Thaler, 1985; De Bondt & Thaler, 1987). Additionally, the overreaction can occur at the short-term (Zarowin, 1989; Atkins & Dyl, 1990; Cox & Peterson, 1994) as well as the long-term (DeBondt & Thaler, 1985; Loughran & Ritter, 1996; Campbell & Limmack, 1997). Price reversal is the phenomenon after the overreaction because stock prices tend to converge back to the fundamental values. The price reversal has been widely empirically studied in different markets (Bremer & Sweeney, 1991; Liang & Mullineaux, 1994; Farag, 2014). To the best of our knowledge, no diffusion process in the finance study has considered the price reversal.

In this chapter, we propose a new diffusion process referred to as the "camel process" in order to model the cumulative return of a financial asset. The camel process has two contributions. First, it is capable of modelling the cumulative return in two market conditions, either sidewalk or trending[2]. Second, the process consider the price reversal after the long-term overreaction behaviour in the financial market. The form of the camel process is parsimonious with three parameters, the market condition parameter α, the price reversal parameter β, and the volatility parameter γ. The market condition can be identified by the sign of α. The magnitude of price reversal is measured by β. γ controls the level of volatility.

The beauty of the camel process is that it considers the market condition and the price reversal. The beast is that the time-dependent solution cannot be obtained analytically, but can be numerically solved by means of a finite difference method. The name of the "camel process" is inspired by its property indicating that the steady state probability density function (PDF) could be unimodal or bimodal, depending on the sign of the

[1] It is not always overreaction, but sometimes be slow or underreaction. Hong & Stein (1999) construct a model with two groups of boundedly rational agents "newwatchers" and "momentum traders" and show the underreaction at short horizons and overreaction at long horizons. Fama (1998) claims that overreaction to information is as frequent as underreaction. Veronesi (1999) uses a dynamic, rational expectations equilibrium model of asset prices to demonstrate that stock prices underreact to good news in bad times and overreact to bad news in good times.

[2] A trending market includes both the bull market and the bear market.

market condition parameter. The price reversal is realised through the non-linear drift term which incorporates the cube term of the instantaneous cumulative return.

3.2 Literature Review

In this section, we summarize alternative models to the Black-Scholes model. The existing literature attempted to improve the Black-Scholes by explaining the stylized facts of asset returns. It is well documented that empirical daily returns have stylized facts which are the heavy-tails, the "long-memory", the volatility clustering, the Taylor effect, and so forth. (see Granger & Ding, 1995; Pagan, 1996; Cont, 2001). Those stylized facts indicate that the independent normality assumption in the Black-Scholes model is unrealistic. In order to explain the stylized facts, many research studies have been devoted to modifying the Geometric Brownian motion used in the derivation of the Black-Scholes model.

The first type of alternative models is represented by the fractional Brownian motions. Mandelbrot (1997) argues that successive price changes are not independent, and employs the fractional Brownian motion to capture the dependent increments. In the finance study, a model should be self-consistent and show no arbitrage opportunity (Kou, 2007). Nevertheless, Rogers (1997) proves that the fractional Brownian motion is not semi-martingale and shows the construction of arbitrage in the fractional Brownian motion.

The stochastic volatility and GARCH models are developed to capture the stylized fact of volatility clustering. Jäckel (2004) reviews various stochastic volatility models with a focus on the dynamic replication of exotic derivatives and their implementation. Bollerslev et al. (1992) provides a comprehensive review on the ARCH-family models. In addition to the price process, these models introduce another process for the evolution of volatility so that the time dependence of volatility could be captured.

Bingham & Kiesel (2001) asserts that the hyperbolic model is a good choice if someone wants a model that is more complex than the benchmark Black-Scholes model, but less

complicated than the stochastic volatility models. Hyperbolic diffusion models are designed due to the empirical evidence that the hyperbolic distributions could be fitted to daily returns with high accuracy (Eberlein & Keller, 1995). These models use hyperbolic distributions rather than normal distributions. Bibby & Sørensen (1996) models the logarithm of the stock price by an ergodic process using the hyperbolic invariance measure, but their simulation shows that there is no significant difference between the option price inferred by the hyperbolic diffusion model and by the Black-Scholes model.

Merton (1976) derives an option pricing formula based on the assumption that the underlying stock returns are generated by the combination of continuous and jump processes. The abnormally large empirical returns can be explained by the jump-diffusion model, which can also replicate the heavy tails of the daily return distribution. Kou (2002) proposes a double exponential jump-diffusion model which gives analytical solutions for path-dependent options. Cont & Tankov (2004) reviews the models based on the jump processes. There are some other alternative models, namely the "implied binomial tress" (Dupire et al., 1994), time changed Lévy process (Carr et al., 2003), and the affine jump-diffusion models (Duffie et al., 2000).

The reminder of the chapter is structured as follows. Section 3.3 defines the camel process and discusses its properties. Section 3.4 presents empirical estimation results of ten market indexes in two different periods. Section 3.5 summarises the chapter.

3.3 The SDE and its properties

The "camel process" captures the dynamically non-linear interaction between the increment of the cumulative return and the instantaneous cumulative return with the consideration of the market condition and the price reversal. The non-linear relationship is achieved by the inclusion of the cube term of the instantaneous cumulative return, which facilitates the modelling of price reversal after the overreaction behaviour. The sign of drift term is determined by the market condition, whether the cumulative return deviating from zero in the trending market condition or moving towards zero in the sidewalk market condition. The camel process is defined as:

Definition 3.1. The camel process solves the stochastic differential equation (SDE)

$$\mathrm{d}X_t = (\alpha X_t - \beta X_t^3)\,\mathrm{d}t + \gamma\,\mathrm{d}W_t\,, \quad X_0 = 0 \tag{3.1}$$

where α, β, and γ are three parameters with $\alpha \in \mathbb{R}$, $\beta \in \mathbb{R}_{\geq 0}$, and $\gamma \in \mathbb{R}_{+}$.

Parameter α is referred to as the market condition parameter. If $\alpha > 0$, the market is in a trending market condition. Otherwise, it is in a sidewalk market condition. Parameter β controls the price reversal after the overreaction behaviour in the market. If there is no overreaction, β is essentially zero. Parameter γ measures the volatility of the process. In the camel process, the volatility is constant. In terms of the parameter space, α can be any real number, β is a non-negative real number, and γ can only be a positive real number. Since the underlying process modelled is the cumulative return, the process always starts at zero.

We investigate the cumulative return rather than the price or the log price for two reasons. First, the overreaction can be easily measured by the cumulative return. Second, the cumulative return facilitates the comparison of investments in different financial assets.

The cumulative return investigated by us is defined as

$$X_t = \sum_{i=1}^{t} r_i \tag{3.2}$$

where r_i is the log return [3] of the price process $\{P_t, t \geq 0\}$ of the asset

$$r_i = \log(P_t) - \log(P_{t-1}) \tag{3.3}$$

3.3.1 Steady State PDF

It is difficult to analytically obtain the solution of the camel process due to its high order non-linear term. We here use the Fokker-Planck equation to conduct a partial analytic

[3] Like most researches, we prefer the log return rather than the arithmetic return $Y_i = (P_t - P_{t-1})/P_{t-1}$. The reason is that the cumulative return over an n period is the sum of the log return (shown in Equation 3.2), while the arithmetic return does not have this property.

analysis. For a SDE, the Fokker-Planck equation is a partial differential equation (PDE) which describes the evolution of its probability density $p(X_t, t)$, namely the probability of the realisations being near X_t at time t. The Fokker-Planck equation constructs a useful relationship between the solution of a SDE and its PDF as a function of time.

Applying the general Fokker-Planck equation to Equation 3.1 produces the PDF $p(X_t, t)$ for the camel process.

$$\frac{\partial p(X_t,t)}{\partial t} = -\frac{\partial}{\partial X_t}\left[(\alpha X_t - \beta X_t^3)p(X_t,t)\right] + \frac{\partial^2}{\partial X_t^2}\left[\frac{1}{2}\gamma^2 p(X_t,t)\right] \tag{3.4}$$

The steady state solution of the Fokker-Planck equation is the PDF evolving for a fairly long time so that it converges to a stable function which no longer changes as a function of time t. The steady state PDF $p(X)$ of the camel process satisfies the time-independent Fokker-Planck equation by setting $\frac{\partial p(X_t,t)}{\partial t} = 0$.

$$0 = -\frac{\partial}{\partial X}\left[(\alpha X - \beta X^3)p(X)\right] + \frac{\partial^2}{\partial X^2}\left[\frac{1}{2}\gamma^2 p(X)\right] \tag{3.5}$$

Analytically solving [4] Equation 3.5 gives the solution of the steady state PDF of the camel process

$$p(X) = A\exp\left(\frac{\alpha X^2 - \beta X^4/2}{\gamma^2}\right) \tag{3.6}$$

where A is the integration constant.

We demonstrate that the steady-state PDF of the camel process could be unimodal or bimodal, depending on the sign of the market condition parameter α. Figure 3.1 displays the steady state PDF of the camel process for two combinations of the parameter values. When α is less than zero, the steady state PDF is unimodal, which resembles a one-humped camel. If α is larger than zero, the steady state PDF is bimodal, looking like a two-humped camel.[5] The name of the "camel process" was inspired by the feature implying that its steady-state PDF could be unimodal or bimodal, which reminds people of two types of camels.

[4] Details of the mathematical derivation are presented in 3.A.

[5] The case that α is equal to zero is shown in 3.B.

Parameter α is referred to as the market condition parameter since its sign determines whether the steady state PDF is unimodal or bimodal. The unimodal situation corresponds to the sidewalk market condition. In this situation, the underlying process (the cumulative return) has a tendency to zero because the SDE drift term has an opposite sign to its instantaneous cumulative return. Hence, the price series shows a mean-reverting pattern and the steady state PDF is centralised around zero. The bimodal situation corresponds to the trending market condition in which the price tends to move upside or downside. In a trending market, a positive α generally implies that the SDE drift term has the same sign as the instantaneous cumulative return within the rational region. The cumulative return moves away from the start point, zero. In the steady state, the two modes of the PDF deviate from zero. The camel process is arbitrage-free and self-consistent. Either in a unimodal or a bimodal situation, the moving direction of the cumulative return is unknown.

FIGURE 3.1: Market Condition Parameter α
Unimodal vs. Bimodal

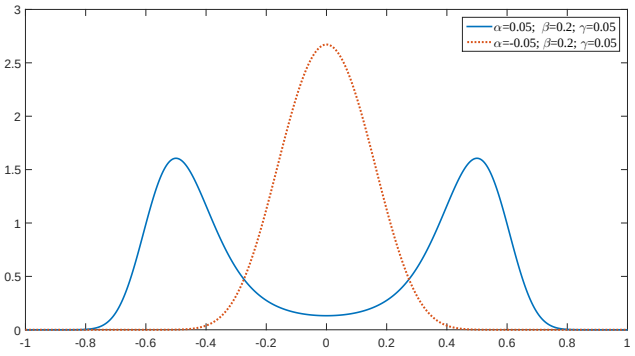

In order to capture the price reversal, we use a non-linear drift term which incorporates the cube of the instantaneous cumulative return. Through this non-linear drift term, the underlying process cannot go to infinity. The price reversal will occur if the cumulative return goes beyond the rational level (i.e. fundamental value). Overreaction behaviour means that the price largely deviates from its rational level. The cumulative return would go back into its rational range if it is in the overreaction area, which will be discussed later. In the "camel process", there is an implicit assumption that the price reversal can only occur in the trending market condition. There is no price reversal in the sidewalk market condition because the drift term always has the opposite sign

as the instantaneous cumulative return in the sidewalk market condition, which will be discussed in detail later.

Parameter β is the parameter which controls the price reversal. Figure 3.2 displays the steady state PDF of both the sidewalk and trending market condition. There is no big effect of the price reversal parameter β on the steady state PDF when the market is in sidewalk. However, the effect of β is vital if the market is in the trending state. A larger value of β forces the mode of the steady state PDF more close to zero. In contrast, the mode of the steady state PDF can move further away if β is small.

The price reversal is realised through the non-linear drift term $\alpha X_t - \beta X_t^3$. Figure 3.3 shows the shape of the non-linear drift term under both market conditions. In a sidewalk market condition, the drift term always has the opposite sign as the instantaneous cumulative return. Hence, the cumulative return moves towards to zero and shows the mean-reverting pattern. Under this situation, the price reversal normally rarely occurs. However, the price reversal plays a vital role in the trending market condition. As you can see in the lower panel of Figure 3.3, there is a middle region that the drift term has the same sign as the instantaneous cumulative return. There are other two side regions indicating that the sign is opposite. The two side regions are deemed as the overreaction area. If the cumulative return goes into the overreaction area, the drift term would force it to move back the rational region, which is the one in the middle.

The range of the rational region is controlled by parameter β. If the value of β is large, then the magnitude of the price reversal is stronger and the rational region is narrower. Conversely, a smaller β means that the market can tolerate overreaction to a larger extent. Thus, the range of the rational region is wider.

Parameter γ is known as the volatility parameter. It controls the volatility magnitude of $\mathrm{d}W_t$. Figure 3.4 illustrates that the steady state PDF is more diversified with a larger value of γ. By contrast, a smaller value of γ results in a more centralised steady state PDF. Importantly, the mode of the steady state PDF remains the same irrespective of the change of the value of γ under both unimodal or bimodal situations. The mode of the steady state PDF only depends on the market condition parameter α and the overreaction parameter β.

FIGURE 3.2: Volatility Parameter β

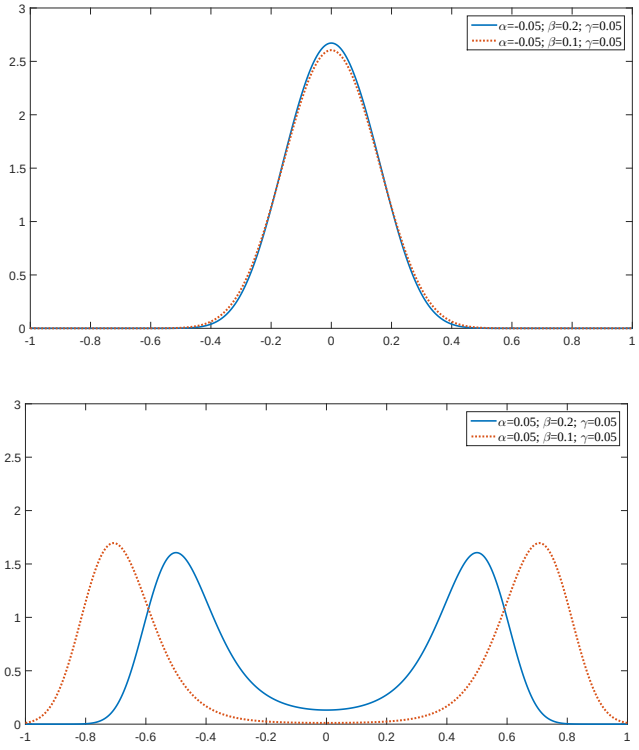

FIGURE 3.3: Drift Term

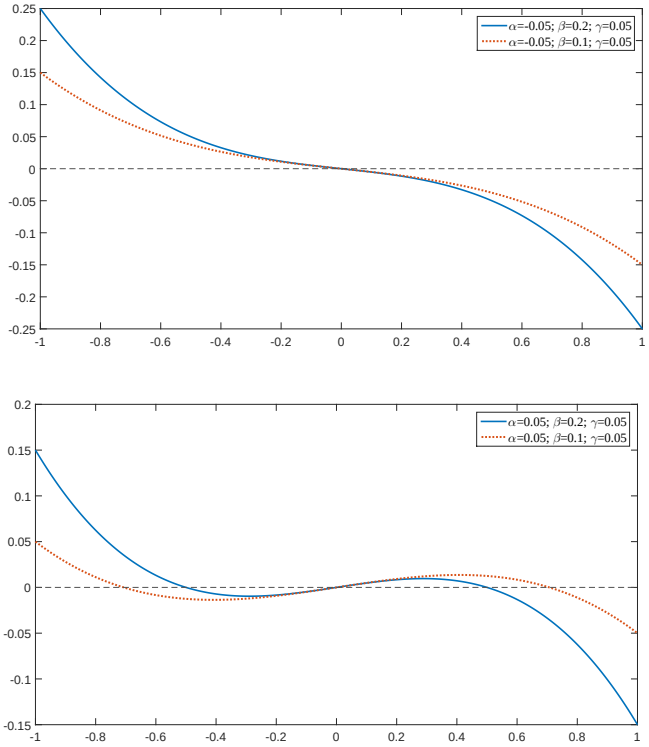

FIGURE 3.4: Volatility Parameter γ

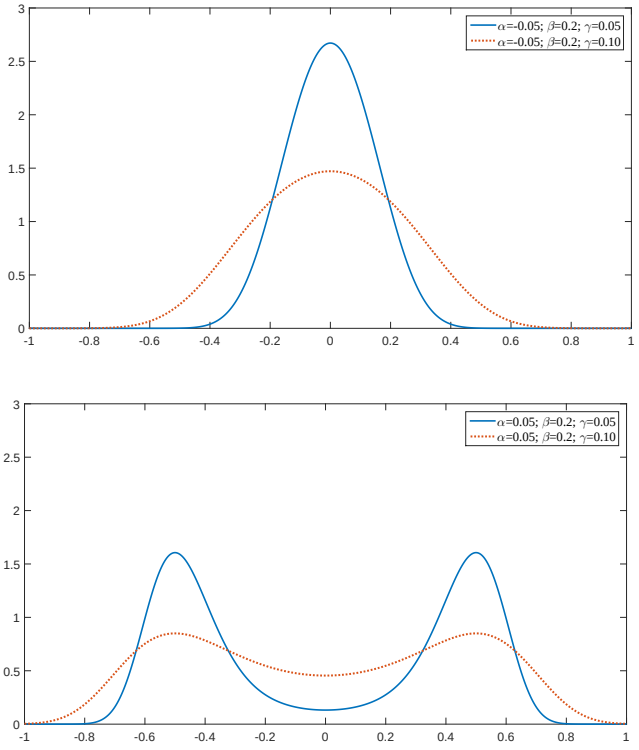

3.3.2 Time Dependent PDF

Without the assumption $\frac{\partial p(X_t,t)}{\partial t} = 0$, the solution of Equation 3.4 is the time dependent PDF $p(X_t, t)$ of the camel process, which is evolving as a function of time t and converges to its steady state PDF $p(X)$. The analytical solution of the Fokker-Planck equation can only be obtained in limited special cases, and mostly in the steady state (Pichler et al., 2013).

During the past five decades, a number of numerical methods have been developed to obtain the approximated solution of the Fokker-Planck equation. These numerical methods include the weighted residual method, the eigenfunction expansion, the finite differences, and the finite elements. Roberts (1986) use the finite difference method to solve the Fokker-Planck equation for the one-dimensional [6] time dependent PDF. Higham (2004) employ the finite difference method to numerically solve the Black-Scholes PDE with the focus on European calls and puts options.Gaviraghi et al. (2016) and Gaviraghi (2017) provide the theoretical and numberical analysis for the Fokker-Planck models which are

[6] In our case, there is only one spatial variable X_t besides the time variable t.

related to jump-diffusion processes. Although there are more accurate higher order finite difference schemes (see Wojtkiewicz et al., 1997), one dimensional finite difference method is enough for our problem. Our examples show that the numerically solved time dependent PDF converges to a steady state PDF accurately.

In order to use the finite difference method to numerically solve the Fokker-Planck equation, we need to clarify the initial condition, the boundary condition, and the normalisation condition. The initial condition $p(X_0, 0)$ is given by the Dirac delta function

$$p(X_0, 0) = \delta(X_0 - 0) \tag{3.7}$$

where X_0 is zero since the underlying process is the cumulative return.

The boundary condition is imposed by a zero-flux condition at infinity of X_t

$$p(X_t, t) \to 0 \quad \text{as} \quad X_t \to \pm\infty \tag{3.8}$$

Additionally, the normalisation condition for the time dependent PDF is given by

$$\int p(X_t, t)\, \mathrm{d}X_t = 1 \tag{3.9}$$

Here, we derive the explicit scheme of the Finite Difference method. Applying the chain rule on Equation 3.4, we can obtain

$$\frac{\partial p(X_t, t)}{\partial t} = (-\alpha + 3\beta X_t^2)p(X_t, t) + (-\alpha X_t + \beta X_t^3)\frac{\partial p(X_t, t)}{\partial X_t} + \frac{1}{2}\gamma^2 \frac{\partial^2 p(X_t, t)}{\partial X_t^2} \tag{3.10}$$

In order to keep the notation cleaner, we suppress the time subscript of X_t as X, and suppress the argument X_t and t of the time dependent PDF $p(X_t, t)$ and use the notation p.

$$\frac{\partial p}{\partial t} = (-\alpha + 3\beta X^2)p + (-\alpha X + \beta X^3)\frac{\partial p}{\partial X} + \frac{1}{2}\gamma^2 \frac{\partial^2 p}{\partial X^2} \tag{3.11}$$

In terms of central finite differences, the above PDF becomes

$$\frac{p_i^{m+1} - p_i^m}{\Delta t} = (-\alpha + 3\beta X^2)p_i^m + (-\alpha X + \beta X^3)\frac{p_{i+1}^m - p_{i-1}^m}{2\Delta X} + \frac{1}{2}\gamma^2 \frac{p_{i+1}^m - 2p_i^m + p_{i-1}^m}{\Delta X^2} \tag{3.12}$$

where m is the integer index of the mesh on time and i is the integer index of the mesh on space.

The explicit scheme is obtained for the time dependent PDF

$$p_i^{m+1} = p_i^m + \Delta t \left\{ (-\alpha + 3\beta X^2)p_i^m + (-\alpha X + \beta X^3)\frac{p_{i+1}^m - p_{i-1}^m}{2\Delta X} + \frac{1}{2}\gamma^2 \frac{p_{i+1}^m - 2p_i^m + p_{i-1}^m}{\Delta X^2} \right\} \tag{3.13}$$

Using this scheme, the values p_i^{m+1} can be calculated directly from values p_i^m. Under the initial condition, boundary condition, and the normalisation condition, the time dependent PDF can be solved directly.

Figure 3.5 displays two examples of the numerical solution of the time dependent PDF starting at time 1 [7]. The upper panel is the case of the sidewalk market condition in which α is negative. The lower panel is the case of the trending market condition in which α is positive. In the sidewalk market condition, the time dependent PDF is always unimodal. Whereas in the trending market condition, the time dependent PDF at the early stage is unimodal because it evolves from the initial condition which is a Dirac delta function. After some periods, the time dependent PDF appears to be bimodal and the density around the two modes is getting increasingly higher as a function of time.

Figure 3.6 shows some slices of the time dependent PDF and compares them with the steady state PDF. In the upper panel (sidewalk market condition), the time dependent PDF converges to the steady state PDF in a rapid manner. The difference is subtle between the time dependent PDF at $t = 20$ and the steady state. After 50 periods, the time dependent PDF almost overlaps with the steady state PDF. However, the convergence rate in the lower panel (trending market condition) is slower. At $t = 20$, the time dependent PDF is still unimodal. After 40 periods, we can observe that the

[7] The PDF at time 0 is omitted here because that is the initial condition, which is a Dirac delta function.

FIGURE 3.5: Time Dependent PDF

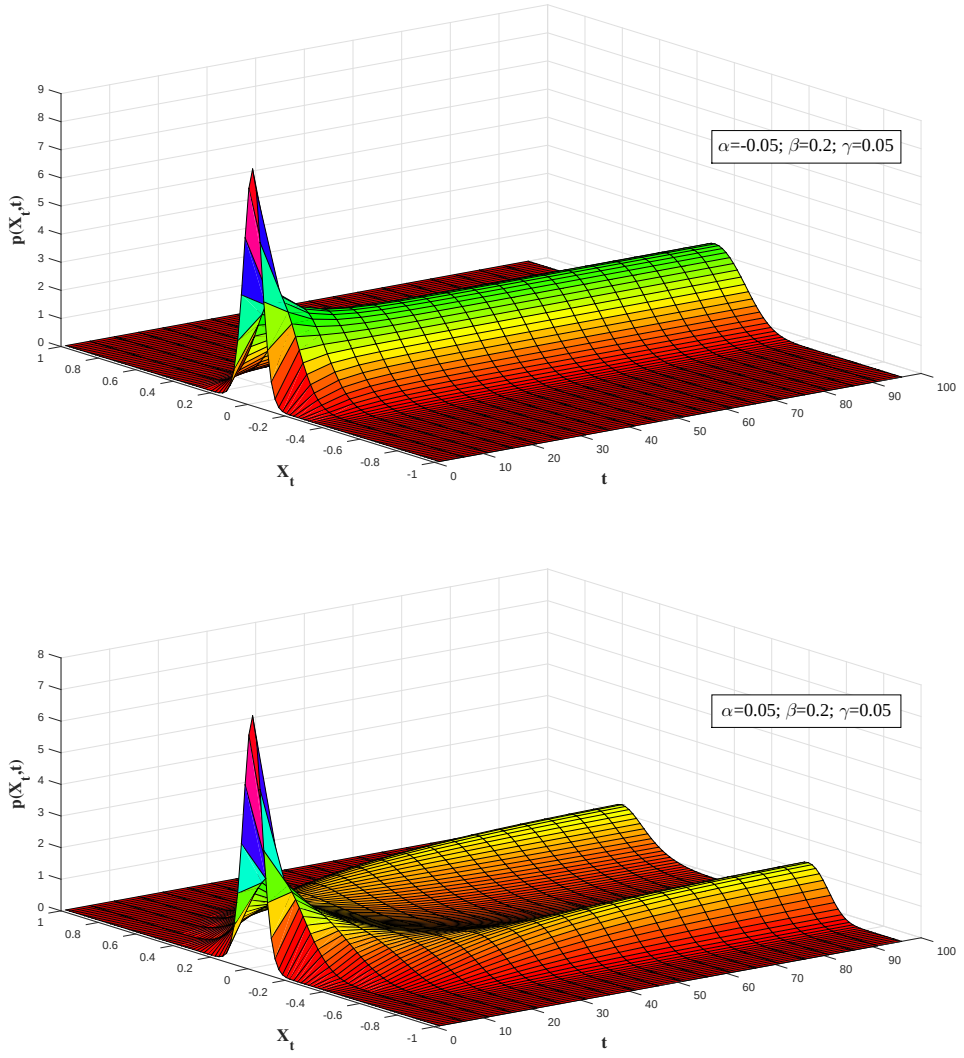

time dependent PDF is bimodal and evolves towards the steady state PDF. At $t = 100$, it is not obvious to distinguish the time dependent PDF and the steady state PDF.

3.4 Empirical Study

3.4.1 Data

The maximum likelihood method is employed in order to estimate the camel process for ten stock market indexes, S&P 500, FTSE 100, CAC 40, DAX, Nikkei 225, STI, ASX

FIGURE 3.6: Time Dependent PDF Slices vs. Steady State PDF

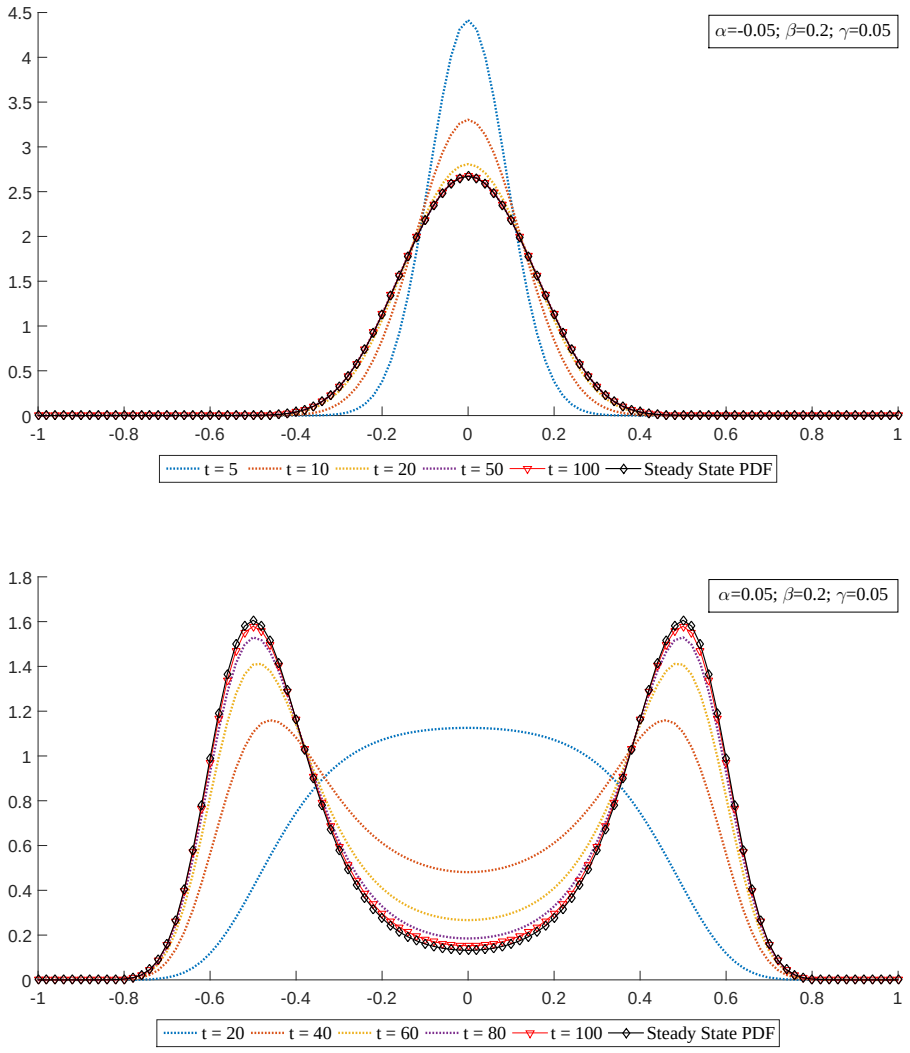

200, CSI 300 (a.k.a. SHSE 300), HSI, and TAIEX. We downloaded the daily closing prices from Yahoo Finance and computed the cumulative returns by Equation 3.2. We are particularly interested in two specific periods, August 1st 2008 to March 31st 2009 and May 1st 2014 to April 30th 2016. The first period is after the financial crisis in 2008 and all markets experienced a declining trend. Thus, we expect to see that the estimated market condition parameters $\hat{\alpha}$ are all positive for different markets. The second period is the recent year and different markets may behave differently. We can use the estimated parameters to investigate their market conditions and the magnitude of the price reversal for the two periods.

3.4.2 Maximum Likelihood Estimator

The log likelihood function for the camel process given a specific dataset is

$$\mathscr{L}(\boldsymbol{\Theta}) = \sum_{t=1}^{T} \log \tilde{p}(X_t, t|\boldsymbol{\Theta}) \tag{3.14}$$

where $\boldsymbol{\Theta} = \{\alpha, \beta, \gamma\}$, X_t is the observation at time t, and $\tilde{p}(X_t, t|\boldsymbol{\Theta})$ is the numerical solver of Equation 3.10. The maximum likelihood method estimates the parameters by maximising the log likelihood function.

$$\hat{\boldsymbol{\Theta}} = \arg\max_{\boldsymbol{\Theta}} \sum_{t=1}^{T} \log \tilde{p}(X_t, t|\boldsymbol{\Theta}) \tag{3.15}$$

where $\hat{\boldsymbol{\Theta}}$ needs to be in the parameter space that $\alpha \in \mathbb{R}$, $\beta \in \mathbb{R}_{\geq 0}$, and $\gamma \in \mathbb{R}_{+}$.

3.4.3 Estimation Result

Table 3.1: Estimation Result

	Aug. 2008 ∼ Apr. 2009				**May. 2015 ∼ Apr. 2016**			
	$\hat{\alpha}$	$\hat{\beta}$	$\hat{\gamma}$	likelihood	$\hat{\alpha}$	$\hat{\beta}$	$\hat{\gamma}$	likelihood
S&P500	0.498	4.217	0.256	98.513	-0.106	0.000	0.025	536.050
FTSE100	0.057	0.680	0.039	193.790	0.010	0.515	0.011	480.400
CAC40	0.070	0.551	0.056	138.760	-0.020	0.666	0.024	436.110
DAX	0.237	1.790	0.113	110.950	0.009	0.568	0.011	439.200
Nikkei225	0.084	0.374	0.034	165.020	-0.039	1.418	0.036	394.420
STI	0.063	2.592	0.349	22.264	0.021	0.351	0.019	357.100
ASX200	0.046	0.407	0.027	223.150	0.020	0.883	0.008	529.300
CSI300	0.092	0.657	0.059	131.820	0.208	1.748	0.109	182.570
HSI	0.085	0.308	0.056	137.570	0.069	0.845	0.041	269.690
TAIEX	0.246	1.624	0.093	123.190	0.016	0.521	0.012	420.130

Table 3.1 presents the estimated parameters for ten indexes during two periods. In the first period (Aug. 2008 to Apr. 2009), the estimated market condition parameters $\hat{\alpha}$ are all positive, indicating that they were all in a trending market condition. This is consistent with the reality that all ten markets had a downside trend after the financial crisis. S&P 500, STI and DAX have relatively large values of $\hat{\beta}$, implying that those three markets had a strong price reversal for the market crash after the financial crisis.

In the second period (May. 2015 to Apr. 2016), S&P, CAC 40 and Nikkei 225 were in a sidewalk condition, while other markets were in a trending condition. CSI 300 has the highest value of the estimated market condition parameter $\hat{\alpha}$ (0.208), suggesting that the Chinese market experienced a relatively large trend. Our estimation result is consistent with reality. Figure 3.1 compares the cumulative return of S&P 500 and CSI 300. It is clear that S&P 500 was in a sidewalk market condition in which its cumulative return was fluctuating around zero, while CSI 300 experienced a significant trend and its cumulative return largely deviated from zero.

FIGURE 3.1: Cumulative Return of S&P 500 and CSI 300 (May 2015 to Apr. 2016)

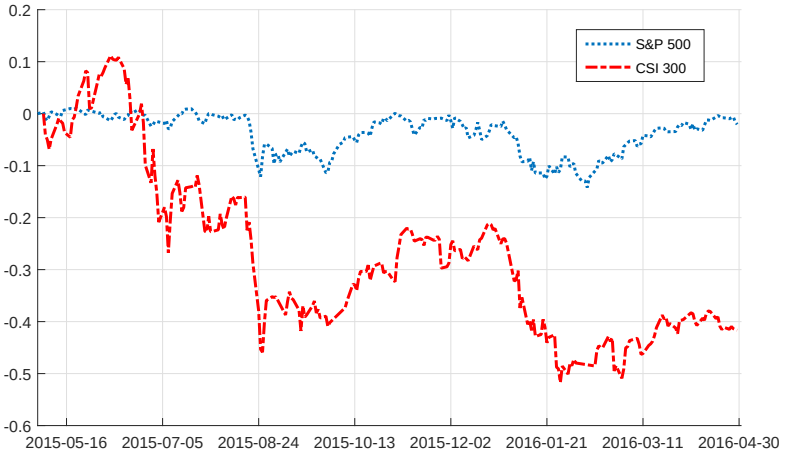

3.5 Conclusion

In this chapter, we propose a new stochastic process for modelling the cumulative return of a financial asset, which is referred to as the "camel process". The process considers the market condition and the price reversal. This new process has three parameters, the market condition parameter α, the price reversal parameter β, and the volatility parameter γ. Its steady state probability density function (PDF) could be unimodal or bimodal, depending on the sign of the market condition parameter. The price reversal is realised through the non-linear drift term which incorporates the cube term of the instantaneous cumulative return. The time-dependent solution of its Fokker-Planck equation cannot be obtained analytically, but can be numerically solved by means of the finite difference method. The properties of the camel process are confirmed by our empirical estimation results of ten market indexes in two different periods. A limitation

of this chapter is that the parameters of the camel process are possibly time-varying. In other words, the parameters may not be stable during the two periods in the empirical analysis. Future research may wish to develop the change point detection for the camel process.

Appendix

3.A Steady State Solution of the Fokker-Planck Equation

Theorem 3.2 (Fokker-Planck equation)**.** *Consider the Ito process X_t with drift $\mu(X_t)$ and volatility $\sigma(X_t)$, and hence satisfying the SDE $dX_t = \mu(x_t)dt + \sigma(x_t)dW_t$. The probability density function (PDF) of the ensemble of realisations $p(X_t, t)$ satisfies the Fokker-Planck equation* [8]*.*

$$\frac{\partial p(X_t,t)}{\partial t} = -\frac{\partial}{\partial X_t}[\mu(X_t)p(X_t,t)] + \frac{\partial^2}{\partial X_t^2}\left[\frac{1}{2}\sigma(X_t)^2 p(X_t,t)\right]$$

The camel process solves the SDE

$$dX_t = (\alpha X_t - \beta X_t^3)dt + \gamma dW_t, \quad X_0 = 0 \tag{3.16}$$

where $\alpha \in \mathbb{R}$, $\beta \in \mathbb{R}_{\geq 0}$, and $\gamma \in \mathbb{R}_+$. The drift term is $\alpha X_t - \beta X_t^3$ and the volatility term is γ.

The Fokker-Planck equation for the camel process is

$$\frac{\partial p(X_t,t)}{\partial t} = -\frac{\partial}{\partial X_t}\left[(\alpha X_t - \beta X_t^3)p(X_t,t)\right] + \frac{\partial^2}{\partial X_t^2}\left[\frac{1}{2}\gamma^2 p(X_t,t)\right] \tag{3.17}$$

[8] The Fokker-Planck equation is also known as the Kolmogorov forward equation.

By setting $\frac{\partial p(X_t,t)}{\partial t} = 0$, we can obtain the steady state PDF $p(X)$ which satisfies the time-independent Fokker-Planck equation

$$0 = -\frac{\partial}{\partial X}\left[(\alpha X - \beta X^3)p(X)\right] + \frac{\partial^2}{\partial X^2}\left[\frac{1}{2}\gamma^2 p(X)\right] \tag{3.18}$$

One integral with respect to X

$$\begin{aligned}
\int 0\,\mathrm{d}X &= \int -\frac{\partial}{\partial X}\left[(\alpha X - \beta X^3)p(X)\right] + \frac{\partial^2}{\partial X^2}\left[\frac{1}{2}\gamma^2 p(X)\right]\mathrm{d}X \\
0 &= -(\alpha X - \beta X^3)p(X) + \frac{\partial}{\partial X}\left[\frac{1}{2}\gamma^2 p(X)\right] + \text{constant} \\
\text{constant} &= -(\alpha X - \beta X^3)p(X) + \frac{\partial}{\partial X}\left[\frac{1}{2}\gamma^2 p(X)\right]
\end{aligned}$$

This constant must be zero, as $p(X)$ and its derivatives have to vanish for a large enough X.

$$\begin{aligned}
0 &= -(\alpha X - \beta X^3)p(X) + \frac{\partial}{\partial X}\left[\frac{1}{2}\gamma^2 p(X)\right] \\
0 &= -(\alpha X - \beta X^3)p(X) + \frac{1}{2}\gamma^2\frac{\mathrm{d}p(X)}{\mathrm{d}X} \\
\frac{1}{2}\gamma^2\frac{\mathrm{d}p(X)}{\mathrm{d}X} &= (\alpha X - \beta X^3)p(X) \\
\frac{1}{p(X)}\,\mathrm{d}p(X) &= \frac{2(\alpha X - \beta X^3)}{\gamma^2}\,\mathrm{d}X
\end{aligned}$$

Integral on both hand sides

$$\begin{aligned}
\int \frac{1}{p(X)}\,\mathrm{d}p(X) &= \int \frac{2(\alpha X - \beta X^3)}{\gamma^2}\,\mathrm{d}X \\
\log p(X) &= \int \frac{2\alpha X}{\gamma^2} - \frac{2\beta X^3}{\gamma^2}\,\mathrm{d}X \\
&= \int \frac{2\alpha X}{\gamma^2}\,\mathrm{d}X - \int \frac{2\beta X^3}{\gamma^2}\,\mathrm{d}X \\
&= \frac{\alpha X^2}{\gamma^2} - \frac{\beta X^4/2}{\gamma^2} + \text{constant} \\
&= \frac{\alpha X^2 - \beta X^4/2}{\gamma^2} + \text{constant}
\end{aligned}$$

Taking the exponential on both hand sides produces the solution

$$p(X) = A \exp\left(\frac{\alpha X^2 - \beta X^4/2}{\gamma^2}\right) \tag{3.19}$$

where A is the integration constant. In order to determine the integration constant A, we can use the property of the PDF indicating that the area underneath must be one.

$$\begin{aligned}
1 &= \int_0^\infty A \exp\left(\frac{\alpha X^2 - \beta X^4/2}{\gamma^2}\right) \mathrm{d}X \\
1 &= A \int_0^\infty \exp\left(\frac{\alpha X^2 - \beta X^4/2}{\gamma^2}\right) \mathrm{d}X \\
A &= \left(\int_0^\infty \exp\left(\frac{\alpha X^2 - \beta X^4/2}{\gamma^2}\right) \mathrm{d}X\right)^{-1}
\end{aligned}$$

Applying series expansion and integrating with respect to individual items

$$A = \left(\frac{1}{2} \sum_{m=0}^{\infty} \frac{\left(\frac{\alpha}{\gamma^2}\right)^m}{m!} \frac{\Gamma\left(\frac{2m+1}{4}\right)}{\left(\frac{\beta}{2\gamma^2}\right)^{\frac{2m+1}{4}}} \right)^{-1} \tag{3.20}$$

where $\Gamma(\cdot)$ is the gamma function.

3.B Steady State PDF when α is zero

FIGURE 3.B.1: when α is zero, the Steady State PDF has a flat area near zero in the x-axis.

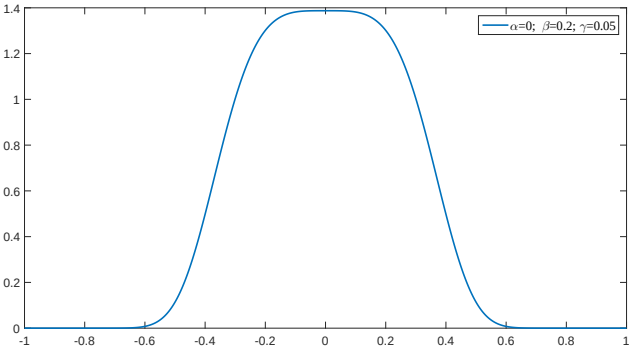

Chapter 4

Forecasting the Log Return of Term Structure for Chinese Commodity Futures:

an h-step Functional Autoregressive Model

This chapter takes the tools in functional data analysis to understand the term structure of Chinese commodity futures and forecast their log returns at both short and long horizons. A functional ANOVA (FANOVA) has been applied in order to examine the calendar effect of the term structure. We use an h-step Functional Autoregressive model to forecast the log return of the term structure. Compared with the naive predictor, the in-sample and out-of-sample forecasting performance indicates that additional forecasting power is gained by using the functional autoregressive structure. Although the log return at short horizons is not predictable, the forecasts appear to be more accurate at long horizons due to the stronger temporal dependence. The predictive factor method has a better in-sample fitting, but it cannot outperform the estimated kernel method for out-of-sample testing, except in the case of 1-quarter-ahead forecasting.

4.1 Introduction

As a matter of fact, investors cannot short sell stocks in the Chinese stock market. The stringent constraints on short selling stocks make it very difficult to manage the downside risk. Although the index futures contracts were launched by the China Financial Futures Exchange in 2010, there are many restrictions on the trading of index futures at the moment. Investors in China are seeking opportunities to broaden the scope of their portfolio to diversify risk. Many studies have shown that investing in commodity futures is an effect way to diversify against falling stock prices (e.g. Edwards & Caglayan, 2001; Jensen et al., 2002; Wang & Yu, 2004; Erb & Harvey, 2006). Gorton & Rouwenhorst (2006) show that the commodity futures returns are negatively correlated with equity returns. Ten years later, Bhardwaj et al. (2015) find that their conclusions largely hold up out-of-sample, and conclude that the negative correlation between commodity futures returns and equity returns is robust. It is worthwhile and meaningful to investigate the commodity futures market in China.

The existing literature mainly focuses on forecasting the term structure of government bond yields. Only a limited number of studies have been devoted to forecasting the term structure of commodity futures. It is even more difficult to find studies on forecasting the term structure of commodity futures in developing countries. This chapter fills the literature gap in the forecasting research on the log return of the term structure for commodity futures, with a particular interest in Chinese markets, since China has the largest trading volume of commodity futures in the world.

In 2015, the total trading volume and the trading value of Chinese commodity futures accounted for 3.237 billion contracts and RMB 136.47 trillion, respectively (Shanghai Institute of Futures and Derivatives, 2016). Table 4.1 lists the top 10 global futures and options exchange in 2015 by the trading volume of the commodity futures and options. Three Chinese commodity futures exchanges, namely the Dalian Commodity Exchange, Zhengzhou Commodity Exchange, and Shanghai Futures Exchange, were ranked among the top 3 largest exchanges. Hence, China plays a vital role in the global futures market, especially for commodity futures.

TABLE 4.1: Top 10 Global Futures and Options Exchange in 2015
by Trading Volume of Commodity Futures and Options

2015 Ranking	**2014 Ranking**	**Exchange**	**2015 (10,000 Contracts)**	**2014 (10,000 Contracts)**
1	5	*Dalian Commodity Exchange*	111632	76964
2	3	*Zhengzhou Commodity Exchange*	107034	67634
3	1	*Shanghai Futures Exchange*	105049	84229
4	2	CME Group	90675	77796
5	4	ICE	70067	64899
6	7	Multi Commodity Exchange	21635	13375
7	6	HKEX	16960	17716
8	10	Moscow Exchange	12328	2022
9	8	National Commodity and Derivatives Exchange	2955	3014
10	9	Tokyo Commodity Exchange	2440	2186

Source: The 2016 Development Report on China's Futures Markets, Futures Industry Association (FIA), China Futures Association
Note: The trading volumes of the DCE as compiled by the FIA are not consistent with those by the China Futures Association. This table uses the data from the latter organisation. CME group: Chicago Mercantile Exchange & Chicago Board of Trade. ICE: Intercontinental Exchange. HKEX: Hong Kong Stock Exchange.

Traditional methods focus on foresting term structure. Nelson & Siegel (1987) develop a parsimonious model that uses exponential components to fit the common shapes of the yield curves, namely monotonic, humped, and S-shaped. The three factors in the Nelson-Siegel model can be interpreted as level, slope, and curvature. Diebold & Li (2006) further develop the Nelson-Siegel model into a three-dimensional parameter model that evolves dynamically. The time-varying parameters have autoregressive structures. Their forecasting is based on the prediction of factors and has an accurate performance at long horizons.

Recent developments in the theory of functional data analysis facilitate the modelling of the term structure. Functional data analysis is a statistical discipline aiming to analyse data represented by curves. When such functional data are collected sequentially and there is dependence between the observations, then this is referred to as functional time series data (Hörmann & Kokoszka, 2010). The collection of term structure and its log return in a period is constituted by functional time series observations.

It is natural to treat term structure and its log return as curves and use a functional data setting rather than a large dimensional VAR model. Bardsley et al. (2017) believe that the term structure of bonds are fundamentally continuous time functions, although

the data are observed only at discrete times. It should be highlighted that the term structure of commodity futures $P_n(t)$ and its log return are also always existing for all t, even if we have observations only for some t, i.e. there is a price of a commodity with delivery t times later after the contract is signed on day n. $P_n(t)$ is a continuous function in nature.

Bosq (2000) developed the theory of general functional linear processes, including the functional autoregressive processes, in the Hilbert and Banach spaces. Ramsay & Silverman (2006), Hörmann & Kokoszka (2010), and Horváth & Kokoszka (2012) provide recent theoretical developments in terms of functional linear processes. The conventional method to estimate the functional autoregressive model is the estimated kernel method using functional principal components. Kargin & Onatski (2008) develop a more refined approach by using predictive factors which focus on the directions more relevant to the predictions. They provide an example using their approach in order to predict the term structure of the Eurodollar futures rates. Didericksen et al. (2012) study the finite sample performance of both the estimated kernel method and the predictive factor method, and their simulation shows that the predictive factor method does not dominate the estimated kernel method.

In the illustrative example of Kargin & Onatski (2008), they firstly demean the data, make the prediction for the demeaned data, and then add the mean back for the real prediction. We believe that it is more natural to forecast the log return of the term structure by means of the functional AR(1) model. There are two advantages of working with the log return of the term structure, rather than with the term structure. First, the log return has zero mean, which can be fed into the functional AR(1) model directly. Second, the log return of the term structure is usually stationary, which meets the conditions of the functional AR(1) model. Since we are working with the log return of the term structure, it is inappropriate to compare our method with traditional methods (e.g. Diebold & Li, 2006). Following Didericksen et al. (2012), we use a naive predictor as our benchmark model.

The remainder of the chapter is as follows. Section 4.2 describes our data and provides the functional descriptive statistics. Section 4.3 applies the functional ANOVA in order to examine the calendar effect. Section 4.4 briefly introduces the two prediction approaches, namely the estimated kernel method and the predictive factor method. In Section 4.5, the forecasting performance is presented with in-depth discussions. Section 4.6 summarises the chapter.

4.2 Data and Functional Descriptive Statistics

Based on two criteria, we select 18 commodity futures traded in China. First, we exclude illiquid commodity futures, such as Wire Rod (symbol: WR), Wheat (symbol: WH), and Early Rice (symbol: RI). Secondly, we exclude commodity futures with too many missing data. Glass (symbol: FG), Methanol (symbol: MA), and Polypropylene (symbol: PP) are not considered because of too many missing data. Table 4.1 shows comprehensive information about the selected commodity futures. Note that the number of observations for the curve is not exactly the same. For instance, there are 8 points in the term structure of A, 12 points in that of AG, and 5 points in that of C. It should be highlighted that this is the reason why a standard multivariate technique cannot be used.

We use the daily settlement price for the commodity futures that we downloaded from Wind. Note that different commodity futures have different periods of data. The in-sample period for training data is from the first date to the middle point of the entire period, and the out-of-sample period for testing data is from one trading day after the in-sample period to the end of the entire period. The number of observations in the in-sample period and the out-of-sample period is approximately the same.

Table 4.1: Commodity Futures Information

Symbol	Commodity	Exchange	Sector	LTD	LD	Contract Month	In-Sample		Out-of-Sample	
A	soybean	DCE	oil and oilseed	10‡	16	1,3,5,7,9,11	2007-01-04	2012-01-11	2012-01-12	2017-01-25
AG	silver	SHF	noble metal	15†	12	1,2,3,4,5,6,7,8,9,10,11,12	2012-09-18	2014-11-27	2014-11-28	2017-01-25
AL	aluminium	SHF	nonferrous metal	15†	12	1,2,3,4,5,6,7,8,9,10,11,12	2007-01-04	2012-01-11	2012-01-12	2017-01-25
C	corn	DCE	agriculture	10‡	10	1,3,5,7,9,11	2007-01-04	2012-01-11	2012-01-12	2017-01-25
CF	cotton	CZC	agriculture	10‡	10	1,3,5,7,9,11	2007-01-04	2012-01-11	2012-01-12	2017-01-25
CS	corn starch	DCE	agriculture	10‡	10	1,3,5,7,9,11	2015-01-20	2016-01-21	2016-01-22	2017-01-25
CU	copper	SHF	nonferrous metal	15†	12	1,2,3,4,5,6,7,8,9,10,11,12	2007-01-04	2012-01-11	2012-01-12	2017-01-25
HC	hot-rolled coil	SHF	ferrous chain	15†	12	1,2,3,4,5,6,7,8,9,10,11,12	2014-07-16	2015-10-23	2015-10-26	2017-01-25
I	iron ore	DCE	ferrous chain	10‡	12	1,2,3,4,5,6,7,8,9,10,11,12	2014-03-17	2015-08-17	2015-08-18	2017-01-25
J	coke	DCE	ferrous chain	10‡	12	1,2,3,4,5,6,7,8,9,10,11,12	2011-09-16	2014-05-30	2014-06-03	2017-01-25
JM	coking coal	DCE	ferrous chain	10‡	12	1,2,3,4,5,6,7,8,9,10,11,12	2013-07-15	2015-04-22	2015-04-23	2017-01-25
L	lastics	DCE	chemical industry	10‡	12	1,2,3,4,5,6,7,8,9,10,11,12	2007-10-22	2012-06-07	2012-06-08	2017-01-25
OI	rapeseed oil	CZC	oil and oilseed	10‡	10	1,3,5,7,9,11	2007-06-08	2012-03-29	2012-03-30	2017-01-25
P	palm oil	DCE	oil and oilseed	10‡	12	1,2,3,4,5,6,7,8,9,10,11,12	2008-01-16	2012-07-20	2012-07-23	2017-01-25
PP	polypropylene	DCE	chemical industry	10‡	12	1,2,3,4,5,6,7,8,9,10,11,12	2014-05-19	2015-09-17	2015-09-18	2017-01-25
RB	screw-thread steel	SHF	ferrous chain	15†	12	1,2,3,4,5,6,7,8,9,10,11,12	2009-09-18	2013-05-30	2013-05-31	2017-01-25
SR	sugar	CZC	agriculture	10‡	16	1,3,5,7,9,11	2008-05-19	2012-09-14	2012-09-17	2017-01-25
ZN	zinc	SHF	nonferrous metal	15†	12	1,2,3,4,5,6,7,8,9,10,11,12	2007-07-20	2012-04-24	2012-04-25	2017-01-25

Note:
Exchange: SHFE stands for the Shanghai Futures Exchange, DCE denotes the Dalian Commodity Exchange, and CZC is the Zhengzhou Commodity Exchange.
LTD: Last trading day in the month. † denotes the calendar day and ‡ denotes the trading day. For example, the last trading day for the AG contract expired in January is the 15^{th} of January.
LM: Longest maturity contract. For example, the contract of AG with the longest maturity on the 4^{th} of January is the AG contract expired in December, 12 months later.
Contract Month: the month in which the commodity futures have contracts expired. For example, AG has contracts expired in every month, but C only has contracts expired in odd months.
In-Sample: the start date of the in-sample period is the first date that the commodity future has a full number of contract contract series. The end date of the in-sample period is in the middle of the entire period.
Out-of-Sample: the start date of the out-of-sample period is one trading day after the end of the in-sample period. The end date of the out-of-sample period is the last day of the entire period.
Source: Shanghai Futures Exchange, Dalian Commodity Exchange and Zhengzhou Commodity Exchange.

4.2.1 Term Structure

On each trading day, the term structure is assembled by the price of the contract serials with the most recent expired contract in the beginning, and the contract expired at the longest maturity in the end. The rolling of the commodity futures is right after the last trading day of the month. For example, the term structure of AG on 2016-01-04 was the sequence of the AG futures contract expired in January 2016, February 2016, up to December 2016. On 2016-01-18, the term structure of AG became the contract serials expired in February 2016, March 2016, up to January 2017. We will use the functional ANOVA in order to examine the calendar effect of the term structure.

4.2.2 Log Return of the Term Structure

Instead of forecasting the term structure, we choose to forecast the log return of the term structure at various horizons (i.e. different h-steps), which is defined in Equation 4.1.

$$X_n(t) = [\log(P_n(t)) - \log(P_{n-h}(t))] * 100, \text{ where } h \in \{1, 5, 20, 60\} \tag{4.1}$$

where t is the time to maturity, and $P_n(t)$ is the term structure at date n.

There are two advantages of working with the log return of the term structure, rather than with the term structure. First, the log return has zero mean, which can be fed into the functional AR(1) model directly. There is no need to demean the data. Second, the functional observations need to be stationary in order to be modelled by the functional AR(1) model. Analogical to the scalar case, the asset price is typically deemed as a non-stationary process, while the log return of the asset price tends to be stationary. Intuitively, the term structure is highly likely to be non-stationary, while the log return would be stationary. We confirm the stationarity of the log returns by checking the existence condition $\|\hat{\Psi}_h\|^2 < 1$. Other recent developed tests, such as the functional stationarity test (Horváth et al., 2014; Aue & Van Delft, 2017), can be used as well.

Regarding forecasting horizons, we select four h-steps, including 1, 5, 20, 60. When $h = 1$, $X_n(t)$ is the daily log return of the term structure, and $\hat{X}_{n+1}(t)$ is the 1-day-ahead forecast. When $h = 5$, $X_n(t)$ is the weekly log return of the term structure, and $\hat{X}_{n+5}(t)$ is the 1-week-ahead forecast. When $h = 20$, $X_n(t)$ is the monthly log return of the term structure, and $\hat{X}_{n+20}(t)$ is the 1-month-ahead forecast. When $h = 60$, $X_n(t)$ is the quarterly log return of the term structure, and $\hat{X}_{n+1}(t)$ is the 1-quarter-ahead forecast. Longer forecasting horizons could be considered, but due to the availability of data, we cap the forecasting horizon at 60 trading days. Figure 4.1 shows the term structure for Steel Rebar (symbol: RB). Figure 4.2 presents the log return of the term structure at four horizons.

FIGURE 4.1: Term Structure (RB)

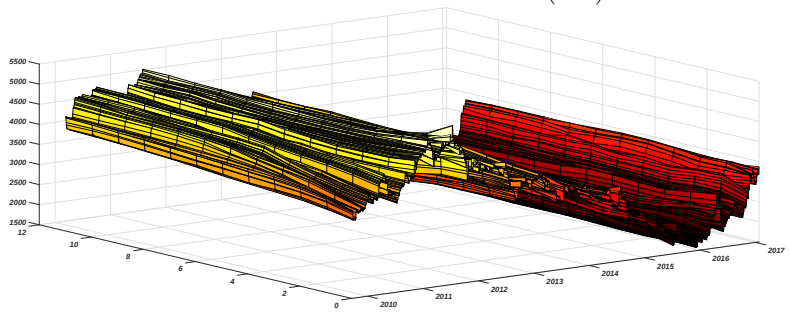

FIGURE 4.2: Log Return of the Term Structure (RB)

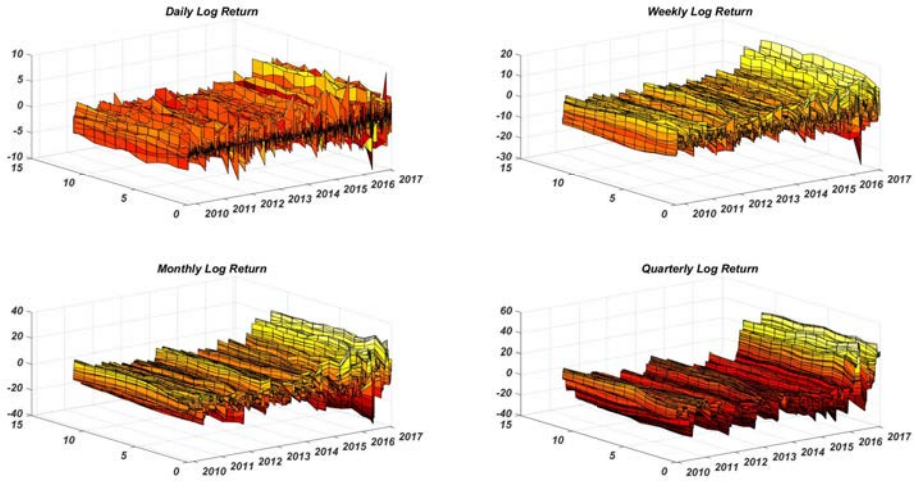

4.2.3 Functional Descriptive Statistics

Following Ramsay & Silverman (2006, Chapter 2), we provide basic functional descriptive statistics, including the functional mean, functional standard deviation, and functional correlation, for both the term structure and the log return of the term structure.

Functional Mean & Functional Standard Deviation

Figure 4.3 shows the sample functional mean and the sample standard deviation of the term structure for 18 commodity futures. Unlike the upside sloping term structure of the government bond yields studied in (Diebold & Li, 2006), the mean curves of the commodity futures term structure are relatively flat. The possible explanation could be that the longest maturity is only 12 months ahead, which is much shorter than that of the term structure of bond yields (120 months). The term structure of all 18 commodity futures has a large standard deviation in our sample period. For the term structure, it is not obvious to observe how the standard deviation varies with the time to maturity.

Figure 4.4 shows the sample functional mean and the sample standard deviation of the log returns of the term structure. The functional means of the log return are very close to a zero function. This fact enables us to use the functional AR(1) model for the log return directly without the demean procedure. The functional standard deviation of the log return increases with h. AL has the smallest magnitude of the functional standard deviation. The commodity futures in the sector of ferrous chain (e.g. HC, I, and J) tend to have a large functional standard deviation.

There are three patterns of the relationship between the functional standard deviation and the time to maturity. The first pattern is that the standard deviation is negatively related to the time to maturity. In other words, the standard deviation is larger when the time to maturity is short. Most commodity futures belong to the first pattern. The second pattern is the positive relationship between the standard deviation and the time to maturity. The example is CU, in which the standard deviation increases after six months of the time to maturity. The third pattern is that the standard deviation is flat, not related to the time to maturity. AG, AL, and ZN are classified into this pattern.

FIGURE 4.3: Functional Mean and Functional Standard Deviation (Term Structure)

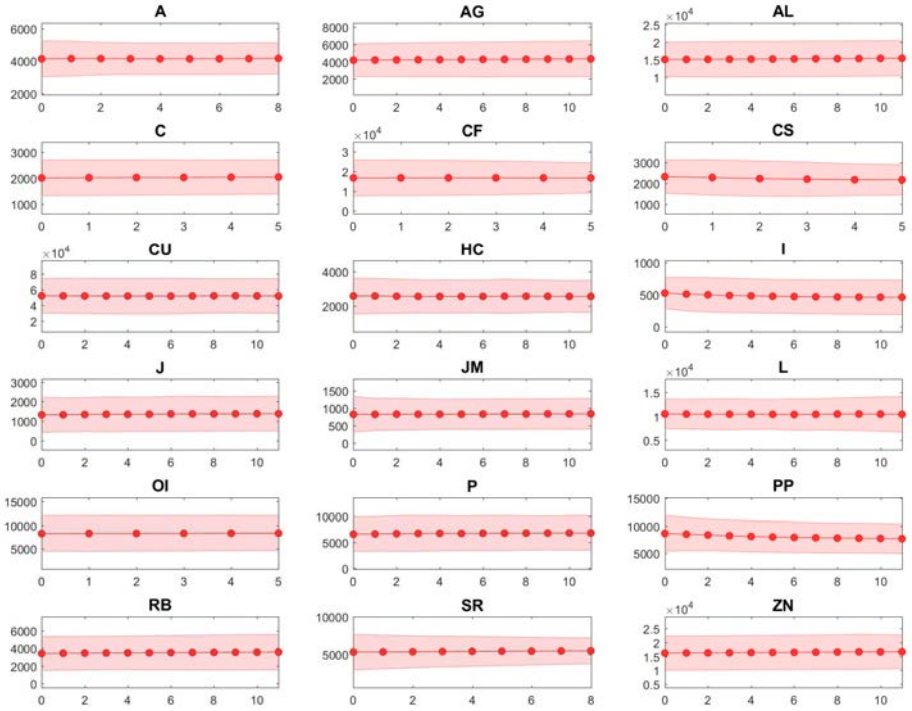

Covariance and Correlation Functions

Figure 4.5 displays the correlation function of the term structure for all 18 commodity futures. All of them show a very high correlation between different time to maturity. Some commodity futures have smooth correlation functions, such as AG, AL, and RB, while some have rigid surfaces, such as L and P. Interestingly, the correlation function of CU and ZN have a sudden drop near 0.9.

Figure 4.6 displays the correlation function of the log return of the term structure for all 18 commodity futures. Compared with the correlation function of the term structure, the correlation function of the log return is significantly lower. With the increase of h, the correlation becomes stronger. Similar to the correlation function of the term structure, some have smooth surfaces, and others have rigid surfaces. A sudden drop in the correlation functions of CU and ZN can also be observed.

FIGURE 4.4: Functional Mean and Functional Standard Deviation (Log Return of the Term Structure)

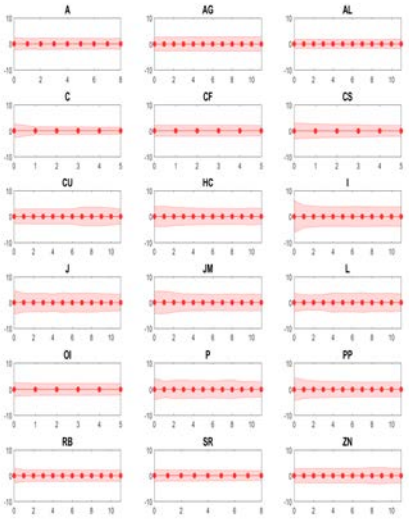

(a) Daily Log Return

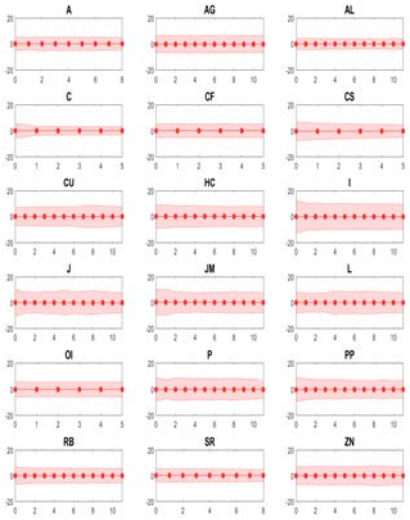

(b) Weekly Log Return

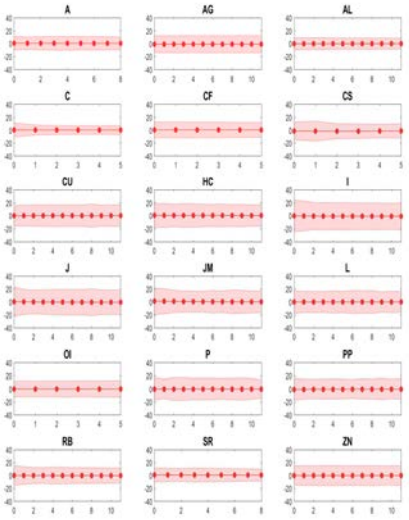

(c) Monthly Log Return

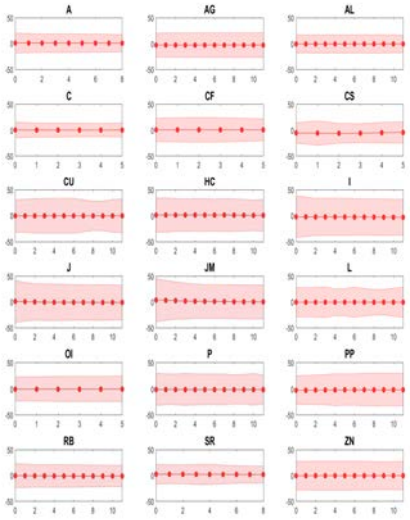

(d) Quarterly Log Return

FIGURE 4.5: Correlation Functions (Term Structure)

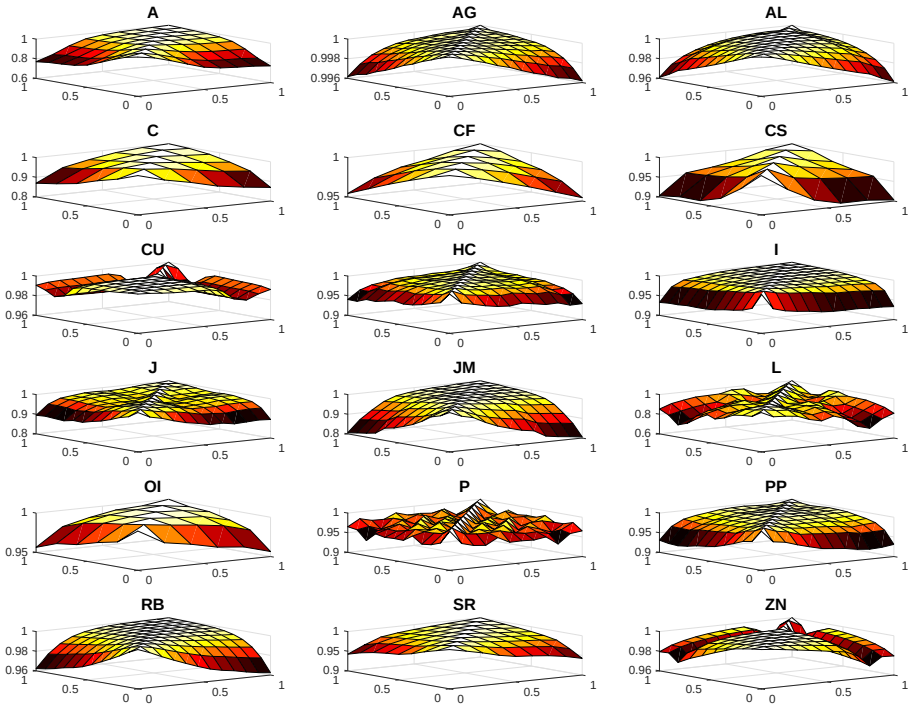

4.3 FANOVA

We employ the one-way functional ANOVA (FANOVA) developed by Horváth & Rice (2015) to examine the season of the year effect (SoY), month of the year effect (MoY), week of the month effect (WoM), and day of the week effect (DoW). It is inappropriate to apply the FANOVA on the log return of the term structure because they all tend to have mean zero functions.

The test has the null hypothesis H_0 that the mean curves of multiple functional populations are the same vs. the alternative H_A that H_0 does not hold.

$$H_0 : \mu_1(\cdot) = \mu_2(\cdot) = ... = \mu_k(\cdot)$$

$$H_A : H_0 \text{ does not hold}$$

FIGURE 4.6: Correlation Functions (Log Return of the Term Structure)

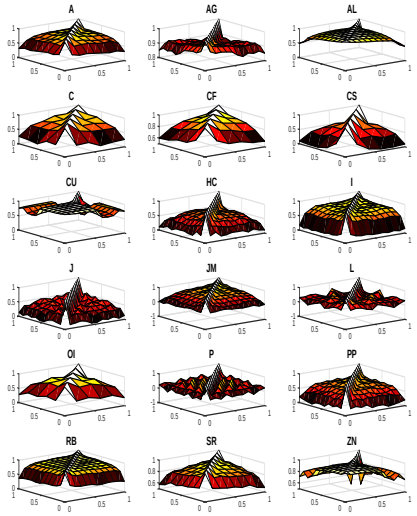

(a) Daily Log Return

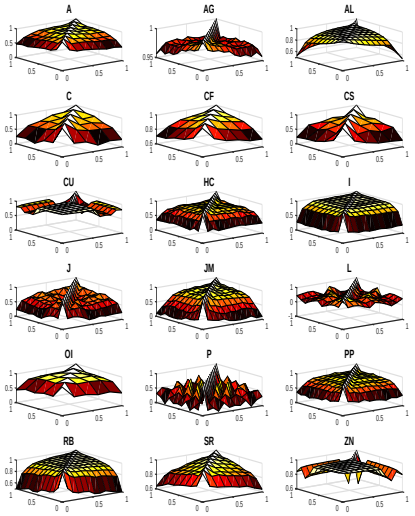

(b) Weekly Log Return

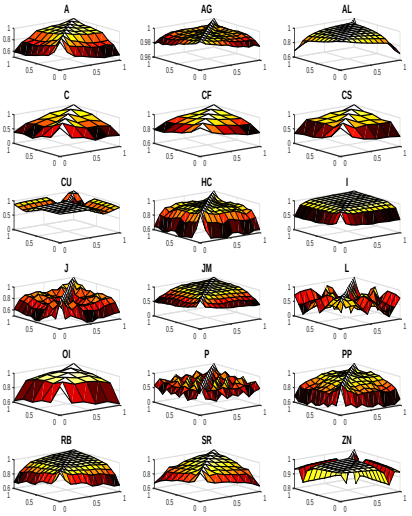

(c) Monthly Log Return

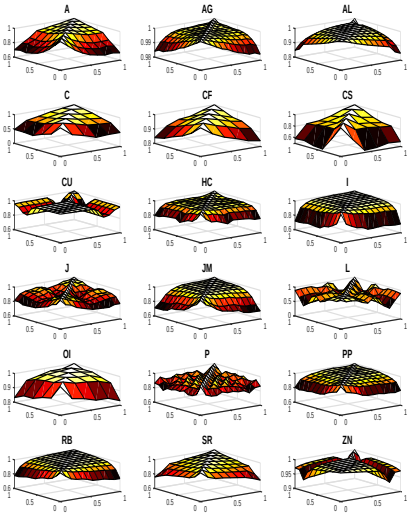

(d) Quarterly Log Return

The core idea of the test is to calculate the empirical score vectors by using the eigenfunctions associated with the d largest eigenvalues of $\hat{D}_{N,p}$ or $\hat{D}_N$ defined as

$$\tilde{\lambda}\tilde{\varphi}_i(t) = \int \tilde{D}_N(t,s)\tilde{\varphi}_i(s)ds \tag{4.2}$$

Then the statistics $\tilde{T}_N$ [1] can be calculated.

$$\tilde{T}_N = \sum_{i=1}^{k} N_i \left(\tilde{\xi}_{i\cdot} - \tilde{\xi}_{\cdot\cdot}\right)^T \tilde{\Sigma}_i^{-1} \left(\tilde{\xi}_{i\cdot} - \tilde{\xi}_{\cdot\cdot}\right) \tag{4.3}$$

where

$$\tilde{\Sigma}_i = \left\{ \int\int \tilde{D}_{N_i,i}(t,s)\tilde{\varphi}_l(t)\tilde{\varphi}_j(s)dtdt,\ 1 \le j,l \le d \right\} \tag{4.4}$$

$$\tilde{\xi}_{\cdot\cdot} = \left(\sum_{i=1}^{k} N_i \tilde{\Sigma}_i^{-1} \right)^{-1} \sum_{i=1}^{k} N_i \tilde{\Sigma}_i^{-1} \tilde{\xi}_{i\cdot} \tag{4.5}$$

$$\tilde{\xi}_{i\cdot} = \frac{1}{N_i} \sum_{i=1}^{N_i} \sum_{i=1}^{N_i} \tilde{\xi}_{ij} \tag{4.6}$$

$$\tilde{\xi}_{ij} = \left(\langle X_{i,j}, \tilde{\varphi}_1 \rangle, \langle X_{i,j}, \tilde{\varphi}_2 \rangle, ..., \langle X_{i,j}, \tilde{\varphi}_d \rangle\right)^T \tag{4.7}$$

The test statistics $\tilde{T}_N$ has the following limit distribution under the null hypothesis.

$$\tilde{T}_N \xrightarrow{\mathcal{D}} \chi^2(d(k-1))$$

where $\chi^2(d(k-1))$ denotes a χ^2 random variable with $d(k-1)$ degrees of freedom. k is the number of functional populations, and d is the number of the basis for the projection. The number d is determined by the rule that approximately $\nu\%$ of the sample variance is explained by the first d principal components. We choose $\nu\% = 95\%$ in this study. Following Horváth & Rice (2015), we also use the flat top kernel to estimate the long-run

[1] There is another version of the statistics $\hat{T}_N$. Interested readers can refer to Horváth & Rice (2015).

covariance kernel, which is shown in Equation 4.8. nan

$$K(x) = \begin{cases} 1, & \text{if } 0 \leq t < 1 \\ 1.1 - |t|, & \text{if } 0.1 \leq t < 1.1 \\ 0, & \text{if } |t| \geq 1.1 \end{cases} \tag{4.8}$$

with the bandwidth parameter equal to $N^{1/4}$.

Our data sample can be divided into different population groups according to four calendar criteria, which are the season of the year (SoY) [2], month of the year (MoY), week of the month (WoM), and day of the week (DoW). The FANOVA is applied to test whether the mean curves in different populations are the same. If the test is rejected, then there could be a market anomaly of the calendar effect.

Since the term structure from different years but the same season/month could have different means just according to the difference in those years, it is necessary to firstly demean the data in each year before the functional AVONA is applied to test the SoY/-MoY. Similarly, the data is demeaned in each month for testing the WoM and the data is demeaned in each week for testing the DoW.

Table 4.1 reports the test statistics and their p-values. Concerning the SoY and MoY, the test of most commodity futures is strongly rejected. There are significant SoY and MoY for most commodity futures. We use JM as a representative example. Figure 4.1 shows the mean curves (demeaned for each year) of the JM term structure for each season and each month. It is apparent that the mean curve of JM in winter is downside sloping, while others are upside sloping. The mean curves of JM in different months show the same pattern with downside sloping curves in November, December, and January. The calendar effect of JM could be explained by the energy consumption in China. JM is one of the main sources of heat in northern China. The demand of JM is typically high in winter. It becomes straightforward that the price of JM in winter is higher, which causes the downside sloping term structure of JM in winter.

[2]The four seasons in China are defined as follows. Spring: February, March, April; Summer: May, June, July; Fall: August, September, October; Winter: November, December, January.

It is reasonable to observe no SoY in HC and ZN. HC is the raw material for the production of automobiles, vessels, and so forth. The main usage of ZN is in order to produce anti-corrosion zinc coating, zinc-base alloy, and zinc oxide, which is commonly utilised in the later stage of the production processes for automobiles, vessels, and light industries. There is no obvious SoY for those industries.

It is expected to observe the SoY in agricultural commodity futures. Interestingly, the FANOVA shows no SoY for SR, while the MoY is very significant for SR. Figure 4.2 shows the mean curves (demeaned for each year) of the SR term structure. The SR term structure in winter seems to be higher than in other seasons, but the FANOVA shows that the difference is not significant. The reason can be explained as follows. It can be observed in Figure 4.3(b) that the SR has a relatively lower term structure in January and comparatively a higher term structure in November and December. Since the spring in China consists of January, November, and December, the mean curve of SR in spring is mixed by relatively high and low curves, which forces it to be closer to the global mean and further makes the SoY of SR insignificant.

Regarding the WoM, there is very strong evidence for RB, strong evidence for AL, I, PP, ZN, and weak evidence for CS and JM. Figure 4.4(a) displays the mean curves (demeaned for each month). Note that the last trading day for the contract of RB expired in the current month is the 15^{th} calendar day in a month. Before the last trading day, the mean curves of Week 1 and 2 are both upside sloping. After the last trading day, the mean curves of Week 3 and 4 are both downside sloping.

In terms of the DoW, the test shows that Al and SR are rejected at the 1% significance level; CF, CS, J, P, and RB are rejected at the 5% significance level; and OI, PP, and ZN are rejected at the 10 % significance level. Taking RB as an example, Figure 4.4(b) depicts the mean curves of the RB term structure (demeaned for each week). The differences among the first four weekdays are not obvious, but the term structure in Friday is clearly relatively lower than the others. This anomaly of lower term structure on Friday can be explained by the investment behaviour. The commodity future of RB in China is a highly volatile investment asset. Some investors in China avoid to take risks during the weekend. They choose to clear their holding positions on Friday

and establish the position again on next Monday. Therefore the RB term structure is abnormally lower than the other weekdays.

TABLE 4.1: FANOVA Results

	SoY	**P-value**	**MoY**	**P-value**	**WoM**	**P-value**	**DoW**	**P-value**
A	59.213***	*(0.00)*	95.399***	*(0.00)*	9.127	*(0.87)*	24.937	*(0.41)*
AG	13.252***	*(0.00)*	53.755***	*(0.00)*	5.179	*(0.16)*	5.254	*(0.26)*
AL	13.087***	*(0.00)*	39.187***	*(0.00)*	14.077**	*(0.03)*	29.589***	*(0.00)*
C	88.965***	*(0.00)*	194.717***	*(0.00)*	17.386	*(0.30)*	20.072	*(0.45)*
CF	8.150**	*(0.04)*	13.994	*(0.23)*	6.934	*(0.64)*	22.134**	*(0.04)*
CS	137.703***	*(0.00)*	399.862***	*(0.00)*	23.769*	*(0.07)*	33.036**	*(0.03)*
CU	8.918**	*(0.03)*	23.675**	*(0.01)*	13.402	*(0.15)*	11.589	*(0.48)*
HC	0.861	*(0.83)*	9.435	*(0.58)*	15.916	*(0.60)*	36.878	*(0.25)*
I	15.971***	*(0.00)*	32.730***	*(0.00)*	18.431**	*(0.03)*	19.184	*(0.74)*
J	72.615***	*(0.00)*	216.472***	*(0.00)*	24.016	*(0.46)*	55.637**	*(0.02)*
JM	11.319**	*(0.01)*	23.421**	*(0.02)*	23.742*	*(0.07)*	30.254	*(0.35)*
L	28.755***	*(0.00)*	88.203***	*(0.00)*	31.407	*(0.25)*	31.538	*(0.68)*
OI	26.519***	*(0.00)*	46.965***	*(0.00)*	10.419	*(0.32)*	26.101*	*(0.05)*
P	33.163***	*(0.00)*	75.643***	*(0.00)*	28.270	*(0.25)*	58.122**	*(0.01)*
PP	27.572***	*(0.00)*	51.428***	*(0.00)*	31.794**	*(0.02)*	45.835*	*(0.05)*
RB	50.549***	*(0.00)*	110.470***	*(0.00)*	23.117***	*(0.00)*	27.393**	*(0.01)*
SR	4.438	*(0.22)*	27.823***	*(0.00)*	6.237	*(0.72)*	35.512***	*(0.00)*
ZN	2.939	*(0.40)*	9.349	*(0.59)*	13.320**	*(0.04)*	19.471*	*(0.08)*

Note: SoY: Season of the Year; MoY: Month of the Year; WoM: Week of the Month; DoW: Day of the Week
For testing the SoY and MoY, the data is demeaned for each year. For testing the WoM, the data is demeaned for each month. For testing the DoW, the data is demeaned for each week.
$^{***}p < 0.01$, $^{**}p < 0.05$, $^{*}p < 0.1$

FIGURE 4.1: Mean Curves for JM (Demeaned for each year)

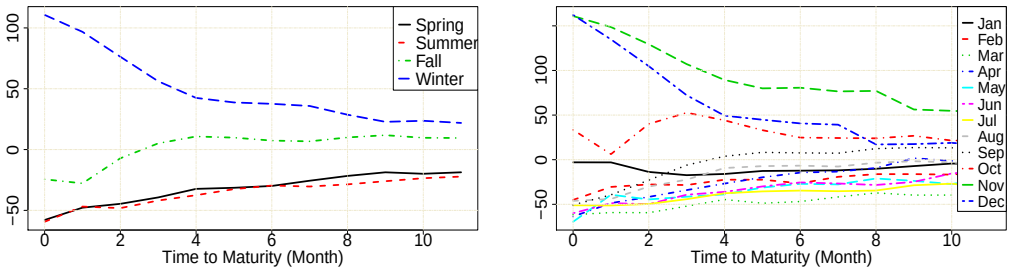

(a) Season of the Year (b) Month of the Year

FIGURE 4.2: Mean Curves for SR (Demeaned for each year)

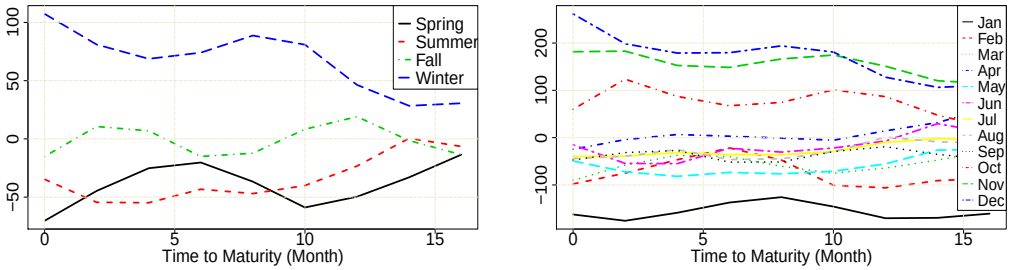

(a) Season of the Year (b) Month of the Year

FIGURE 4.3: Mean Curves for RB (Demeaned for each month/week)

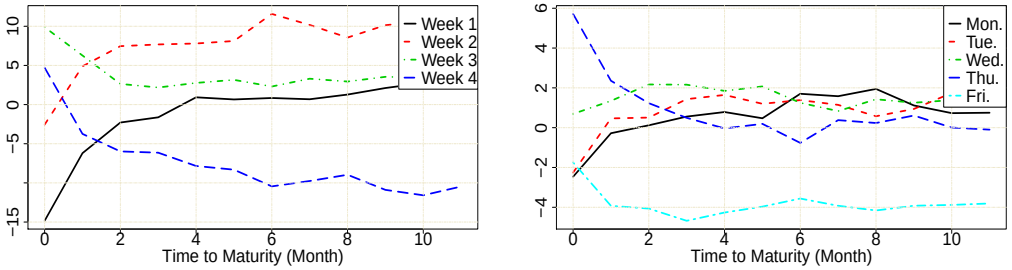

(a) Week of the Month (b) Day of the Week

4.4 h-step Functional Autoregressive Model

Bosq (2000) developed the theory of general functional linear processes, including the functional autoregressive process, in the Hilbert and Banach spaces. Ramsay & Silverman (2006), Hörmann & Kokoszka (2010), and Horváth & Kokoszka (2012) provide recent theoretical developments in functional linear processes. All functions in the Hilbert space $\mathcal{L}^2$ are real square integrable functions on the interval $[0, 1]$ with inner product $\langle f, g\rangle = \int f(t)g(t)dt$. Recall the definition of the functional AR(1) model.

$$X_n(t) = \Psi(X_{n-1}(t)) + \varepsilon_n \tag{4.9}$$

where $\{X_n(t), -\infty < n < \infty\}$ is a sequence of mean zero functional observations in the Hilbert space $\mathcal{L}^2$, $\{\varepsilon_n, -\infty < n < \infty\}$ is a sequence of the i.i.d. mean zero functional errors also in $\mathcal{L}^2$, satisfying $\mathbb{E}\|\varepsilon_n\|^2 < \infty$, and $\Psi \in \mathcal{L}$ is a linear operator mapping a curve into another curve. Here we propose an h-step functional AR(1) model defined in a similar way.

$$X_n(t) = \Psi_h(X_{n-h}(t)) + \varepsilon_n \tag{4.10}$$

where h is the forecasting horizon, and $\Psi_h \in \mathcal{L}$ is also a linear operator. The operator Ψ_h is defined as

$$\Psi_h(X(t)) = \int \psi_h(t, s)X(s)dt \tag{4.11}$$

where $\psi(t, s)$ is a bivariate kernel.

There are two versions of the existence condition for the functional AR(1) model. The weak version is proved by Horváth & Kokoszka (2012), and the strong version is provided by Didericksen et al. (2012). If condition C0 or C1 holds, then there is a unique strictly stationary causal solution to Equation 4.9.

C0 (weak version): There exists an integer j_0 such that $\|\Psi_h^{j_0}\| < 1$.

C1 (strong version): $\|\Psi_h\| < 1$, where $\|\Psi_h\|^2 = \int\int \psi_h(t, s)^2 dtds$.

Note that condition C0 is more general than condition C1. Practically, the condition C1 is more convenient to use.

In this chapter, we employ two prediction methods for the functional AR(1) model under finite sample. The first method is the estimated kernel, which uses only a few of the most important empirical functional principle components (EFPC) to estimate kernel $\psi(t,s)$. The second method is the predictive factor, developed by Kargin & Onatski (2008). The key idea of the second method is to replace the EFPCs by directions which are the most relevant for predictions.

4.4.1 Estimated Kernel

Analogical to the scalar AR(1) model, the most intuitive estimator for Ψ_h would be $\hat{\Psi}_h = \hat{C}_h\hat{C}^{-1}$, where the functional covariance C and lag-h autocovariance C_h operator are defined by

$$C(x) = \mathbb{E}\left[\langle X_n, x\rangle X_n\right], \quad x \in \mathcal{L}^2 \tag{4.12}$$

$$C_h(x) = \mathbb{E}\left[\langle X_n, x\rangle X_{n+h}\right], \quad x \in \mathcal{L}^2 \tag{4.13}$$

The empirical covariance and empirical lag-h autocovariance operator can be estimated by

$$\hat{C}(x) = \frac{1}{N}\sum_{j=1}^{N}\langle X_i, x\rangle X_{j+1} \tag{4.14}$$

$$\hat{C}_h(x) = \frac{1}{N-h}\sum_{k=1}^{N-h}\langle X_i, x\rangle X_{k+h} \tag{4.15}$$

Horváth & Kokoszka (2012) show that the inverse of the covariance operator C is not bounded. In order to avoid working with the reciprocals of very small eigenvalues, it is sensible to use only the first p most important EFPC. Practically, the number of p can be determined by several methods, including the cumulative variance method, cross-validation, and information criteria. Denote the EFPC of the functional observations X_n as, $\hat{\nu}_j$, $j = 1, 2, 3..., p$, the inverse of covariance operator using the first p EFPCs can be defined as

$$\hat{\Gamma}_p(x) = \sum_{j=1}^{p}\hat{\lambda}_j^{-1}\langle x, \hat{\nu}_j\rangle\,\hat{\nu}_j \tag{4.16}$$

Then we can obtain the estimator for $\Psi_{h,p}$

$$\hat{\Psi}_{h,p} = \hat{C}_h \hat{\Gamma}_p(x) \tag{4.17}$$

$$= \hat{C}_h \left(\sum_{j=1}^{p} \hat{\lambda}_j^{-1} \langle x, \hat{\nu}_j \rangle \hat{\nu}_j \right) \tag{4.18}$$

$$= \frac{1}{N-h} \sum_{k=1}^{N-h} \left\langle X_k, \sum_{j=1}^{p} \hat{\lambda}_j^{-1} \langle x, \hat{\nu}_j \rangle \hat{\nu}_j \right\rangle X_{k+h} \tag{4.19}$$

$$= \frac{1}{N-h} \sum_{k=1}^{N-h} \sum_{j=1}^{p} \hat{\lambda}_j^{-1} \langle x, \hat{\nu}_j \rangle \langle X_k, \hat{\nu}_j \rangle X_{k+h} \tag{4.20}$$

If a smoothing procedure is applied on $X_{k+h} \approx \sum_{i=1}^{p} \langle X_{k+h}, \hat{\nu}_i \rangle \hat{\nu}_i$, the estimator further becomes

$$\hat{\Psi}_{h,p} = \frac{1}{N-h} \sum_{k=1}^{N-h} \sum_{j=1}^{p} \sum_{i=1}^{p} \hat{\lambda}_j^{-1} \langle x, \hat{\nu}_j \rangle \langle X_k, \hat{\nu}_j \rangle \langle X_{k+h}, \hat{\nu}_i \rangle \hat{\nu}_i \tag{4.21}$$

The estimated kernel for the estimator in Equation 4.21 is

$$\hat{\psi}_{h,p}(t,s) = \frac{1}{N-h} \sum_{k=1}^{N-h} \sum_{j=1}^{p} \sum_{i=1}^{p} \hat{\lambda}_j^{-1} \langle X_k, \hat{\nu}_j \rangle \langle X_{k+h}, \hat{\nu}_i \rangle \hat{\nu}_j(s) \hat{\nu}_i(t) \tag{4.22}$$

Using the estimated kernel, we can make h-step predictions as

$$\hat{X}_{n+h}(t) = \int \hat{\psi}_{h,p} X_n(s) ds \tag{4.23}$$

$$= \sum_{j=1}^{p} \left(\sum_{i=1}^{p} \hat{\psi}_{h,p} \langle X_n, \hat{\nu}_i \rangle \right) \hat{\nu}_j(t) \tag{4.24}$$

4.4.2 Predictive Factors

Kargin & Onatski (2008) develop the predictive factor decomposition for the estimation of the functional autoregression operator, which is a dimension-reduction technique aiming to minimise the prediction error. This method is different from the estimated kernel method, which is based on the functional principle analysis, because it is designed to identify the directions (linear combinations of components) that are most relevant for prediction rather than describing variance. Here we briefly explain the regularised version of the method for the h-step prediction.

The method aims to find an operator A which can minimise the prediction error

$$min\left\{\mathbb{E}\|X_{n+h} - A(X_n)\|^2;\ A \in \mathcal{R}_k\right\} \tag{4.25}$$

where R_k is the set of all rank k operators mapping $\mathcal{L}^2$ into a subspace of dimension k. In order to solve this problem, Kargin & Onatski (2008) employ the polar decomposition of $\Psi C^{1/2}$

$$\Psi C^{1/2} = U\Phi^{1/2}, \quad \Phi = C^{1/2}\Psi^T\Psi C^{1/2} \tag{4.26}$$

Then the optimisation problem becomes

$$\mathbb{E}\|X_{n+h} - \Psi_{h,k}(X_n)\|^2 \tag{4.27}$$

where $\Psi_{h,k}$ is defined as

$$\Psi_{h,k}(y) = \sum_{i=1}^{k} \sigma_i^{-1} \left\langle y, \Psi^T\Psi C^{1/2}(x_i)\right\rangle U(x_i) \tag{4.28}$$

where $\sigma_1^2 > ... > \sigma_k^2 > 0$ are the largest k eigenvalues of Φ. The operation in Equation 4.28 is equivalent to

$$\Psi_{h,k}(y) = \sum_{i=1}^{k} \langle y, b_i\rangle C_h(b_i), \quad b_i = C^{-1/2}(x_i) \tag{4.29}$$

where the processes $\{\langle y, b_i\rangle, i = 1, ..., k)\}$ are named as the predictive factors, and the functions $\{C_h(b_i), i = 1, ..., k)\}$ are named as the corresponding predictive loadings, which are the most relevant "directions" in $\mathcal{L}^2$ for prediction.

Since $C^{-1/2}$ is also not a bounded estimator, Kargin & Onatski (2008) proposed the following regularised version for consistent estimation.

$$\hat{\Phi}_{\alpha,h} = \hat{C}_\alpha^{-1/2}\hat{C}_h^T\hat{C}_h\hat{C}_\alpha^{-1/2}, \quad \hat{C}_\alpha = \hat{C} + \alpha I \tag{4.30}$$

where $\alpha \in \mathbb{R}^+$ is a regularisation parameter and I is the identity operator. Then the h-step prediction can be made by

$$\begin{aligned}\hat{X}_{n+h}(t) &= \hat{\Psi}_{\alpha,h,k}(X_n(t)) \\ &= \sum_{i=1}^{k} \left\langle X_n(t), \hat{b}_{\alpha,i} \right\rangle \hat{C}_h(\hat{b}_{\alpha,i}), \quad \hat{b}_{\alpha,i} = \hat{C}_\alpha^{-1/2}(\hat{x}_{\alpha,i})\end{aligned} \tag{4.31}$$

where $\sigma^2_{\alpha,1} > ... > \sigma^2_{\alpha,k}$ are the largest k eigenvalues of $\hat{\Phi}_{\alpha,h}$, and $\hat{x}_{\alpha,1}, ..., \hat{x}_{\alpha,k}$ are the corresponding eigenfunctions.

In practice, we need to select the value of the regularisation parameter α. In this study, we use a numerical optimiser to choose α which minimises the total prediction error in the in-sample period data.

4.4.3 Forecast Performance Evaluation

For the sake of measuring the overall forecasting performance in a period, we propose to use the functional RMSE (FRMSE)

$$FRMSE = \sqrt{\frac{1}{N} \sum_{i=1}^{N} \left(\int_0^1 \left(X_i(t) - \hat{X}_i(t) \right)^2 dt \right)} \tag{4.32}$$

In order to compare forecasting performance among different commodities, we developed the functional R^2. Since the functional AR(1) sequence has a zero mean, we define the functional total sum of squares (FTSS) for a functional observation as

$$FTSS = \sum_{i=1}^{N} \left(\int_0^1 X_i(t)^2 dt \right) \tag{4.33}$$

The functional residual sum of squares (FRSS) is defined as

$$FRSS = \sum_{i=1}^{N} \left(\int_0^1 \left(X_i(t) - \hat{X}_i(t) \right)^2 dt \right) \tag{4.34}$$

The functional R^2 (FR^2) is defined as

$$FR^2 = \frac{FTSS - FRSS}{FTSS} \tag{4.35}$$

4.5 Forecasting Performance

Traditional methods (e.g. Diebold & Li, 2006) focus on foresting the term structure. Our functional AR(1) model is more suitable to forecast the log return of the term structure. It is not appropriate to compare our method with traditional methods. Following Didericksen et al. (2012), we use a naive prediction (NP) method as the benchmark model. The naive predictor set $\hat{X}_{n+h}(t) = X_n(t)$, which does not consider the temporal dependence. Compared with the naive predictor, we can see the additional forecasting power gained by using the functional autoregressive structure of the data.

Prior to forecasting, we need to choose the number of EFPCs (p) for the estimated kernel method, and the number of predictive factors (k) for the predictive factor method. In order not to use future information, the parameter optimisation is conducted only by the in-sample period data. We have experimented with the cross-validation procedure, but the optimised p and k tend to be the maximum number of EFPCs or predictive factors. Section 4.4.1 has shown the potential danger of working with the reciprocals of very small eigenvalues. We decide to report the results of $\{p, k\} = 3, 4, 5$.

Regarding the values of the regularisation parameter α for the predictive factor method, we employ a numerical optimiser[3] in order to find the optimised value of α that minimises the forecasting FRMSE in the in-sample period for each commodity futures. Table 4.1 reports the optimised values [4] of α for four forecasting horizons of each commodity futures. When the forecasting horizon is short, like 1-day-ahead and 1-week-ahead, the optimised α has very small values. When the forecasting horizon is long, like 1-month-ahead and 1-week-ahead, the optimised α could be very large for some commodity futures, such as HC and CS.

[3]The numerical optimiser used is *fminunc* in Matlab.

[4]Notice that the values reported in the table are $\alpha \times 1000$

The strong existence condition for the functional AR(1) model is that $\|\Psi_h\| < 1$. In order to ensure that the model is used in a proper way, we calculate the norm of the estimated kernel, i.e. $\|\hat{\Psi}_h\|$. As described in Section 4.4.1, the kernel can be estimated by only the first p most important EFPCs. In order to avoid redundancy, we only report the value of $\|\hat{\Psi}_h\|$ by using the first 5 EFPCs for both the in-sample period and out-of-sample period.

With the purpose of saving space, we only report the best model FR^2. Notice that FR^2 could have negative values because of our definition in Equation 4.35. The interpretation of a negative FR^2 would be that the model produces more variation than the FTSS. In this case, the prediction of a zero function could outperform the model.

4.5.1 In-Sample Fitting

The upper panel of Table 4.2 to Table 4.5 present the in-sample forecasting errors (FRMSE), $\|\hat{\Psi}_h\|$, and FR^2 for four different forecasting horizons. We will use EK to denote the estimated kernel method and PF to denote the predictive factors method. Within the same forecasting horizon, there are three observations about the in-sample fitting.

- Both the EK and PF method can consistently outperform the naive predictor, based on the FRMSE. This indicates that additional forecasting power could be gained by using the functional autoregressive structure.
- Using the same p/k, the PF method has a better fitting than EK. The better performance of PF could be the idea that PF focuses on the directions that are most relevant for the prediction, rather than the directions describing variance. Compared with the EK method, the PF has one additional turning parameter α. The improved performance may also come from the introduction of an additional parameter.
- For both EK and PF, the FRMSE is decreasing with more EFPCs or predictive factors. Using more EFPCs or predictive factors can always give a better fitting

TABLE 4.1: Optimised Values of $\alpha \times 1000$

	1-day-ahead			**1-week-ahead**		
	k=3	**k=4**	**k=5**	**k=3**	**k=4**	**k=5**
A	0.060	0.068	0.077	2.840	2.822	2.823
AG	0.127	0.129	0.128	0.057	0.057	0.057
AL	0.057	0.057	0.057	0.039	0.039	0.039
C	0.060	0.060	0.039	1.060	1.063	1.063
CF	0.039	0.039	0.039	1.940	1.942	1.943
CS	3.741	3.461	3.470	0.057	0.057	0.057
CU	0.057	0.057	0.057	0.072	0.063	0.063
HC	0.057	0.057	0.057	20.821	15.894	11.379
I	1.747	1.612	1.230	0.057	0.057	0.057
J	1.120	1.189	1.213	15.638	16.290	14.465
JM	0.057	0.057	0.057	0.057	0.057	0.057
L	0.057	0.057	0.057	10.612	10.624	11.030
OI	0.279	0.284	0.284	3.260	3.175	3.139
P	1.456	1.296	1.219	0.057	0.057	0.057
PP	0.057	0.057	0.057	0.057	0.057	0.057
RB	0.098	0.086	0.087	0.057	0.057	0.057
SR	0.063	0.063	0.063	0.057	0.057	0.057
ZN	0.039	0.039	0.039	0.157	0.160	0.161
	1-month-ahead			**1-quarter-ahead**		
	k=3	**k=4**	**k=5**	**k=3**	**k=4**	**k=5**
A	27.197	27.058	27.089	55.082	57.272	56.083
AG	0.057	0.057	0.057	0.057	0.057	0.057
AL	0.457	0.451	0.451	0.057	0.057	0.057
C	5.023	5.051	5.064	31.881	32.030	31.616
CF	6.149	6.683	6.710	62.583	62.745	62.825
CS	0.057	0.057	0.057	5122.523	5072.378	5055.936
CU	0.675	0.671	0.641	0.057	0.057	0.057
HC	39.459	43.514	49.998	1683.064	1668.080	1654.022
I	4.773	5.008	4.789	97.297	96.015	96.018
J	316.294	326.450	334.966	695.041	666.286	684.190
JM	51.358	48.081	44.871	16.683	17.996	15.517
L	272.091	268.958	257.877	647.480	630.016	633.118
OI	21.161	21.070	20.989	107.871	107.390	106.798
P	0.057	0.057	0.057	15.900	14.478	12.007
PP	162.848	161.898	158.533	0.057	0.057	0.057
RB	3.539	3.576	3.530	28.105	27.637	27.650
SR	12.694	12.630	12.609	68.255	68.211	68.060
ZN	1.378	1.379	1.369	2.650	2.657	2.660

Note: The numerical optimisation is applied to find the value of α under the principle to minimise the FRMSE. The values reported in the table are $\alpha \times 1000$.

for the in-sample period data, but more p/k may overfit the data, as indicated by the out-of-sample forecasting performance. PF with five predictive factors can always give the best in-sample fitting.

Across different forecasting horizons, there are four comments about the in-sample fitting.

- With a longer forecasting horizon, the FRMSE becomes larger. This is an intuitive result because more uncertainty will arise with a longer forecasting horizon. The quarterly log return has a larger magnitude of variation than the daily log return.
- $\|\hat{\Psi}_h\|$ are mostly less than 1, expect for the 1-quarter-ahead forecasting of four commodity futures, namely AG, CF, CS, and OI. The strong existence condition of the functional AR(1) model is that $\|\Psi_h\| < 1$. Most log returns of different commodity futures at different horizons meet the condition, except that the quarterly log return of those four commodity futures is larger than 1. This suggests that the quarterly log return of those four commodity futures could be non-stationary, and cannot be modelled by the functional AR(1) model.
- With a longer forecasting horizon, $\|\hat{\Psi}_h\|$ becomes larger. For the 1-day-ahead and 1-week-ahead forecasting, $\|\hat{\Psi}_h\|$ is very small, generally less than 0.1. The temporal dependence of the daily and weekly log return is relatively weak, which is the reason for the low FR^2 of the functional AR(1) model. Hence, the log returns at short horizons are not predictable. The temporal dependence of the monthly and quarterly log return becomes stronger, implied by the larger values of $\|\hat{\Psi}_h\|$. Thus, the forecasts appear to be more accurate at long horizons due to the stronger temporal dependence.
- When the forecasting horizon is short, FR^2 is normally less than 15%, indicating a small power of forecasting. With the increase of the forecasting horizon, FR^2 is getting larger. For the 1-month-ahead forecasting, FR^2 is around 40% for many commodities, such as I, L, and P. For the 1-quarter-ahead forecasting, FR^2 can be larger than 50 %, with CF, HC, and I close to 80%.

Our results are consistent with Horváth & Kokoszka (2012, Chapter 13) and Didericksen et al. (2012). Their simulation results show that a larger value of $\|\hat{\Psi}_h\|$ significantly and visibly improves the predictions using the functional autoregressive structure.

4.5.2 Out-of-Sample Forecasting

For the out-of-sample forecasting, we recursively estimate the model and use the most updated parameter to make the next forecast. At date n, the model is firstly estimated by the data $\{X_d(t), 1 \leq d \leq n\}$, and then the h-step forecast for $\hat{X}_{n+h}(t)$ is conducted by either the EK or PF method. The optimised α for the PF method is always the same as the in-sample [5]. In this recursively updated manner, we can reduce the potential danger of over-fitting in the in-sample period since the values of the parameters are updated with new coming observations.

The lower panels of Table 4.2 to Table 4.5 present the in-sample forecasting errors (FRMSE), $\|\hat{\Psi}_h\|$, and FR^2 for four different forecasting horizons. There are three observations about the out-of-sample testing.

- Both EK and PF outperform the naive predictor for the out-of-sample forecasting. This double-confirm the benefit of using functional autoregressive structure to forecast the log return of the term structure.
- When the forecasting horizon is short, EK outperforms PF. As for the 1-quarter-ahead forecasting, PF shows increased predictive power than EK. Similarly to the in-sample results, the value of $\|\hat{\Psi}_h\|$ is larger when the forecasting horizon is longer. It suggests that PF could outperform EK under the condition that the temporal dependence is strong.
- As can be seen from FR^2, the out-of-sample forecasting is less accurate than the in-sample fitting. There are two possible reasons for a good in-sample fitting but a bad out-of-sample forecasting. First, the data generation process (DGP) could be changed. At least the parameter of the DGP could be different. Second, there could be over-fitting in the in-sample period data. Using more EFPCs or predictive

[5] We do not choose to update α recursively because of extremely high computational costs.

factors does not produce a better forecasting. This also suggests that there could be overfitting in the in-sample period data. However, we have conducted out-of-sample forecasting in a recursive way. The parameters are recursively updated. The danger of overfitting is already mitigated.

It is interesting to see that the log returns at short horizons are not predictable, and the forecasts appear much accurate at long horizons. Diebold & Li (2006) also find that their model is more accurate at long horizons. The possible reason could be that the magnitude of noise at short horizons is relatively larger than the fundamental values of the term structure and its log returns. Under longer horizons, the relative magnitude of noise would be smaller, with the comparison to the fundamental values. Then the temporal dependence becomes stronger, which further enables the functional AR(1) model to have a better forecast.

4.6 Conclusion

In this chapter, our aim is to forecast the log return of the term structure for Chinese commodity futures. There are two advantages of working with the log return of the term structure, rather than with the term structure. First, the log return has zero mean, which can be fed into the functional AR(1) model directly. Second, the log return of the term structure is stationary which can be modelled by the functional AR(1).

We start our analysis by inspecting the functional descriptive statistics. Compared with the term structure of bond yields, the functional mean curves show that the term structure for Chinese commodity futures is relatively flat. The relationship between the functional standard deviation and the time to maturity has three patterns, negative, positive, and not related.

The FANOVA has been applied to examine the calendar effect of the term structure. SoY and MoY are found in most commodity futures. HC and ZN do not have both SoY and MoY; CF has SoY but no MoY; while SR has MoY but no SoY. There is very strong evidence for the WoM on RB. Before the last trading day in the month, the RB term

TABLE 4.2: 1-day-ahead Forecasting Results

	Estimated Kernel			*Predictive Factors*			NP	$\|\hat{\Psi}_1\|$	FR^2
In-Sample	**p=3**	**p=4**	**p=5**	**k=3**	**k=4**	**k=5**			
A	3.741	3.738	3.735	3.727	3.725	***3.724***	5.193	0.036	1.839%
AG	4.929	4.923	4.919	4.884	4.880	***4.877***	6.732	0.118	5.593%
AL	3.554	3.551	3.543	3.518	3.516	***3.514***	4.891	0.062	3.725%
C	1.965	1.965	1.963	1.963	1.963	***1.963***	2.807	0.060	0.666%
CF	2.720	2.716	2.715	2.710	2.710	***2.710***	3.522	0.079	5.069%
CS	3.012	3.007	2.989	2.988	2.983	***2.983***	4.168	0.078	4.898%
CU	6.782	6.780	6.779	6.749	6.745	***6.743***	9.273	0.017	2.151%
HC	4.626	4.619	4.615	4.535	4.524	***4.516***	6.440	0.030	7.187%
I	5.720	5.715	5.704	5.634	5.627	***5.622***	7.900	0.044	9.950%
J	5.769	5.765	5.760	5.738	5.730	***5.725***	8.139	0.029	3.578%
JM	4.234	4.230	4.224	4.192	4.185	***4.180***	5.954	0.034	5.059%
L	7.142	7.139	7.135	7.100	7.093	***7.087***	9.953	0.027	3.852%
OI	3.474	3.467	3.460	3.458	3.457	***3.456***	4.752	0.096	2.820%
P	7.000	6.995	6.990	6.983	6.977	***6.974***	9.705	0.028	2.433%
PP	5.222	5.214	5.206	5.173	5.164	***5.155***	7.527	0.034	3.212%
RB	3.074	3.068	3.066	3.049	3.045	***3.043***	4.150	0.042	5.078%
SR	3.525	3.524	3.524	3.512	3.511	***3.510***	4.694	0.032	3.259%
ZN	6.083	6.081	6.078	6.032	6.029	***6.027***	8.131	0.031	4.607%
Out-of-Sample									
	Estimated Kernel			*Predictive Factors*			NP	$\|\hat{\Psi}_1\|$	FR^2
	p=3	**p=4**	**p=5**	**k=3**	**k=4**	**k=5**			
A	2.529	2.527	2.528	2.530	2.529	***2.526***	3.477	0.039	2.112%
AG	***4.318***	4.327	4.325	4.398	4.394	4.388	5.901	0.088	0.921%
AL	2.231	2.226	***2.222***	2.234	2.232	2.231	2.954	0.062	3.344%
C	***2.200***	2.202	2.203	2.201	2.202	2.202	3.070	0.036	0.106%
CF	2.260	2.258	2.256	2.254	2.254	***2.254***	3.049	0.100	2.809%
CS	3.061	3.063	***3.059***	3.063	3.062	3.062	4.188	0.096	3.221%
CU	3.443	3.443	3.443	***3.434***	3.435	3.434	4.639	0.100	1.830%
HC	6.416	6.408	***6.402***	6.420	6.421	6.413	8.652	0.057	7.072%
I	7.804	***7.779***	7.784	7.846	7.839	7.837	10.377	0.093	8.516%
J	6.618	***6.617***	6.618	6.638	6.635	6.632	9.010	0.045	3.390%
JM	***7.293***	7.296	7.308	7.349	7.350	7.348	9.906	0.045	2.753%
L	4.387	***4.385***	4.387	4.410	4.411	4.411	6.168	0.021	0.374%
OI	2.134	2.130	2.131	2.131	2.131	***2.130***	2.923	0.079	2.975%
P	4.196	4.197	4.195	***4.185***	4.186	4.186	5.893	0.040	2.635%
PP	5.677	5.673	***5.672***	5.740	5.736	5.729	7.804	0.046	2.588%
RB	4.470	4.471	***4.466***	4.485	4.485	4.483	5.728	0.042	6.070%
SR	2.551	2.550	***2.549***	2.552	2.552	2.551	3.501	0.046	1.420%
ZN	3.347	3.346	***3.343***	3.372	3.369	3.369	4.577	0.067	1.483%

Note: The lowest FRMSE for each commodity future is highlighted by the bold font. $\|\hat{\Psi}_1\|$ is calculated based on the estimated kernel method with 5 EFPCs. Only the best model FR^2 is reported.

TABLE 4.3: 1-week-ahead Forecasting Results

In-Sample

	Estimated Kernel			***Predictive Factors***			**NP**	$\|\hat{\Psi}_5\|$	FR^2
	p=3	**p=4**	**p=5**	**k=3**	**k=4**	**k=5**			
A	9.007	8.987	8.917	8.773	8.769	***8.766***	12.624	0.116	5.471%
AG	12.315	12.273	12.258	12.185	12.182	***12.180***	16.541	0.238	3.885%
AL	8.418	8.400	8.360	8.275	8.270	***8.268***	11.518	0.115	5.637%
C	4.276	4.242	4.240	4.235	4.235	***4.235***	5.988	0.172	2.602%
CF	7.147	7.145	7.100	7.096	7.095	***7.094***	9.608	0.270	8.130%
CS	6.797	6.755	6.740	6.684	6.673	***6.668***	9.245	0.121	14.297%
CU	16.763	16.653	16.573	16.191	16.170	***16.154***	23.386	0.071	7.784%
HC	10.391	10.327	10.240	10.034	9.981	***9.938***	14.681	0.070	14.366%
I	13.608	13.535	13.455	13.176	13.147	***13.125***	18.858	0.095	15.201%
J	13.050	13.035	13.007	12.876	12.842	***12.813***	18.325	0.030	5.738%
JM	9.419	9.366	9.306	9.089	9.063	***9.040***	13.444	0.080	10.124%
L	17.411	17.351	17.283	16.987	16.921	***16.891***	24.165	0.044	8.071%
OI	8.448	8.422	8.400	8.371	8.365	***8.359***	11.543	0.186	5.407%
P	16.391	16.335	16.289	16.099	16.028	***15.990***	23.873	0.053	10.753%
PP	11.056	11.029	10.950	10.755	10.714	***10.689***	16.220	0.075	11.689%
RB	7.506	7.481	7.444	7.311	7.305	***7.301***	10.511	0.122	7.071%
SR	8.894	8.833	8.789	8.778	8.775	***8.774***	12.689	0.165	3.405%
ZN	15.755	15.735	15.675	15.518	15.502	***15.498***	21.932	0.086	4.250%

Out-of-Sample

	Estimated Kernel			***Predictive Factors***			**NP**	$\|\hat{\Psi}_5\|$	FR^2
	p=3	**p=4**	**p=5**	**k=3**	**k=4**	**k=5**			
A	***5.887***	5.896	5.930	5.990	5.986	5.981	8.456	0.076	-0.064%
AG	***10.296***	10.319	10.321	10.402	10.397	10.393	14.819	0.132	-1.235%
AL	***5.484***	5.492	5.534	5.558	5.555	5.552	7.656	0.111	-0.243%
C	***5.084***	5.088	5.088	5.088	5.087	5.085	7.044	0.070	0.871%
CF	5.587	***5.584***	5.585	5.587	5.587	5.587	7.378	0.095	-2.412%
CS	7.425	7.431	***7.421***	7.472	7.469	7.464	10.192	0.117	-0.660%
CU	8.291	***8.279***	8.290	8.355	8.356	8.358	11.724	0.266	-0.206%
HC	16.834	***16.717***	16.752	16.751	16.733	16.717	23.285	0.116	3.165%
I	21.102	20.947	***20.916***	21.026	21.019	21.014	30.105	0.141	-0.916%
J	16.359	16.311	16.309	16.308	16.292	***16.277***	22.095	0.094	7.928%
JM	17.553	17.575	***17.518***	17.592	17.549	17.534	25.677	0.083	7.228%
L	***9.711***	9.723	9.744	9.904	9.901	9.897	13.961	0.046	-0.666%
OI	5.103	5.086	***5.085***	5.097	5.093	5.089	7.293	0.131	-0.466%
P	9.719	9.707	***9.677***	9.767	9.767	9.761	13.996	0.064	-2.462%
PP	13.785	***13.688***	13.707	13.726	13.716	13.701	19.044	0.119	3.218%
RB	12.266	12.269	12.237	12.208	12.207	***12.207***	16.742	0.117	2.389%
SR	5.938	***5.933***	5.975	5.958	5.956	5.954	8.686	0.104	-0.516%
ZN	7.828	7.827	***7.791***	7.905	7.904	7.903	11.051	0.120	0.704%

Note: The lowest FRMSE for each commodity future is highlighted by the bold font. $\|\hat{\Psi}_5\|$ is calculated based on the estimated kernel method with 5 EFPCs. Only the best model FR^2 is reported.

TABLE 4.4: 1-month-ahead Forecasting Results

In-Sample

	Estimated Kernel			*Predictive Factors*			**NP**	$\|\hat{\Psi}_{20}\|$	FR^2
	p=3	**p=4**	**p=5**	**k=3**	**k=4**	**k=5**			
A	18.568	18.352	18.200	17.872	17.860	***17.853***	27.518	0.217	10.535%
AG	27.158	27.041	26.997	26.730	26.728	***26.727***	36.145	0.496	4.600%
AL	18.097	17.934	17.925	17.678	17.674	***17.671***	24.716	0.129	10.606%
C	8.376	8.263	8.239	8.213	8.209	***8.208***	12.518	0.345	15.378%
CF	16.505	16.485	16.436	16.425	16.419	***16.418***	22.414	0.354	9.402%
CS	16.328	16.268	16.205	15.983	15.963	***15.954***	25.085	0.209	22.942%
CU	33.939	33.397	33.298	32.197	32.145	***32.101***	46.810	0.166	22.310%
HC	21.209	20.511	20.269	19.596	19.466	***19.360***	30.302	0.150	27.608%
I	28.761	27.294	25.623	24.616	24.521	***24.489***	43.202	0.445	38.816%
J	25.723	24.844	23.836	23.292	22.625	***22.162***	39.566	0.153	33.719%
JM	17.262	17.056	16.888	16.539	16.444	***16.401***	24.929	0.127	15.889%
L	33.417	31.336	31.188	29.229	28.732	***28.417***	55.611	0.176	41.785%
OI	18.943	18.612	18.208	18.207	18.201	***18.198***	26.544	0.808	9.864%
P	30.947	30.211	29.666	26.805	26.538	***26.306***	49.268	0.161	44.554%
PP	21.549	20.759	20.379	18.557	18.375	***18.298***	30.102	0.224	39.874%
RB	15.793	15.756	15.727	15.062	15.049	***15.043***	21.828	0.113	12.176%
SR	18.168	18.111	18.062	17.379	17.370	***17.363***	25.572	0.172	10.892%
ZN	33.859	33.769	32.760	32.539	32.495	***32.479***	48.973	0.338	10.753%

Out-of-Sample

	Estimated Kernel			*Predictive Factors*			**NP**	$\|\hat{\Psi}_{20}\|$	FR^2
	p=3	**p=4**	**p=5**	**k=3**	**k=4**	**k=5**			
A	***11.452***	11.512	11.588	11.792	11.792	11.790	16.274	0.092	-2.481%
AG	18.778	***18.767***	18.888	19.031	19.030	19.028	29.216	0.225	-0.861%
AL	11.865	11.753	11.752	11.636	11.632	***11.631***	15.598	0.094	0.497%
C	9.724	9.768	9.704	9.712	9.701	***9.695***	15.360	0.184	13.897%
CF	12.347	12.302	12.333	***12.287***	12.288	12.288	16.772	0.195	-3.661%
CS	13.235	13.191	***13.089***	13.103	13.093	13.095	21.179	0.322	18.857%
CU	17.702	***17.699***	17.700	18.014	18.023	18.024	24.654	0.188	-3.593%
HC	37.642	37.785	37.470	36.555	***36.530***	36.530	53.164	0.213	5.419%
I	***43.053***	43.614	44.027	43.272	43.267	43.259	59.767	0.312	0.349%
J	39.641	39.494	***38.067***	38.218	38.199	38.201	54.019	0.226	12.280%
JM	39.176	38.342	38.000	37.277	37.192	***37.112***	50.181	0.166	14.528%
L	18.285	18.455	***18.093***	18.727	18.754	18.758	26.066	0.119	2.563%
OI	***9.728***	9.993	10.277	10.223	10.214	10.210	13.158	0.147	1.831%
P	19.000	18.962	***18.726***	19.805	19.782	19.770	26.267	0.111	-2.935%
PP	29.774	28.894	28.979	27.854	27.825	***27.799***	40.236	0.245	12.320%
RB	26.225	25.917	25.756	24.584	24.570	***24.560***	37.757	0.423	16.428%
SR	11.931	11.943	11.925	***11.804***	11.805	11.807	16.279	0.098	0.441%
ZN	***16.039***	16.052	16.459	16.468	16.467	16.468	21.426	0.286	-2.798%

Note: The lowest FRMSE for each commodity future is highlighted by the bold font. $\|\hat{\Psi}_{20}\|$ is calculated based on the estimated kernel method with 5 EFPCs. Only the best model FR^2 is reported.

TABLE 4.5: 1-quarter-ahead Forecasting Results

	In-Sample								
	Estimated Kernel			***Predictive Factors***			**NP**	$\|\hat{\Psi}_{60}\|$	FR^2
	p=3	**p=4**	**p=5**	**k=3**	**k=4**	**k=5**			
A	29.385	29.098	28.904	28.741	28.658	***28.632***	46.266	0.364	29.885%
AG	54.710	54.708	54.424	53.941	53.941	***53.940***	73.916	1.034	4.064%
AL	37.200	37.174	36.839	36.015	36.006	***36.002***	49.118	0.404	13.684%
C	15.163	15.102	14.912	14.767	14.756	***14.749***	21.812	0.597	18.315%
CF	31.224	28.574	27.115	26.841	26.800	***26.789***	41.997	1.561	38.381%
CS	24.554	23.073	22.154	20.989	20.857	***20.850***	40.932	1.037	74.104%
CU	68.779	68.686	68.650	66.200	66.174	***66.160***	98.285	0.180	17.496%
HC	34.352	32.772	29.451	20.846	20.473	***20.274***	38.825	0.522	79.725%
I	30.237	30.063	29.918	26.757	26.670	***26.612***	48.928	0.399	77.555%
J	43.998	43.490	42.443	38.997	38.588	***38.221***	72.003	0.244	39.394%
JM	27.751	27.676	26.701	24.342	24.286	***24.243***	40.652	0.414	57.539%
L	59.289	55.134	54.642	51.621	51.499	***51.391***	92.266	0.293	30.272%
OI	33.279	32.364	31.875	31.888	31.867	***31.863***	47.955	1.309	25.557%
P	65.251	58.074	57.826	50.954	50.830	***50.743***	90.603	0.343	41.668%
PP	49.516	49.427	48.260	40.428	40.373	***40.317***	77.547	0.354	40.790%
RB	26.460	26.289	26.275	26.097	26.089	***26.084***	42.977	0.456	16.239%
SR	30.588	30.355	30.117	28.203	28.150	***28.119***	43.788	0.429	27.623%
ZN	56.786	56.599	56.463	55.468	55.451	***55.439***	80.821	0.307	12.301%
	Out-of-Sample								
	Estimated Kernel			***Predictive Factors***			**NP**	$\|\hat{\Psi}_{60}\|$	FR^2
	p=3	**p=4**	**p=5**	**k=3**	**k=4**	**k=5**			
A	22.269	19.939	20.093	19.723	19.719	***19.700***	25.943	0.390	-10.460%
AG	***31.121***	31.177	31.373	31.366	31.365	31.364	42.563	0.347	-2.175%
AL	21.810	***21.764***	22.060	22.288	22.288	22.286	28.609	0.474	0.091%
C	16.686	16.325	***15.894***	16.267	16.227	16.199	24.474	0.392	19.390%
CF	***22.901***	24.266	24.905	24.859	24.836	24.835	27.598	0.405	-7.625%
CS	27.824	26.833	26.587	25.326	25.329	***25.308***	45.817	0.794	0.117%
CU	29.824	***29.796***	29.805	31.272	31.272	31.272	40.967	1.670	-3.214%
HC	60.852	61.162	56.924	56.343	56.325	***56.313***	69.062	0.753	26.967%
I	79.216	76.969	76.717	76.280	76.274	***76.270***	107.459	0.615	-3.562%
J	74.867	74.913	74.056	***73.460***	73.461	73.494	75.841	0.385	12.532%
JM	71.617	70.651	71.355	67.126	67.089	***67.049***	74.510	0.310	37.507%
L	***32.253***	33.073	33.250	34.861	34.852	34.834	49.016	0.193	1.462%
OI	***21.298***	22.163	22.522	22.391	22.379	22.376	23.031	0.392	-22.396%
P	***29.854***	31.005	31.181	31.910	31.908	31.859	44.004	0.177	0.707%
PP	48.108	47.100	46.966	45.889	45.858	***45.839***	70.788	0.324	6.553%
RB	45.308	45.178	45.096	44.268	44.259	***44.254***	53.102	0.445	11.321%
SR	21.554	21.691	21.966	20.907	20.885	***20.882***	31.512	0.720	6.894%
ZN	29.260	29.201	29.180	29.083	29.078	***29.077***	32.645	0.151	8.997%

Note: The lowest FRMSE for each commodity future is highlighted by the bold font. $\|\hat{\Psi}_{60}\|$ is calculated based on the estimated kernel method with 5 EFPCs. Only the best model FR^2 is reported.

structure is upward sloping. While after the last trading day, the RB term structure becomes downward sloping. As for the DoW, the test is rejected for AL and SR at the 1% significance level. Additionally, it is found that the RB term structure is relatively lower on Friday than on other weekdays.

We employ an h-step Functional Autoregressive model to forecast the log return of the term structure for Chinese commodity futures at both short and long horizons. Two prediction approaches are used. The estimated kernel method is a conventional approach using functional principal components, and the predictive factor method is a more refined approach focusing on the directions more relevant to predictions. Compared with the naive predictor, the in-sample and out-of-sample forecasting performance indicates that additional forecasting power is gained by using the functional autoregressive structure. Although the log return at short horizons is not predictable, the forecasts appear to be more accurate at long horizons due to the stronger temporal dependence. The predictive factor method has a better in-sample fitting, but it cannot outperform the estimated kernel method for out-of-sample testing, except for the 1-quarter-ahead forecasting.

The limitation of our research is that our functional AR(1) only uses the temporal dependence information. The exogenous variables, such as interest rates and convenience yields, are not used for the forecasting, which could potentially contribute to a better forecasting performance. Future research will consider incorporating exogenous variables into the functional AR(1) model.

Conclusions, Limitations and Future Research

In this collection of four loosely related essays, several advanced quantitative methods, hidden semi-Markov model, diffusion process, and functional data analysis, have been applied to understand and model the asset returns in the Chinese financial market.

In the introduction, we firstly provide background information about the Chinese stock market, including basic statistics, unique features, and two historical events. Those unique features are closely related to the quantitative results from the statistical methods. Then, we review the relevant finance theories, including the efficient market hypothesis (EMH), technical analysis, and behavioural finance. Furthermore, we present the research question, motivations, and contributions.

HSMM is a generalisation of the HMM by explicitly specifying the sojourn time distribution (Yu, 2010). Bulla & Bulla (2006) examine the reproduction of the stylized facts of the asset returns by the US industry stock indices and show that HSMM is superior to HMM because the stylized facts of the daily returns were entirely reproduced. Due to the merits of HSMM in the literature, we employ a three-state HSMM to decode the Chinese stock market returns in Chapter 1. The research question is divided into three research sub-questions, which have been answered separately. Firstly, it is appropriate to employ a three-state HSMM to explain the time-varying distribution of Chinese stock market returns. In terms of the model performance, our three-state HSMM along with a SV model and a tGARCH(1,1) can reproduce the stylized facts of the "long-memory" and the Taylor effect, but tGARCH(1,1) fails to reduce the fat tails. Secondly,

the hidden states in the HSMM correspond to the market conditions, namely the bear, sidewalk, and bull market. Unlike the definition of market conditions in the literature (Fabozzi & Francis, 1977; Chauvet & Potter, 2000; Edwards & Caglayan, 2001; Lunde & Timmermann, 2004; Gonzalez et al., 2006; Cheng et al., 2013), we provide a systematic way to find the timing of three-category classification, namely the bull, sidewalk, and bear market, for the daily data. Thirdly, we show the inefficiency of the market by design a trading strategy based on the expanding window decoding. The trading strategy generates risk-adjusted return with a Sharpe ratio of 1.14 in the testing sample. The result of our simple trading strategy is consistent with the previous studies shown that technical trading strategies are profitable for the stock market indices in emerging markets (Ratner & Leal, 1999; Ito, 1999; Coutts & Cheung, 2000; Gunasekarage & Power, 2001).

The by-product of Chapter 1 is our statistical definition of market conditions, i.e. bear, sidewalk, and bull markets, which correspond to the three states in the HSMM. Since the regulation and the investor structure of the Chinese stock market are different from the developed markets, it is natural to question the difference in terms of market conditions between the Chinese stock market and developed market. Many studies have investigated the Chinese stock market. Herding behaviour, overreaction, and speculation in the Chinese stock market are well-documented (Tan et al., 2008; Mei et al., 2009; Ni et al., 2015). However, less attention has been to paid from the perspective of the market condition. In Chapter 2, we are interested in investigating the unique characteristics of market conditions in China with particular comparison to developed markets. Using the Viterbi algorithm to globally decode the most likely sequence of the market conditions, we systematically find the precise timing of bear, sidewalk, and bull markets for all eight markets. Through the comparison of the estimation and decoding results, many unique characteristics of the Chinese stock market are found, such as “Crazy Bull”, “Frequent and Quick Bear”, and “No Buffer Zone”. In China, the bull market is more volatile than in developed markets, the bear market occurs more frequently than in developed markets, and the sidewalk market has not functioned as a buffer zone since 2005. Lastly, possible causes of the unique characteristics. For the policy suggestions,

it is very important to adjust the investor structure, to provide risk management tools, and to strengthen supervision on the excess leverage from other source financing.

Many parametric diffusion processes have been developed to improve the Black-Scholes by explaining the stylized facts (Mandelbrot, 1997; Jäckel, 2004; Bingham & Kiesel, 2001; Eberlein & Keller, 1995; Merton, 1976). To the best of our knowledge, there is no parametric diffusion process considering the market condition and the price reversal, although they have been widely studied in the literature of technical analysis and behavioural finance. Financial economists often argue that asset price may behaves differently in different market conditions(Levy, 1974; Kim & Zumwalt, 1979; Chen, 1982). Price reversal is the phenomenon after the overreaction because stock prices tend to converge back to the fundamental values. The price reversal has been widely empirically studied in different markets (Bremer & Sweeney, 1991; Liang & Mullineaux, 1994; Farag, 2014). Chapter 3 propose a new diffusion process referred to as the "camel process" in order to model the cumulative return of a financial asset. This new process includes three parameters, the market condition parameter α, the price reversal parameter β, and the volatility parameter γ. Its steady state probability density function could be unimodal or bimodal, depending on the sign of the market condition parameter. The price reversal is realised through the non-linear drift term which incorporates the cube term of the instantaneous cumulative return. The time-dependent solution of its Fokker-Planck equation cannot be obtained analytically, but can be numerically solved using the finite difference method. The properties of the camel process are confirmed by our empirical estimation results of ten market indexes in two different periods.

In the last chapter, we shift from the stock market to the commodity futures market because the stringent constraints on short selling stocks make it very difficult to manage the downside risk and investing in commodity futures is an effect way to diversify against falling stock prices (Edwards & Caglayan, 2001; Jensen et al., 2002; Wang & Yu, 2004; Erb & Harvey, 2006). Chapter 4 takes the tools in functional data analysis to understand the term structure of Chinese commodity futures and forecast their log returns at both short and long horizons. A functional ANOVA (FANOVA) has been applied in order to examine the calendar effect of the term structure. We use an h-step Functional

Autoregressive model to forecast the log return of the term structure. Compared with the naive predictor, the in-sample and out-of-sample forecasting performance indicates that additional forecasting power is gained by using the functional autoregressive structure. Although the log return at short horizons is not predictable, the forecasts appear to be more accurate at long horizons due to the stronger temporal dependence. The predictive factor method has a better in-sample fitting, but it cannot outperform the estimated kernel method for out-of-sample testing, except in the case of 1-quarter-ahead forecasting. We conclude that the log returns at short horizons are not predictable, and the forecasts appear much accurate at long horizons, which is consistent with Diebold & Li (2006) that also find that their model is more accurate at long horizons.

Limitations and Further Research

One limitation of the HSMM is that the empirical results can be largely changed by the model setting. Finding the appropriate model settings can involve many times of trial and error. Another limitation is that the transition matrix is static. It should be pointed out that the transition matrix can be time-varying and can also depend on the macroeconomic variables. Kim et al. (1999) designed a HMM with time-varying transition matrix depending on the macroeconomic variables. It is possible to develop a HSMM with time-varying transition matrix in a similar manner.

Furthermore, our three-state HSMM can be used to explore the link between the market conditions and macroeconomic variables. But there are two potential challenges that need extra care to deal with. Firstly, the market conditions obtained from our three-state HSMM are daily, but the macroeconomic variables are most likely to be monthly or longer frequencies. Effort should be taken to design the aggregation rule to convert daily market conditions into monthly market conditions. There is no aggregation rule for this conversion at the moment. Secondly, selecting the appropriate macroeconomic variables also need extreme care to avoid multicollinearity and potential endogeneity. It would be interesting to compare the monthly market conditions obtained from our three-state HSMM and other traditional market condition definitions. From this comparison,

we can evaluate whether different definitions of market conditions can produce different conclusions.

In Chapter 2, we only compare China with other developed markets. It is interesting to compare China with other emerging markets as well. Since some other emerging market may also have price limit and individual investors dominating structure, we can investigate on whether the features of market conditions are similar between the emerging markets. Through the comparison with other emerging markets, we can gain more understanding on the Chinese stock market.

As for the "camel process", the parameters of the camel process are possibly time-varying, especially for the parameter α, because the market condition can change along with time. Hence, the parameters may not be stable during the two periods in the empirical analysis. The first possible research is to design a change-point detection test to find the change-point for the "camel process". This research is promising because it can provide another way to systemically find the exact dates of the change in market condition. The second potential research is to develop a "time-varying camel process". Specifically, the parameter α is assumed to be time-varying according to another diffusion process.

Regarding the functional autoregressive model, the limitation is that our functional AR(1) only uses the temporal dependence information. The exogenous variables, such as interest rates and convenience yields, are not used for the forecasting, which could potentially contribute to a better forecasting performance. Future research will consider incorporating exogenous variables into the functional AR(1) model.

Bibliography

Allen, H., & Taylor, M. P. (1990). Charts, noise and fundamentals in the London foreign exchange market. *The Economic Journal*, *100*, 49–59.

Arrow, K. J. (1982). Risk perception in psychology and economics. *Economic inquiry*, *20*, 1–9.

Atkins, A. B., & Dyl, E. A. (1990). Price reversals, bid-ask spreads, and market efficiency. *Journal of Financial and Quantitative Analysis*, (pp. 535–547).

Aue, A., & Van Delft, A. (2017). Testing for stationarity of functional time series in the frequency domain. *arXiv preprint*, *arXiv:1701.01741*.

Barber, B. M., & Odean, T. (1999). The courage of misguided convictions. *Financial Analysts Journal*, (pp. 41–55).

Barber, B. M., & Odean, T. (2008). All that glitters: The effect of attention and news on the buying behavior of individual and institutional investors. *Review of Financial Studies*, *21*, 785–818.

Barberis, N., & Xiong, W. (2009). What drives the disposition effect? An analysis of a long-standing preference-based explanation. *The Journal of Finance*, *64*, 751–784.

Bardsley, P., Horváth, L., Kokoszka, P., & Young, G. (2017). Change point tests in functional factor models with application to yield curves. *The Econometrics Journal*, *20*, 86–117.

Baum, L. E., Petrie, T., Soules, G., & Weiss, N. (1970). A maximization technique occurring in the statistical analysis of probabilistic functions of Markov chains. *The Annals of Mathematical Statistics*, *41*, 164–171.

Beechey, M., Gruen, D. W., Vickery, J. et al. (2000). *The efficient market hypothesis: a survey*. Reserve Bank of Australia, Economic Research Department Sydney.

Bhardwaj, G., Gorton, G., & Rouwenhorst, G. (2015). *Facts and fantasies about commodity futures ten years later*. Technical Report National Bureau of Economic Research.

Bibby, B. M., & Sørensen, M. (1996). A hyperbolic diffusion model for stock prices. *Finance and Stochastics*, *1*, 25–41.

Bingham, N. H., & Kiesel, R. (2001). Modelling asset returns with hyperbolic distributions. In J. Knight, & S. Satchell (Eds.), *Return Distributions in Finance* chapter 1. (pp. 1–20). Oxford: Butterworth-Heinemann.

Black, F., & Scholes, M. (1973). The pricing of options and corporate liabilities. *Journal of Political Economy*, *81*, 637–654.

Blattberg, R. C., & Gonedes, N. J. (1974). A comparison of the stable and student distributions as statistical models for stock prices. *The Journal of Business*, *47*, 244–280.

Boehmer, E., & Kelley, E. K. (2009). Institutional investors and the informational efficiency of prices. *Review of Financial Studies*, *22*, 3563–3594.

Bollerslev, T. (1986). Generalized autoregressive conditional heteroskedasticity. *Journal of Econometrics*, *31*, 307–327.

Bollerslev, T., Chou, R. Y., & Kroner, K. F. (1992). ARCH modeling in finance: A review of the theory and empirical evidence. *Journal of Econometrics*, *52*, 5–59.

Bollerslev, T., & Wooldridge, J. M. (1992). Quasi-maximum likelihood estimation and inference in dynamic models with time-varying covariances. *Econometric reviews*, *11*, 143–172.

Bosq, D. (2000). *Linear Processes in Function Spaces: Theory and Applications, volume 149 of Lecture Notes in Statistics*. Springer-Verlag New York Inc.

Bremer, M., & Sweeney, R. J. (1991). The reversal of large stock-price decreases. *The Journal of Finance*, *46*, 747–754.

Brock, W., Lakonishok, J., & LeBaron, B. (1992). Simple technical trading rules and the stochastic properties of stock returns. *The Journal of Finance*, *47*, 1731–1764.

Broto, C., & Ruiz, E. (2004). Estimation methods for stochastic volatility models: a survey. *Journal of Economic Surveys*, *18*, 613–649.

Bulla, J. (2006). *Application of hidden Markov models and hidden semi-Markov models to financial time series*. Ph.D. thesis.

Bulla, J., & Bulla, I. (2006). Stylized facts of financial time series and hidden semi-Markov models. *Computational Statistics & Data Analysis*, *51*, 2192–2209.

Bulla, J., & Bulla, I. (2013). *hsmm: Hidden Semi Markov Models*. URL: `https://CRAN.R-project.org/package=hsmm` r package version 0.4.

Campbell, J. Y., Lo, A. W.-C., & MacKinlay, A. C. (1997). *The econometrics of financial markets*. Princeton University Press.

Campbell, K., & Limmack, R. J. (1997). Long-term over-reaction in the UK stock market and size adjustments. *Applied Financial Economics*, *7*, 537–548.

Carr, P., Geman, H., Madan, D. B., & Yor, M. (2003). Stochastic volatility for Lévy processes. *Mathematical Finance*, *13*, 345–382.

Chan, K., Menkveld, A. J., & Yang, Z. (2008). Information asymmetry and asset prices: Evidence from the China foreign share discount. *The Journal of Finance*, *63*, 159–196.

Chan, L. K., Jegadeesh, N., & Lakonishok, J. (1996). Momentum strategies. *The Journal of Finance*, *51*, 1681–1713.

Chauvet, M., & Potter, S. (2000). Coincident and leading indicators of the stock market. *Journal of Empirical Finance*, *7*, 87–111.

Chen, S.-N. (1982). An examination of risk-return relationship in bull and bear markets using time-varying betas. *Journal of Financial and Quantitative Analysis*, *17*, 265–286.

Chen, S.-S., Lee, C.-f., & Shrestha, K. (2003). Futures hedge ratios: a review. *The Quarterly Review of Economics and Finance*, *43*, 433–465.

Cheng, T. Y., Lee, C. I., & Lin, C. H. (2013). An examination of the relationship between the disposition effect and gender, age, the traded security, and bull–bear market conditions. *Journal of Empirical Finance*, *21*, 195–213.

Cont, R. (2001). Empirical properties of asset returns: stylized facts and statistical issues. *Quantitative Finance*, *1:2*, 223–236.

Cont, R., & Tankov, P. (2004). *Financial modelling with jump processes*. Chapman & Hall.

Coutts, J. A. (2010). Trading rules and stock returns: some further short run evidence from the hang seng 1997–2008. *Applied Financial Economics*, *20*, 1667–1672.

Coutts, J. A., & Cheung, K.-C. (2000). Trading rules and stock returns: some preliminary short run evidence from the hang seng 1985-1997. *Applied Financial Economics*, *10*, 579–586.

Cox, D. R., & Peterson, D. R. (1994). Stock returns following large one-day declines: Evidence on short-term reversals and longer-term performance. *The Journal of Finance*, *49*, 255–267.

Curcio, R., Goodhart, C., Guillaume, D., & Payne, R. (1997). Do technical trading rules generate profits? Conclusions from the intra-day foreign exchange market. *International Journal of Finance & Economics*, *2*, 267–280.

Day, T. E., & Wang, P. (2002). Dividends, nonsynchronous prices, and the returns from trading the Dow Jones industrial average. *Journal of Empirical Finance*, *9*, 431–454.

De Bondt, W. F., & Thaler, R. H. (1987). Further evidence on investor overreaction and stock market seasonality. *The Journal of Finance*, (pp. 557–581).

DeBondt, W. F., & Thaler, R. (1985). Does the stock market overreact? *The Journal of Finance*, *40*, 793–805.

Didericksen, D., Kokoszka, P., & Zhang, X. (2012). Empirical properties of forecasts with the functional autoregressive model. *Computational statistics*, *27*, 285–298.

Diebold, F. X., & Li, C. (2006). Forecasting the term structure of government bond yields. *Journal of Econometrics*, *130*, 337–364.

Ding, Z., & Granger, C. W. (1996). Modeling volatility persistence of speculative returns: a new approach. *Journal of Econometrics*, *73*, 185–215.

Ding, Z., Granger, C. W., & Engle, R. F. (1993). A long memory property of stock market returns and a new model. *Journal of Empirical Finance*, *1*, 83–106.

Duffie, D., Pan, J., & Singleton, K. (2000). Transform analysis and asset pricing for affine jump-diffusions. *Econometrica*, *68*, 1343–1376.

Dupire, B. et al. (1994). Pricing with a smile. *Risk*, *7*, 18–20.

Eberlein, E., & Keller, U. (1995). Hyperbolic distributions in finance. *Bernoulli*, (pp. 281–299).

Edwards, F. R., & Caglayan, M. O. (2001). Hedge fund and commodity fund investments in bull and bear markets. *The Journal of Portfolio Management*, *27*, 97–108.

Engle, R. F. (1982). Autoregressive conditional heteroscedasticity with estimates of the variance of United Kingdom inflation. *Econometrica*, (pp. 987–1007).

Erb, C. B., & Harvey, C. R. (2006). The strategic and tactical value of commodity futures. *Financial Analysts Journal*, *62*, 69–97.

Fabozzi, F. J., & Francis, J. C. (1977). Stability tests for alphas and betas over bull and bear market conditions. *The Journal of Finance*, *32*, 1093–1099.

Fama, E. F. (1965). The behavior of stock-market prices. *The Journal of Business*, *38*, 34–105.

Fama, E. F. (1970). Efficient capital markets: A review of theory and empirical work. *The Journal of Finance*, *25*, 383–417.

Fama, E. F. (1998). Market efficiency, long-term returns, and behavioral finance. *Journal of Financial Economics*, *49*, 283–306.

Fama, E. F., & French, K. R. (1988). Permanent and temporary components of stock prices. *Journal of Political Economy*, *96*, 246–273.

Fama, E. F., & French, K. R. (1993). Common risk factors in the returns on stocks and bonds. *Journal of Financial Economics*, *33*, 3–56.

Farag, H. (2014). Investor overreaction and unobservable portfolios: Evidence from an emerging market. *Applied Financial Economics*, *24*, 1313–1322.

Frazzini, A. (2006). The disposition effect and underreaction to news. *The Journal of Finance*, *61*, 2017–2046.

French, K. R. (1980). Stock returns and the weekend effect. *Journal of Financial Economics*, *8*, 55–69.

Gaviraghi, B. (2017). *Theoretical and numerical analysis of Fokker-Planck optimal control problems for jump-diffusion processes*. Ph.D. thesis Dissertation, Würzburg, Universität Würzburg, 2017.

Gaviraghi, B., Schindele, A., Annunziato, M., & Borzì, A. (2016). On optimal sparse-control problems governed by jump-diffusion processes. *Applied Mathematics*, *7*, 1978.

Gencay, R. (1998). Optimization of technical trading strategies and the profitability in security markets. *Economics Letters*, *59*, 249–254.

Girardin, E., & Liu, Z. (2003). The Chinese stock market: A casino with 'buffer zones'? *Journal of Chinese Economic and Business Studies*, *1*, 57–70.

Girardin, E., & Liu, Z. (2005). Bank credit and seasonal anomalies in China's stock markets. *China Economic Review*, *16*, 465–483.

Girardin, E., & Liu, Z. (2007). The financial integration of China: New evidence on temporally aggregated data for the A-share market. *China Economic Review*, *18*, 354–371.

Gonzalez, L., Hoang, P., Powell, J. G., & Jing, S. (2006). Defining and dating bull and bear markets: two centuries of evidence. *Multinational Finance Journal*, *10*, 81–116.

Gorton, G., & Rouwenhorst, K. G. (2006). Facts and fantasies about commodity futures (digest summary). *Financial Analysts Journal*, *62*, 47–68.

Granger, C. W., & Ding, Z. (1995). Some properties of absolute return: An alternative measure of risk. *Annales d'Economie et de Statistique*, (pp. 67–91).

Guédon, Y. (2003). Estimating hidden semi-Markov chains from discrete sequences. *Journal of Computational and Graphical Statistics*, *12*, 604–639.

Guillaume, D. M. (2012). *Intradaily exchange rate movements*. Springer Science & Business Media.

Gunasekarage, A., & Power, D. M. (2001). The profitability of moving average trading rules in south asian stock markets. *Emerging Markets Review*, *2*, 17–33.

Hamm, L., & Wade Brorsen, B. (2000). Trading futures markets based on signals from a neural network. *Applied Economics Letters*, *7*, 137–140.

Han, X., & Li, Y. (2017). Can investor sentiment be a momentum time-series predictor? Evidence from China. *Journal of Empirical Finance*, .

Hansen, P. R., & Lunde, A. (2005). A forecast comparison of volatility models: does anything beat a GARCH(1, 1)? *Journal of Applied Econometrics*, *20*, 873–889.

Haugen, R. A., & Lakonishok, J. (1988). The incredible january effect: The stock market's unsolved mystery (Dow Jones-Irwin, homewood, il). *HaugenThe Incredible January Effect: The Stock Markets Unsolved Mystery1988*, .

Higham, D. (2004). *An introduction to financial option valuation: mathematics, stochastics and computation* volume 13. Cambridge University Press.

Hong, H., & Stein, J. C. (1999). A unified theory of underreaction, momentum trading, and overreaction in asset markets. *The Journal of Finance*, *54*, 2143–2184.

Hörmann, S., & Kokoszka, P. (2010). Weakly dependent functional data. *The Annals of Statistics*, *38*, 1845–1884.

Horváth, L., & Kokoszka, P. (2012). *Inference for functional data with applications* volume 200. Springer Science & Business Media.

Horváth, L., Kokoszka, P., & Rice, G. (2014). Testing stationarity of functional time series. *Journal of Econometrics*, *179*, 66–82.

Horváth, L., & Rice, G. (2015). Testing equality of means when the observations are from functional time series. *Journal of Time Series Analysis*, *36*, 84–108.

Hou, Y., & Li, S. (2014). The impact of the CSI 300 stock index futures: Positive feedback trading and autocorrelation of stock returns. *International Review of Economics & Finance*, *33*, 319–337.

Hsu, S. (2015). Chinas volatile stock market and its implications. *University of Nottingham, China Policy Institute Policy Paper*, *7*.

Hudson, R., Dempsey, M., & Keasey, K. (1996). A note on the weak form efficiency of capital markets: The application of simple technical trading rules to UK stock prices-1935 to 1994. *Journal of Banking & Finance*, *20*, 1121–1132.

Ito, A. (1999). Profits on technical trading rules and time-varying expected returns: Evidence from Pacific-Basin equity markets. *Pacific-Basin Finance Journal*, *7*, 283–330.

Jäckel, P. (2004). *Stochastic volatility models: past, present and future*. Chichester, UK: Wiley.

Jacquier, E., Polson, N. G., & Rossi, P. E. (1994). Bayesian analysis of stochastic volatility models. *Journal of Business & Economic Statistics*, *20*, 69–87.

Jamshidian, M., & Jennrich, R. I. (2000). Standard errors for EM estimation. *Journal of the Royal Statistical Society: Series B (Statistical Methodology)*, *62*, 257–270.

Jensen, G. R., Johnson, R. R., & Mercer, J. M. (2002). Tactical asset allocation and commodity futures. *The Journal of Portfolio Management*, *28*, 100–111.

Jiang, F. (2014). Bull leverage funds. *Caixin Weekly*, *December 5*.

Kargin, V., & Onatski, A. (2008). Curve forecasting by functional autoregression. *Journal of Multivariate Analysis*, *99*, 2508–2526.

Kastner, G., & Frühwirth-Schnatter, S. (2014). Ancillarity-sufficiency interweaving strategy (asis) for boosting MCMC estimation of stochastic volatility models. *Computational Statistics & Data Analysis*, *76*, 408–423.

Keynes, J. M. (1964). *The general theory of employment, interest, and money*. London: Harcourt Brace Jovanovich.

Kim, C.-J., Nelson, C. R. et al. (1999). State-space models with regime switching: classical and Gibbs-sampling approaches with applications. *MIT Press Books*, *1*.

Kim, M. K., & Zumwalt, J. K. (1979). An analysis of risk in bull and bear markets. *Journal of Financial and Quantitative analysis*, *14*, 1015–1025.

Kim, S., Shephard, N., & Chib, S. (1998). Stochastic volatility: likelihood inference and comparison with ARCH models. *The review of economic studies*, *65*, 361–393.

Kim, W., & Wei, S.-J. (2002). Foreign portfolio investors before and during a crisis. *Journal of International Economics*, *56*, 77–96.

Kou, S. (2007). Jump-diffusion models for asset pricing in financial engineering. *Handbooks in Operations Research and Management Science*, *15*, 73–116.

Kou, S. G. (2002). A jump-diffusion model for option pricing. *Management science*, *48*, 1086–1101.

Kumar, A., & Lee, C. (2006). Retail investor sentiment and return comovements. *The Journal of Finance*, *61*, 2451–2486.

Lakonishok, J., Shleifer, A., & Vishny, R. W. (1994). Contrarian investment, extrapolation, and risk. *The Journal of Finance*, *49*, 1541–1578.

Lao, P., & Singh, H. (2011). Herding behaviour in the Chinese and Indian stock markets. *Journal of Asian Economics*, *22*, 495–506.

Lee, C., & Swaminathan, B. (2000). Price momentum and trading volume. *The Journal of Finance*, *55*, 2017–2069.

Leigh, W., Paz, N., & Purvis, R. (2002). Market timing: a test of a charting heuristic. *Economics Letters*, *77*, 55–63.

Levy, R. A. (1974). Beta coefficients as predictors of return. *Financial Analysts Journal*, (pp. 61–69).

Liang, Y., & Mullineaux, D. J. (1994). Overreaction and reverse anticipation: two related puzzles? *Journal of Financial Research*, *17*, 31–43.

Liao, L., Liu, B., & Wang, H. (2014). China's secondary privatization: Perspectives from the split-share structure reform. *Journal of Financial Economics*, *113*, 500–518.

Lien, D., & Tse, Y. K. (2000). Hedging downside risk with futures contracts. *Applied Financial Economics*, *10*, 163–170.

Lien, D., & Tse, Y. K. (2002). Some recent developments in futures hedging. *Journal of Economic Surveys*, *16*, 357–396.

Lo, A. W., & MacKinlay, A. C. (2002). *A non-random walk down Wall Street*. Princeton University Press.

Lo, A. W., Mamaysky, H., & Wang, J. (2000). Foundations of technical analysis: Computational algorithms, statistical inference, and empirical implementation. *The Journal of Finance*, *55*, 1705–1770.

Los, C. A., & Yu, B. (2008). Persistence characteristics of the Chinese stock markets. *International Review of Financial Analysis*, *17*, 64–82.

Loughran, T., & Ritter, J. R. (1996). Long-term market overreaction: The effect of low-priced stocks. *The Journal of Finance*, *51*, 1959–1970.

Louis, T. A. (1982). Finding the observed information matrix when using the EM algorithm. *Journal of the Royal Statistical Society. Series B (Methodological)*, (pp. 226–233).

Lucke, B. (2003). Are technical trading rules profitable? Evidence for head-and-shoulder rules. *Applied Economics*, *35*, 33–40.

Lunde, A., & Timmermann, A. (2004). Duration dependence in stock prices: An analysis of bull and bear markets. *Journal of Business & Economic Statistics*, *22*, 253–273.

Malkiel, B. G. (2003). The efficient market hypothesis and its critics. *The Journal of Economic Perspectives*, *17*, 59–82.

Mandelbrot, B. B. (1997). *The variation of certain speculative prices*. Springer.

Mei, J., Scheinkman, J. A., & Xiong, W. (2009). Speculative trading and stock prices: Evidence from Chinese AB share premia. *Annals of Economics and Finance*, *10*, 225–255.

Meng, L. (2016). Method for computation of the fisher information matrix in the Expectation-Maximization algorithm. *arXiv preprint*, *arXiv:1608.01734*.

Meng, X.-L., & Rubin, D. B. (1991). Using EM to obtain asymptotic variance-covariance matrices: The SEM algorithm. *Journal of the American Statistical Association*, *86*, 899–909.

Merton, R. C. (1973). Theory of rational option pricing. *The Bell Journal of Economics and Management Science*, (pp. 141–183).

Merton, R. C. (1976). Option pricing when underlying stock returns are discontinuous. *Journal of Financial Economics*, *3*, 125–144.

Mills, T. C. et al. (1997). Technical analysis and the London stock exchange: Testing trading rules using the FT30. *International Journal of Finance & Economics*, *2*, 319–331.

Mittnik, S., & Rachev, S. T. (1993). Modeling asset returns with alternative stable distributions. *Econometric reviews*, *12*, 261–330.

Nartea, G. V., Wu, J., & Liu, Z. (2013). Does idiosyncratic volatility matter in emerging markets? Evidence from China. *Journal of International Financial Markets, Institutions and Money*, *27*, 137–160.

Neely, C., Weller, P., & Dittmar, R. (1997). Is technical analysis in the foreign exchange market profitable? A genetic programming approach. *Journal of Financial and Quantitative Analysis*, *32*, 405–426.

Nelson, C. R., & Siegel, A. F. (1987). Parsimonious modeling of yield curves. *Journal of Business*, (pp. 473–489).

Nelson, D. B. (1991). Conditional heteroskedasticity in asset returns: A new approach. *Econometrica*, (pp. 347–370).

Ni, Z.-X., Wang, D.-Z., & Xue, W.-J. (2015). Investor sentiment and its nonlinear effect on stock returns: New evidence from the Chinese stock market based on panel quantile regression model. *Economic Modelling*, *50*, 266–274.

Nielsen, S., Olesen, J. O. et al. (2001). *Regime-switching stock returns and mean reversion*. Technical Report.

Okunev, J., & White, D. (2003). Do momentum-based strategies still work in foreign currency markets? *Journal of Financial and Quantitative Analysis*, *38*, 425–447.

Pagan, A. (1996). The econometrics of financial markets. *Journal of Empirical Finance*, *3*, 15–102.

Park, C.-H., & Irwin, S. H. (2007). What do we know about the profitability of technical analysis? *Journal of Economic Surveys*, *21*, 786–826.

Pichler, L., Masud, A., & Bergman, L. (2013). Numerical solution of the Fokker–Planck Equation by Finite Difference and Finite Element Methods – A comparative study. In *Computational Methods in Stochastic Dynamics* (pp. 69–85). Springer.

Platanioti, K., McCoy, E., & Stephens, D. (2005). *A review of stochastic volatility: univariate and multivariate models*. Technical Report working paper.

Poterba, J. M., & Summers, L. H. (1988). Mean reversion in stock prices: Evidence and implications. *Journal of Financial Economics*, *22*, 27–59.

Praetz, P. D. (1972). The distribution of share price changes. *The Journal of Business*, *45*, 49–55.

Pruitt, S. W., & White, R. E. (1988). The CRISMA trading system: Who says technical analysis can't beat the market? *The Journal of Portfolio Management*, *14*, 55–58.

Ramsay, J. O., & Silverman, B. W. (2006). *Functional data analysis*. Wiley Online Library.

Ratner, M., & Leal, R. P. (1999). Tests of technical trading strategies in the emerging equity markets of Latin America and Asia. *Journal of Banking & Finance*, *23*, 1887–1905.

Roberts, J. (1986). First-passage time for randomly excited non-linear oscillators. *Journal of Sound and Vibration*, *109*, 33–50.

Rogers, L. C. G. (1997). Arbitrage with fractional Brownian motion. *Mathematical Finance*, *7*, 95–105.

Rogers, L. C. G., & Zhang, L. (2011). An asset return model capturing stylized facts. *Mathematics and Financial Economics*, *5*, 101–119.

Rydén, T., Teräsvirta, T., Åsbrink, S. et al. (1998). Stylized facts of daily return series and the hidden Markov model. *Journal of applied econometrics*, *13*, 217–244.

Samuelson, P. A. (1965). Proof that properly anticipated prices fluctuate randomly. *Industrial Management Review*, *6*, 41–49.

Schaller, H., & Norden, S. V. (1997). Regime switching in stock market returns. *Applied Financial Economics*, *7*, 177–191.

Shanghai Institute of Futures and Derivatives (2016). The 2016 development report on China's futures markets. `http://www.shfe.com.cn/upload/20160711/1468201417695.pdf`.

Shiller, R. J. (2003). From efficient markets theory to behavioral finance. *The Journal of Economic Perspectives*, *17*, 83–104.

Tan, L., Chiang, T. C., Mason, J. R., & Nelling, E. (2008). Herding behavior in Chinese stock markets: An examination of A and B shares. *Pacific-Basin Finance Journal*, *16*, 61–77.

Taylor, S. J. (1986). *Modelling financial time series*. World Scientific.

Taylor, S. J. (1994). Modeling stochastic volatility: A review and comparative study. *Mathematical finance*, *4*, 183–204.

Tian, M. (2015). Umbrella trusts in China: An RMB 400 billion problem. URL: `http://knowledge.ckgsb.edu.cn/2015/06/04/finance-and-investment/umbrella-trusts-in-china-an-rmb-400-billion-problem/`.

Veronesi, P. (1999). Stock market overreactions to bad news in good times: a rational expectations equilibrium model. *Review of Financial Studies*, *12*, 975–1007.

Viterbi, A. (1967). Error bounds for convolutional codes and an asymptotically optimum decoding algorithm. *IEEE Transactions on Information Theory*, *13*, 260–269.

Wang, C., & Yu, M. (2004). Trading activity and price reversals in futures markets. *Journal of Banking & Finance*, *28*, 1337–1361.

Wang, J., Burton, B., & Power, D. (2004). Analysis of the overreaction effect in the Chinese stock market. *Applied Economics Letters*, *11*, 437–442.

Weber, M., & Camerer, C. F. (1998). The disposition effect in securities trading: An experimental analysis. *Journal of Economic Behavior & Organization*, *33*, 167–184.

Williams, J. B. (1938). *The theory of investment value* volume 36. JSTOR.

Wojtkiewicz, S., Bergman, L., & Spencer Jr, B. (1997). High fidelity numerical solutions of the fokker-planck equation. In *Proceedings of the ICOSSAR 97, The Seventh International Conference on Structural Safety and Reliability, Kyoto, Japan, Nov* (pp. 24–28).

Yang, J., Yang, Z., & Zhou, Y. (2012). Intraday price discovery and volatility transmission in stock index and stock index futures markets: Evidence from China. *Journal of Futures Markets*, *32*, 99–121.

Yap, C.-W. (2015). China crackdown on margin lending hits peer-to-peer lenders. *Dow Jones News, July*, *13*.

Yeh, Y.-H., Shu, P.-G., Lee, T.-S., & Su, Y.-H. (2009). Non-tradable share reform and corporate governance in the Chinese stock market. *Corporate Governance: An International Review*, *17*, 457–475.

Yu, J. (2002). Forecasting volatility in the New Zealand stock market. *Applied Financial Economics*, *12*, 193–202.

Yu, S.-Z. (2010). Hidden semi-Markov models. *Artificial Intelligence*, *174*, 215–243.

Zarowin, P. (1989). Short-run market overreaction: size and seasonality effects. *The Journal of Portfolio Management*, *15*, 26–29.